UNIVERSITY OF CALIFORNIA,
IRVINE

Contributions of Microglia in the Healthy and Injured Brain

DISSERTATION

submitted in partial satisfaction of the requirements
for the degree of

DOCTOR OF PHILOSOPHY

in Biological Sciences

by

Rachel Anne Rice

Dissertation Committee:
Assistant Professor Kim Green, Chair
Professor Leslie Thompson
Professor Charles Glabe

2015

DEDICATION

To my family.

I know why families were created, with all their imperfections. They humanize you. They are made to make you forget yourself occasionally, so that the beautiful balance of life is not destroyed.

Anaïs Nin

TABLE OF CONTENTS

LIST OF FIGURES AND TABLES

LIST OF ABBREVIATIONS

3xTg	triple transgenic
Aβ	beta-amyloid
AD	Alzheimer's disease; sAD(sporadic) or fAD(familial)
ALS	Amyotrophic lateral sclerosis
APP	amyloid precursor protein
ASD	Autism spectrum disorder
BBB	Blood brain barrier
BDNF	Brain-derived neurotrophic factor
CA	Cornu Ammonis subfield of hippocampus
CCI	Controlled cortical impact
CCR2	C-C chemokine receptor type 2
CD11b	Cluster of differentiation 11b; *aka* ITGAM, *aka* CR3
CD80	Cluster of differentiation 80
CD86	Cluster of differentiation 86
cDNA	Complementary DNA
CNS	Central nervous system
CR3	Complement receptor 3, *aka* ITGAM, *aka* CD11b
CSF	Cerebrospinal fluid
CSF1	Colony-stimulating factor 1
CSF1R	Colony-stimulating factor 1 receptor
DT_A	Diphtheria toxin A chain
EC	Entorhinal cortex
FTD	Frontotemporal dementia
GFAP	Glial fibrillary acidic protein
GWAS	Genome-wide association studies
HC	Hippocampus
HD	Huntington's disease
HDLS	Hereditary diffuse leukoencephalopathy with spheroids
HVAC	High voltage-activated calcium channel
IBA1	Ionophore calcium-binding adapter molecule 1
IFNγ	Interferon gamma
IL	Interleukin
IP_3R	Inositol 1,4,5-trisphosphate receptor
ITGAM	Integrin alpha M; a*ka* CD11b, *aka* CR3
KA	Kainic acid
KO	Knock out
LPS	Lipopolysaccharide
LSPS	Laser scanning photostimulation
LVAC	Low voltage-activated calcium channel
MeCP2	Methyl-CpG-binding protein-2
MHC-II	Major histocompatibility complex class II
mRNA	Messenger RNA
NFT	Neurofibrillary tangle

NSAID	Non-steroidal anti-inflammatory drug
NTg	Non-transgenic
pcDNA	Plasmid Cytomegalovirus promoter DNA
PCG	Posterior cingulate gyrus
PD	Parkinson's disease
PHF	Paired helical filaments
PSD-95	Postsynapstic density protein 95
RyR	Ryanodine receptor
SFG	Superior frontal gyrus
SBDP	Spectrin breakdown production
SNP	Single nucleotide polymorphism
Syn	Synaptophysin
TBI	Traumatic brain injury
TLR	Toll-like receptor
TNF-α	Tumor necrosis factor-alpha
TREM2	Triggering receptor expressed on myeloid cells 2
WT	Wild-type

ACKNOWLEDGMENTS

I am forever grateful for the teachings and support of my mentor, Dr. Kim N. Green. His brilliance is rivaled only by his enthusiasm. I also thank the entire lab of Dr. Frank M. LaFerla for their technical support and intellectual input throughout the course of my graduate career.

I would like to thank my committee members, Professors Leslie Thompson and Charles Glabe, for providing helpful suggestions and critique.

I thank Dr. Denis Drygin for his strict training and genuine concern for my development as a scientist.

Thanks to Elizabeth Spangenberg, Hana Yamate-Morgan, Rajan Arora, and Jason Pham for their technical assistance.

This work was supported in parts by NINDS 1R01NS083801 to KNG, NINDS F31NS086409 to RAR, American Federation for Aging Research to KNG, Whitehall Foundation to KNG, and Alzheimer's Association to KNG. I thank Cell Press, Neurobiology of Aging, Elsevier, and PLoS ONE for permission to include copyrighted figures and text as part of my dissertation.

CURRICULUM VITAE

Rachel Anne Rice

2008	Student Intern, Cylene Pharmaceuticals, San Diego, CA Dr. Denis Drygin
2009	Research Assistant, Department of Cell and Neurobiology, University of Southern California, Los Angeles, CA Dr. Ruth I. Wood
2009	B.A. in Neuroscience, University of Southern California, Los Angeles, CA
2010	Research Scientist I at Cylene Pharmaceuticals, San Diego, CA Caroline B. Ho
2015	Ph.D. in Biological Sciences, University of California, Irvine Dr. Kim N. Green

FIELD OF STUDY

The roles of microglia in healthy and disease states; Age-related changes in APP processing due to downregulation of the $CaV_{3.1}$ T-type calcium channel

HONORS AND AWARDS

2006	Resident Honors Program, University of Southern California
2006-2009	Presidential Scholar, University of Southern California
2008, 2009	Undergraduate Research Associates Program, University of Southern California
2009	Provost Undergraduate Fellowship, University of Southern California
2012	AAIC Travel Award
2012, 2013	UCI-HHMI Teaching Fellows Program Graduate Fellow Award, University of California, Irvine
2013	School of Biological Sciences, Fine Science Tools Graduate Travel Award, University of California, Irvine
2013	Carl W. Cotman Scholar's Award, University of California, Irvine
2014	NIH National Research Service Award
2014	FASEB Conference Travel Award

PUBLICATIONS

Original Reports

"Protein Kinase CK2 Modulates IL-6 Expression in Inflammatory Breast Cancer." Drygin D, Ho CB, Omori M, Bliesath J, Proffitt CC, **Rice R**, Siddiqui-Jain A, O'Brien S, Padgett C, Lim JK, Anderes K, Rice WG, Ryckman D. Biochemical and Biophysical Research Communications. 2011 Nov 11;415(1):163-167.

"Ethanol-induced Conditioned Partner Preference in Female Mice." Wood RI and **Rice R**. Behavioral Brain Research. 2013 Apr 15;243:273-277.

"Age-related Downregulation of the $CaV_{3.1}$ T-type Calcium Channel as a Mediator of Amyloid Beta Production." **Rice RA,** Berchtold NC, Cotman CW, Green KN. Neurobiology of Aging. 2014 May;35(5):1002-1011.

"Colony-stimulating Factor 1 Receptor Signaling is Necessary for Microglia Viability, Unmasking a Microglia Progenitor Cell in the Adult Brain." Elmore MR, Najafi AR, Koike MA, Dagher NN, Spangenberg EE, **Rice RA**, Kitazawa M, Matusow B, Nguyen H, West BL, Green KN. Neuron. 2014 Apr 16;82(2):380-397.

"Microglial Elimination Improves Functional Recovery Following Extensive Neuronal Loss in the Hippocampus." **Rice RA**, Spangenberg EE, Yamate-Morgan H, Lee R, Arora RP, Hernandez MX, Tenner AJ, West BL, Green KN. Journal of Neuroscience. *Under review.*

"Chronic Elimination of Microglia in the 5xfAD Mouse Model of Alzheimer's Disease Attenuates Dendritic Spine Loss and Cognitive Impairments Without Modulating Amyloid Pathology." Spangenberg EE, **Rice RA**, Elmore MRP, Blurton-Jones M, West BL, Green KN. Journal of Neuroscience. *Under review*.

Reports in Progress

"Microglial Repopulation Resets the Inflammatory Milieu in the Injured Adult Brain." **Rice RA**, Pham JC, West BL, Green KN.

Abstracts and Posters

"Serotonin 5HT2A Receptor Immunoreactivity in Mouse Forebrain: Examination of Sex Differences and Effects of Hormones." **Rice R** and Wood, RI. Society for Neuroscience Conference 2010, San Diego, CA.

"CX-4945, a Selective and Orally Bioavailable Inhibitor of Protein Kinase CK-2 Inhibits PI3K/AKT, JAK-STAT, and NFkB Signaling and Induces Apoptosis in Multiple Myeloma Cells." Ho CB, **Rice R**, Drygin D, Bliesath J, Streiner N, Siddiqui-Jain A, Proffitt CC, O'Brien S, Anderes K. American Society of Hematology Conference 2010, Orlando, FL.

"Age-related Changes in T-type Calcium Channels and Their Effects on Alzheimer's Disease Pathogenesis." **Rice RA**, Green KN. Alzheimer's Association International Conference 2012, Vancouver, BC.

"Elimination of Microglia Improves Functional Recovery Following Extensive Neuronal Loss." **Rice RA**, Green KN. Society for Neuroscience Conference 2013, San Diego, CA.

"Elimination of Microglia Improves Functional Recovery Following Extensive Neuronal Loss." **Rice RA**, Green KN. FASEB Translational Neuroimmunology Conference 2014, Big Sky, MT.

PRESENTATIONS

May 2012	Neuroblitz Seminar, UC Irvine
February 2013	Neuroblitz Seminar, UC Irvine
February 2013	ReMIND Emerging Scientists Symposium, UC Irvine
January 2014	Neuroblitz Seminar, UC Irvine
July 2014	FASEB Translational Neuroimmunology Conference, Big Sky, MT
February 2015	Neuroblitz Seminar, UC Irvine
February 2015	ReMIND Emerging Scientists Symposium, UC Irvine

ADMINISTRATIVE SERVICE

2010-2012	Admissions Committee Student Representative Interdepartmental Neuroscience Program (INP), UC Irvine
2012-2013	Member of Organizing Committee School of Biological Sciences Professional Development Seminar Series, UC Irvine
2010-2015	Financial, Education Chair Research and Education in Memory Impairments and Neurological Disorders (ReMIND), UC Irvine

TEACHING

2011	Bio 93: From DNA to Organisms
2012	N113L: Neurobiology Laboratory
2012	Bio 93: From DNA to Organisms
2013	Bio 38: Learning and Memory
2014	Bio 44: Stem Cells in the Brain

ABSTRACT OF THE DISSERTATION

Contributions of Microglia in the Healthy and Injured Brain

By

Rachel Anne Rice

Doctor of Philosophy in Biological Sciences

University of California, Irvine, 2015

Assistant Professor Kim Green, Chair

Microglia are the immune competent cells of the central nervous system (CNS). During development, microglia play critical roles in pruning synapses and refining neuronal connectivity. In the adult brain, microglia constantly survey the parenchyma for cellular damage or invading pathogens. Upon detection of such events, microglia become activated and shift to a phagocytic phenotype, secreting pro-inflammatory molecules and adopting an amoeboid morphology. As part of the resolution/repair process, microglia return to a surveillant state and produce anti-inflammatory molecules. Unfortunately, with severe insults, such as traumatic brain injury or chronic neurodegeneration, microglia remain activated and contribute to an inflammatory process that is never, or poorly, resolved. In this way, we hypothesize that microglia contribute deleteriously to functional outcomes.

The goal of my dissertation is to determine the contributions of microglia to neuronal health and cognition in both the healthy and injured brain. The direct assessment of microglia-specific contributions is possible due to the discovery by our lab that microglia are dependent upon signaling through the colony-stimulating factor 1 receptor (CSF1R)

for their survival. Treatment with a small-molecule CSF1R inhibitor eliminates >99% of microglia from the adult mouse brain. Critically, microglia fully repopulate the CNS upon withdrawal of the CSF1R inhibitor, effectively renewing this cellular compartment.

Using a genetic model of inducible neuronal loss, I have determined that the elimination of microglia *during* a lesion is detrimental to cellular health, while the elimination of microglia *following* a lesion results in the reversal of many lesion-induced deficits. Importantly, this research suggests that the microglia-mediated immune response is beneficial during insult or injury, but deleterious after such an event. Moreover, repopulation of the brain with new microglia following neuronal lesioning largely resets the inflammatory milieu and confers functional benefits.

Finally, long-term elimination of microglia was employed in order to determine if these cells shape the synaptic landscape in the healthy adult brain, as they do during development. Indeed, I found that microglial elimination in healthy adult mice results in brain-wide and robust increases in dendritic spine numbers and excitatory neuronal connectivity, indicating that microglia modulate synaptic function throughout the course of the lifetime.

INTRODUCTION

Microglia are the resident immune cells of the central nervous system and comprise approximately 10% of all cells in the brain. These cells play homeostatic roles in neuronal maintenance, but also mediate immune responses to neuronal damage or invading pathogens. It is known that microglia regulate synapse number and type during development through the pruning of dendritic spines. Moreover, microglial abnormalities result in deficient neuronal connectivity in mice, and also are implicated in human developmental disorders that display synaptic aberrations, such as autism spectrum disorder (ASD) and Rett syndrome. It is not known, however, if microglia continue to serve as synaptic architects past development.

In the adult brain, microglia constantly monitor the parenchyma for the presence of stress signals, dead or dying cells, and pathogens. The detection of such by molecular receptors on microglia results in activation of the cells and subsequent elimination of debris or microbes, by way of phagocytosis. In this way, microglia serve as the guardians of our central nervous system. However, these cells can become overwhelmed by severe and/or long-lasting insults. For example, it has been shown that microglia remained activated in a human for 17 years following a traumatic brain injury (Ramlackhansingh et al., 2011). The chronic inflammation produced under such circumstances likely contributes to functional impairment in the individual, as studies have shown that the production of individual pro-inflammatory molecules can affect cognition and behavior. It is therefore critical to understand which pro-inflammatory molecules microglia produce and if such microglia-specific signaling contributes to functional outcomes.

On the whole, my dissertation seeks to understand the roles that microglia play during and after neuronal injury, and if the manipulation of microglial homeostasis can remodel the brain at a synaptic level to facilitate functional recovery.

A. Microglial Origins

Microglia are the resident macrophages of the CNS and were first described by Franz Nissl in the late 1800s. These cells did not become known as “microglia” until del Rio-Hortega introduced the term in 1939, in an effort to distinguish them from neuron and astrocyte populations in the brain (Rio-Hortega, 1939). While it was previously believed that microglia and astrocytes derive from a common neuroectodermal lineage, similarities among microglia, monocytes, and macrophages prompted studies that ultimately revealed microglia to be of myeloid origin (Kitamura et al., 1984; Beers et al., 2006). Indeed, microglia progenitors originate as KIT^+ hematopoietic stem cells in the yolk sac and migrate to the central nervous system during embryonic development, at which point the blood brain barrier (BBB) forms, effectively separating these cells from the periphery, as well as from their pool of progenitors (Ginhoux and Merad, 2010; Kierdorf et al., 2013) (Figure 1).

Once in the central nervous system, progenitors rapidly expand and differentiate into $CD11b^+/F4/80^+$ microglia (Alliot et al., 1999). Such microgliogenesis is critically dependent on many transcription factors including PU.1, RUNX1, and IRF8; mice lacking any one of these have severely reduced microglial numbers and/or functionality as a result of either yolk sac or CNS disruptions in microglial maturation (McKercher et al., 1996; Zusso et al., 2012; Kierdorf et al., 2013).

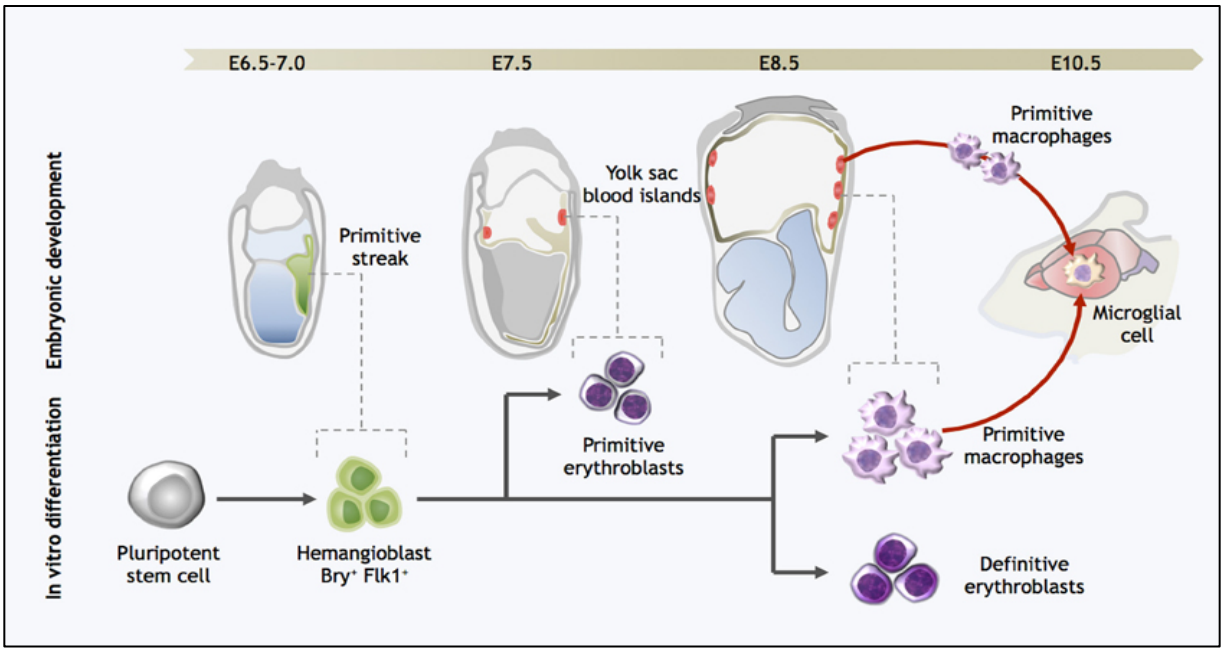

Figure 1 "Strategy for directed differentiation of microglial precursors from pluripotent stem cells" from Ginhoux *et al.*, Copyright 2013. Available at: http://journal.frontiersin.org/Journal/10.3389/fncel.2013.00045/full

It is suggested that bone marrow-derived cells may be able to contribute to the immunocompetent population in the CNS during the early postnatal period, though most of the work demonstrating this phenomenon was done under abnormal conditions (e.g. In PU.1$^{-/-}$ mice) (Beers et al., 2006). In the adult CNS, appreciable numbers of infiltrating monocytes are only observed when the blood brain barrier is compromised, such as with Alzheimer's disease, stroke, or traumatic brain injury (de Groot et al., 1992). In fact, researchers have shown that 15 weeks following bone marrow transplant in adult mice, the vast majority of microglia in the brain were of host origin (Priller et al., 2001). Even with injury, monocytes do not seem to contribute to microgliosis and do not remain in the brain for substantial amounts of time (Priller et al., 2001; Ajami et al., 2007).

Because no readily available progenitor source has been identified within the CNS, and bone marrow-derived cells do not seem to contribute to the immune cell population of

the healthy brain, microglia are believed to have low proliferation rates and long lifespans. In this way, microglia represent an autonomous, self-renewing cell population.

B. Microglial Functions in Development and Adulthood

Roles in Development

A role for microglia as synaptic architects has emerged over the last decade. During development, there is an overproduction of synapses in the brain, and these must be pruned back in order to refine and establish appropriate neuronal connectivity. To this end, multiple groups have shown that microglia are capable of phagocytosing pre- and post-synaptic inputs. Importantly, this ability is dependent upon two key receptors expressed by microglia: chemokine fractalkine receptor 3 (CX3CR1) and complement receptor 3 (CR3).

CX3CR1 is exclusively expressed by microglia in the healthy brain and allows for crosstalk with neurons, which express its ligand, CX3CL1 (Erblich et al., 2011). Neurons upregulate expression of CX3CL1 during development, and this phenomenon led researchers to believe that this signaling pathway underlies microglia-mediated synaptic pruning (Mody et al., 2001). Indeed, researchers found that mice lacking CX3CR1 had a higher number of PSD-95 puncta in the early postnatal brain, as well as a higher density of dendritic spines, compared to wild-type littermates (Paolicelli et al., 2011). Moreover, electrophysiological measurements indicated that synaptic signaling remained immature for a longer period of time in the knockout (KO) mice, as evidenced by enhanced long-term depression and a depressed seizure threshold. It is important to note a caveat of this study: CX3CR1 KO mice exhibit a transient reduction in microglia during the early

postnatal period, and so it is plausible that the increase in synaptic components was due to a reduction in the number of microglia available to prune, and not a lack of CX3CL1-CX3CR1 signaling. A follow-up study by the same group further revealed that 1) post-natal microglial pruning acts primarily on excitatory synapses and 2) a transient reduction in microglia number during development (as a result of CX3CR1 deficiency) results in changes that persist into adulthood (P40), including decreased functional brain connectivity and impairments in social behaviors (Zhan et al., 2014).

The classical complement pathway, part of the innate immune system, is another signaling cascade by which microglia identify and phagocytose synaptic components. It was first discovered that mice deficient for C1q, or the downstream complement protein C3, exhibit an excess of synapses as a result of a pruning failure (Stevens et al., 2007). As microglia express CR3 and are capable of phagocytosis, these cells were identified as the prime candidate for complement-mediated synaptic pruning. Studying the retinogeniculate system, researchers discovered that both CR3 and neuronal activity are critical for the elimination and refinement of synapses by microglia (Stevens et al., 2007). A pharmacologic approach to reduce microglial phagocytic ability was also employed by treating mice with minocycline, and a similar decrease in pre-synaptic terminal engulfment was found. Together, these data definitively determined that microglia are capable of phagocytosing synaptic inputs during neuronal development/maturation, and that this ability is critically dependent upon complement signaling.

That CX3CR1 deficiency produces long-lasting impairments in neuronal connectivity and social behaviors led many researchers to believe that microglia-mediated

impairments may underlie neurodevelopmental disorders. Indeed, at a clinical level, aberrant numbers, signaling, and activation of microglia are found in Rett Syndrome and ASD, and just a single prenatal injection of lipopolysaccharide (LPS) in a pregnant rat leads to communication and cognitive deficits in pups (Maezawa and Jin, 2010; Kirsten et al., 2012; Tetreault et al., 2012; Suzuki et al., 2013). Rett syndrome is a neurodevelopmental disorder, primarily affecting female children haplodeficient for the methyl-CpG-binding protein-2 (MeCP2) gene. Of note, expression of the MeCP2 gene is frequently downregulated in males with autism, as a result of promoter methylation (Nagarajan et al., 2006). In 2010, it was discovered that $MeCP2^{-/-}$ microglia release glutamate at five-times higher levels than MeCP2-intact microglia, and that such increased glutamate release results in dendritic spine abnormalities in cultured hippocampal neurons (Maezawa and Jin, 2010). Moreover, *in vivo* studies revealed that the introduction of wild-type microglia, via bone-marrow transplantation into MeCP2 null male or $MeCP2^{+/-}$ female mice, resulted in the restoration of many functional impairments (Derecki et al., 2012). These studies led microglia to be identified as the key cell type underlying many neuronal abnormalities in this syndrome.

Over the last decade, it has become abundantly clear that microglia play essential roles in refining neuronal connectivity during development and the early post-natal period. Moreover, the failure of these cells to properly execute this function can result in aberrant connectivity, and may likely contribute to, or account for, developmental disorders such as autism and Rett syndrome. While microglia serve as synaptic architects in early life, it remains unknown if these cells carry out similar functions in the mature adult brain, and this is a fundamental question my dissertation aims to answer.

Roles in Adulthood

In the adult, microglia serve as guardians of the central nervous system. At rest, microglia constantly survey the brain in an effort to identify potential hazards, which can range from dying neurons to invading pathogens. These duties require that microglia are highly motile and make frequent contacts with neurons. Upon neural insult or invasion by a pathogenic species, microglia migrate to the site of injury and rapidly proliferate. The cells also change in morphology, exhibiting a swollen cell body and shorter processes, indicative of their activation. Such an activation state is often termed "M1." This morphological switch occurs in concert with changes in inflammatory signaling, favoring secretion of pro-inflammatory cytokines such as TNF-α, IL-1β, and IL-6. Subsequently, the microglia take on an anti-inflammatory role, secreting molecules such as IL-4 and IL-10 as part of the resolution and repair process (Colton and Wilcock, 2010). In this stage, microglia are often termed "M2." While the M1 and M2 designations each encapsulate a variety of differential microglial characteristics, they also represent a tendency of the field to oversimplify microglial phenotypes. Microglia can exhibit different signaling profiles in different regions of the brain, and do not appear to be an entirely homogenous population of cells, even within a particular region (Hanisch, 2013). Therefore, I do not make use of these terms throughout my dissertation, despite their popularity in the fields of microglia research.

In addition to responding to many secreted molecular signals, microglia also rely on physical contact with other cells for surveillance purposes. In a live-imaging study, researchers found that microglia made contacts with pre- and post-synaptic structures at a rate of about once per hour in the healthy adult brain, with each contact lasting

approximately five minutes (Wake et al., 2009). The monitoring of synapses by microglia appears to be activity-dependent, as reducing neuronal activity reduced the frequency of contacts. Following an ischemic injury, microglia made contact with synaptic terminals for longer than an hour at a time, and more importantly, many of the previously present pre-synaptic terminals were absent following this prolonged period. This study suggests that microglia can detect injured cells in the adult brain, and also that the prolonged contact of microglia with neurons following such an event may allow for the support or elimination of damaged cellular components.

Microglia can also phagocytose uninjured cells in the adult brain. During adult neurogenesis, more neuroprogenitor cells are produced in the adult dentate gyrus than will survive. Non-activated microglia phagocytose these extranumerous cells within the first few days of their lives, effectively regulating the rate at which newborn neurons mature and become incorporated into existing circuitry (Sierra et al., 2010). Importantly, the authors of this study reported that this ability of microglia was not compromised by aging or inflammation.

On the whole, microglia are critically important in the adult brain for maintaining the integrity of the parenchyma and can function quickly to eliminate toxic, injured, or superfluous cells.

C. Microglial Senescence

Because microglia are long-lived and do not have a readily available progenitor source, they are prone to senescence with increasing age. Senescence describes a constellation of age-related changes in the phenotype of microglia that ultimately render

these cells less effective at carrying out both homeostatic and stimulus-induced functions. Alterations can be observed in microglia number, morphology, expression profile, reaction to stimuli, and phagocytic ability.

The morphology of aged microglia can resemble that of activated microglia in the young brain, in that the cell body becomes larger, while the processes appear shorter and thicker (Hefendehl et al., 2014). In a study comparing the cerebral cortex of young (38-year-old) and aged (68-year-old) cognitively normal individuals, researchers found de-ramified microglia to be more than nine times more prevalent in the aged sample, compared to the young sample (Streit et al., 2004). Of importance, this morphological switch does not occur in all microglia; de-ramified microglia were found scattered throughout the parenchyma, residing next to ramified microglia (Streit et al., 2004). Moreover, in certain brain regions, microglia become more numerous and dense with age, and often, these cells do not maintain the stereotyped spacing observed in a younger, healthy brain (Tremblay et al., 2012; Hefendehl et al., 2014). It is not known, however, if this increase in microglial density is a compensatory response to the reduced individual abilities of microglia, or if it is a result of microglia proliferating and becoming activated over time, and subsequently failing to return to a resting state.

Shortening microglial telomeres has also been proposed as a mechanism contributing to the senescence of this cell type. When cells divide, DNA polymerase cannot entirely replicate the telomeres, or the furthest ends of our linear DNA, and so cells lose telomere length over time. When telomere length is critically shortened, cells enter replicative senescence and change their expression profiles (Baird et al., 2003). Indeed, studies have shown that the telomeres of rat microglia shorten with time *in vitro* and with

normal aging *in vivo*, and that the longest telomeres actually demonstrate the most shortening (Flanary and Streit, 2003). The same research group later compared microglial telomere length in four individuals with AD and one non-demented individual (Flanary et al., 2007). They found the longest telomeres to be in the non-demented individual, while individuals with AD had significantly shorter telomeres, on average. Moreover, shorter telomeres were absent in the brain of the non-demented individual. The researchers also found the presence of dystrophic microglia to be significantly higher in demented and high pathology, non-demented individuals, compared to low pathology, non-demented individuals. Thus, there appear to be correlations between 1) microglial telomere shortening and dementia, as well as 2) dystrophic/de-ramified microglia and AD pathology. Finally, one can imagine that the more microglia divide in response to stimuli over a lifetime, the faster this process of telomere shortening might happen, possibly expediting disease pathogenesis.

Aged microglia exhibit increased expression of many inflammatory molecules, even when unchallenged. In comparing 2 month-old and 18 month-old mice, researchers found that microglia in the older mice produced higher levels of the pro-inflammatory cytokines IL-1β, IL-6, IL-12β, and TNF-α (Sierra et al., 2007). Another group comparing young (3-6 months-old) and aged (20-24 months-old) mice found expression levels of major histocompatibility complex class two (MHC-II), a marker of microglial activation, to be increased in the aged brain (Godbout et al., 2005).

Besides exhibiting increased basal expression of pro-inflammatory molecules, senescent microglia also react more severely and less effectively to inflammatory stimuli. The aforementioned study found that the aged brain responds more strongly to

an injection of LPS than does the young brain, and sickness behavior associated with this stimulus was exaggerated in the aged mice, as measured by testing motivation, locomotion, food consumption, and body weight (Godbout et al., 2005). Specifically, LPS-induced increases in IL-6 and IL-1β expression are significantly greater in the aged brain (Godbout et al., 2005). In the controlled cortical impact (CCI) model of traumatic brain injury, aged mice displayed much larger increases in markers of both microglia and astrocyte activation than did young mice, though this study did not assess functional outcomes (Sandhir et al., 2008). Interestingly, young rats display more activated microglia one day following intracerebral hemorrhage, and fewer activated microglia three days following intracerebral hemorrhage, than do aged rats, again demonstrating the failure of aged microglia to respond appropriately to neural insult (Wasserman et al., 2008). Moreover, the ability of microglia to *physically* respond to stimuli has been studied extensively in the mouse retina, as it is an easily accessed compartment of the CNS. In these studies, researchers found that young microglia respond to ATP by extending processes, while aged microglia respond by retracting processes (Damani et al., 2011). Additionally, both the homeostatic and injury-induced mobility of microglial processes is decreased with aging (Damani et al., 2011; Hefendehl et al., 2014). These findings support the idea that microglia manifest age-related deficits in phagocytosis, as the regulation of cell structure is critical to this process.

Together, these results demonstrate that the basal inflammation state of aged microglia is already “primed,” meaning that 1) they respond to less severe insults and 2) they respond more strongly than do microglia in the youthful brain. Such changes have many implications for disease and injury states, in which aged microglia fail to resolve insults

and instead, contribute to excessive and chronic inflammation. Figure 2 summarizes the phenotypical changes associated with microglial aging/senescence.

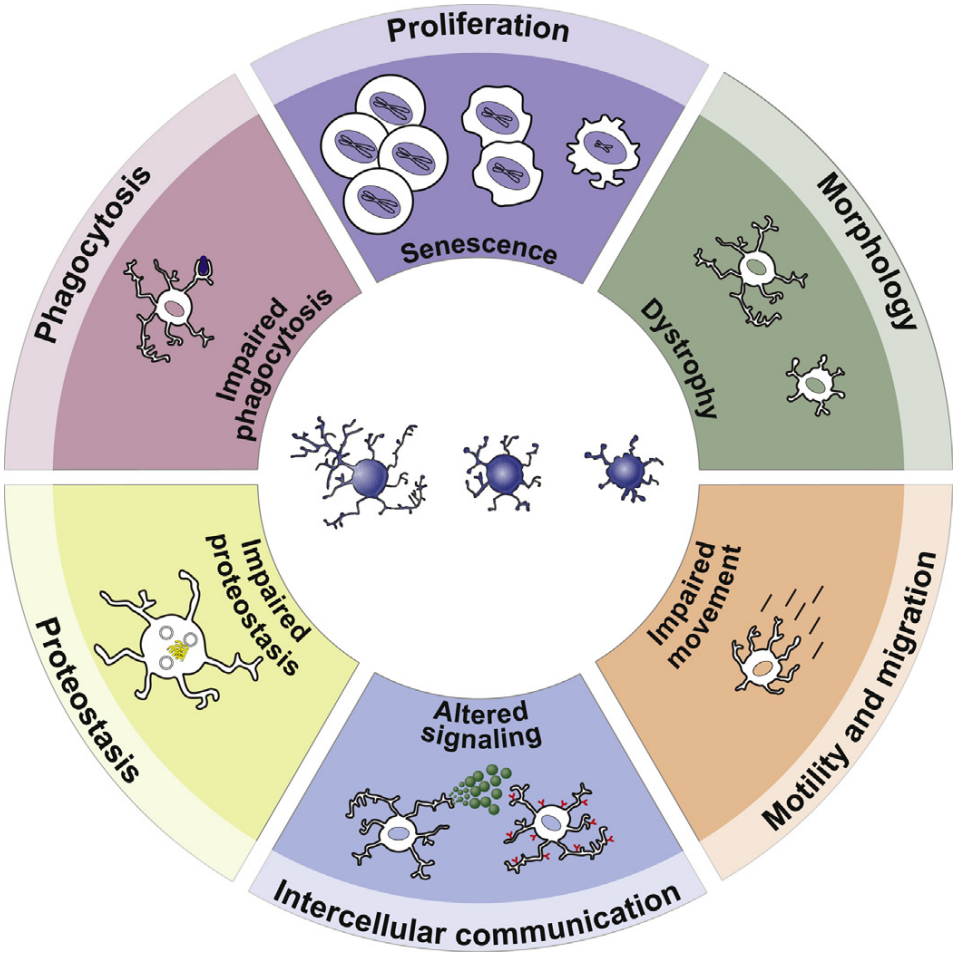

Figure 2 "The hallmarks of microglial aging" from Mosher and Wyss-Coray, Copyright 2014. Available at: www.sciencedirect.com/science/article/pii/S000629521400032X

D. Neurodegeneration, Inflammation, and Injury

Alzheimer's disease

Microglia-derived inflammation is implicated in many neurodegenerative conditions, including Alzheimer's disease (AD), Parkinson's disease, amyotrophic lateral sclerosis, frontotemporal dementia (FTD) and Huntington's disease. Over the last decade,

genome-wide association studies (GWAS) have identified mutations in microglia-specific and microglia-related genes that increase the likelihood of developing AD, leading many researchers to focus on how microglial dysregulation drives this disease in particular.

AD is a crippling neurodegenerative disease that specifically targets an individual's memory and cognitive abilities. Over time, personality changes can occur, along with the ability to take care of one's self and carry out daily tasks. Age is the biggest risk factor for AD, while other risk factors include family history, head trauma, and heart health (Association, 2012). The disease is characterized by the presence of two hallmark pathologies in the brain: amyloid plaques and neurofibrillary tangles (NFT). Plaques are composed primarily of the Aβ peptide and are found extracellularly, while tangles are composed primarily of hyperphosphorylated tau protein and are found intracellularly. The Aβ peptide is produced by sequential cleavage of the amyloid precursor protein (APP) by BACE1, a β-secretase, and then γ-secretase, as part of the amyloidogenic pathway. Alternatively, APP can undergo non-amyloidogenic processing and be cleaved within the Aβ sequence by ADAM10, an α-secretase, precluding the formation of this toxic peptide (Figure 3). Additionally, extensive synaptic and neuronal loss occurs over the course of the disease, likely as a result of pathology, as well as the inflammatory response to this pathology. The extent of this loss, and not plaque burden, correlates with cognitive decline (Giannakopoulos et al., 2003).

As age is the biggest risk factor, it is important to understand what changes in the aged body and brain to allow for the development of Alzheimer's disease. As an individual ages, microglia may contribute to disease onset and progression by multiple

mechanisms. It is believed that systemic inflammation, or a history of immune insults, can lead to microglial priming and/or senescence in aged individuals, though this represents an indirect mechanism. There are still other changes that occur in aged microglia to compromise their abilities, and these changes represent direct mechanisms.

Senescent microglia become less efficient at carrying out many of their normal functions, including phagocytosis. It has been postulated that an age-related decline in the phagocytic ability of these cells may allow for the aggregation of Aβ and resulting plaque deposition in the brain. Indeed, studies have revealed that microglia specifically lose their capacity to phagocytose Aβ with age (Floden and Combs, 2011).

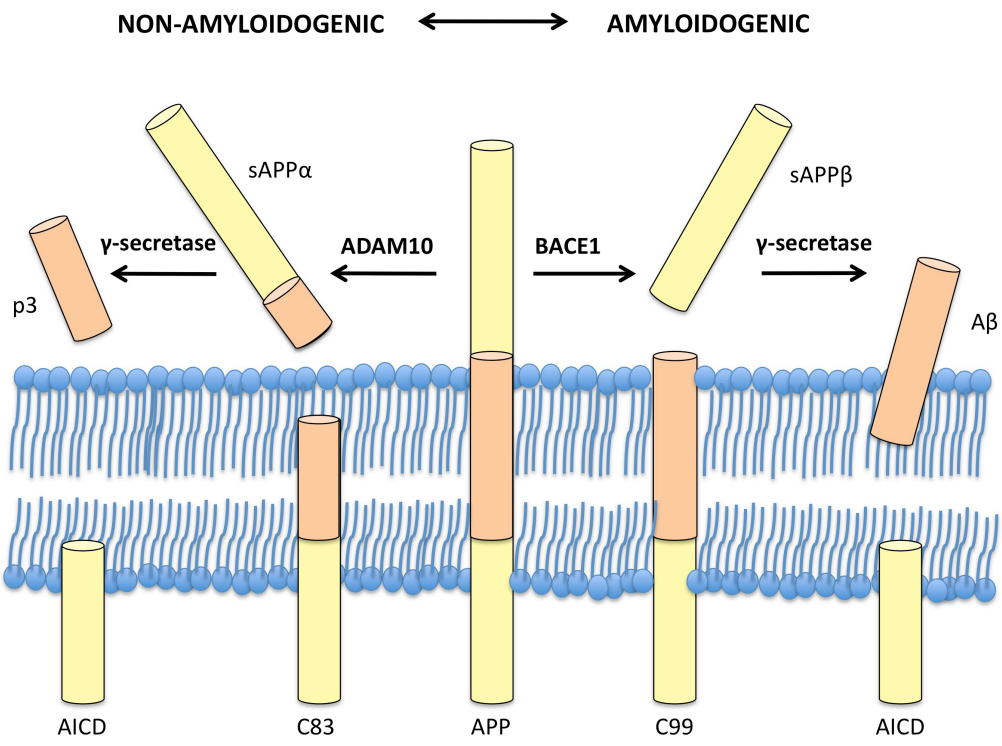

Figure 3 "APP processing pathways" APP can be processed via the non-amyloidogenic pathway, in which it is cleaved by ADAM10 within the Aβ sequence, or via the amyloidogenic pathway, in which it is cleaved sequentially by BACE1 and γ-secretase.

In the same vein, genome-wide association studies found that single nucleotide polymorphisms (SNPs) in TREM2, a gene highly expressed by microglia, are associated with an increased risk of Alzheimer's disease (Guerreiro et al., 2013; Jonsson et al., 2013). Researchers believe that TREM2 function is essential for microglia-mediated phagocytosis of Aβ, and that these SNPs represent loss of function mutations, by way of inhibiting TREM2 maturation (Kleinberger et al., 2014). Accordingly, these studies found soluble TREM2 levels to be reduced in the cerebrospinal fluid (CSF) of individuals with AD and FTD, further implicating impaired microglial phagocytosis in these neurodegenerative conditions (Kleinberger et al., 2014). Taken together, these results support the hypothesis that TREM2 function may decline with age, or in the context of neurodegenerative diseases, such as Alzheimer's.

In a reciprocal fashion, the pathology associated with Alzheimer's disease may also impair microglial phagocytosis. It has been found that oligomeric species of Aβ inhibit the phagocytosis of fibrillar species of Aβ (Pan et al., 2011). Ultimately, the vicious cycle by which microglial dysfunction leads to increased pathology, and pathology furthers this dysfunction, leaves microglia in a state of "frustrated phagocytosis," whereby these cells cannot effectively clear aggregating proteins, but exist in a chronically activated state, pumping out pro-inflammatory molecules. Studies have demonstrated that the removal of a single pro-inflammatory molecule alone can restore cognitive abilities in mouse models of AD (Kitazawa et al., 2011), suggesting that chronically activated microglia could hugely contribute to functional decline.

Expanding upon the interplay between microglia and Alzheimer's disease, there exists a link between microglial activation in response to amyloid species and the *APOE*ε4

genotype, which is the greatest known genetic risk factor for sporadic AD (Roses, 1996). Researchers co-cultured primary microglia and hippocampal neurons in a fashion that still allowed for the isolated treatment of microglia. They found that treating microglia with secreted APPα induced microglial activation and microglia-mediated neurotoxicity, and that these effects can be inhibited by the presence of APOε3, but not APOε4 (Barger and Harmon, 1997). Further analyses revealed that APOε3, but not APOε4, is capable of binding secreted APPα, likely sequestering the species in a way that prevents its activation of microglia. Thus, like missense mutations in TREM2, the presence of the APOEε4 allele represents another genetic risk factor for AD that involves microglial dysfunction.

Peripheral inflammation

Additionally, because aged microglia are primed, they can become activated by systemic inflammation. In elderly populations, it is commonly found that an infection or other source of peripheral inflammation produces deleterious cognitive effects and can even expedite decline associated with neurodegenerative conditions (Holmes et al., 2009; Trollor et al., 2012). Researchers have been able to validate this hypothetical framework by peripherally injecting LPS in mouse models of Alzheimer's and prion diseases, and observing an exaggeration of pathology, as well as behavioral decline (Combrinck et al., 2002; Lee et al., 2008). Intriguingly, studies by Dr. Tony Wyss-Coray and colleagues have found that one can rejuvenate the aged brain and improve cognition by supplying the body with young blood (Villeda et al., 2011). His studies employ a parabiosis paradigm, in which the peritoneal walls of a young and old mouse are sewn together, so that capillaries eventually grow across, and the two mice share

blood supply. Effectively, learning and memory are improved in the aged mouse, and impaired in the young mouse. It is believed that this phenomenon is mediated by circulating bloodborne factors, such as chemokines (Villeda et al., 2011). Together, these studies demonstrate the extent to which peripheral immune signaling can influence behavior and cognition, and microglia appear to be the main mediator of these effects. Through both direct and indirect mechanisms, it is clear that microglial dysfunction contributes to functional decline in the aging and diseased brain.

Brain injury

Aside from disease, microglia also regulate the brain's response to injuries, such as stroke and traumatic brain injury (TBI). TBIs are extremely common in children, the elderly, and military personnel. A paper published in 2010 found that each year in the United States, traumatic brain injuries result in over one million individuals receiving emergency room services, 235,000 requiring hospital stays, and 50,000 deaths (Corrigan et al., 2010). Critically, over 40% of Americans who experience a TBI are still disabled one year after the event, and as of 2010, over 3 million Americans were living with disability following a hospital stay for TBI (Corrigan et al., 2010). Microglial activation in certain areas of the brain is correlated with degree of cognitive impairment post-TBI, suggesting that microglia may mediate long-term cognitive disabilities associated with these types of injuries (Ramlackhansingh et al., 2011). Microglia become activated within minutes of a traumatic brain injury, phagocytose dead and dying cells, and secrete a host of pro-inflammatory molecules and reactive oxygen species. Unfortunately, research has revealed that microglia remain activated following TBI and fail to resolve neuroinflammatory insults. Indeed, using a ligand that only binds

activated microglia, researchers imaged brains of individuals that had previously experienced TBIs and found that microglia can remain activated for up to 17 years (Ramlackhansingh et al., 2011). However, while microglial activation around the injury site is believed to be detrimental to outcomes, it is hypothesized that microglial activation in other regions of the brain could promote plasticity and repair, potentially through the release of brain-derived neurotrophic factor (BDNF) (Nagamoto-Combs et al., 2007). Many of these same microglia-mediated mechanisms are in place following ischemic stroke. Stroke is the leading cause of long-term disability in the US, with about 800,000 individuals experiencing a new or recurring stroke each year (Go et al., 2014). Microglia are known to phagocytose compromised neurons following stroke, though it is possible that microglial signaling through toll-like receptors (TLR) leads to the activation of cell death pathways that result in the death of viable neurons, as well. Evidence that healthy neurons may be phagocytosed comes from studies showing that the blockade of TLR2 or TLR4 massively reduces infarct volume following stroke (Tang et al., 2007).

The activation of microglia in response to severe injuries and neurodegeneration represents a double-edged sword, in that other immune cells are recruited to help resolve the insult and dysfunctional cells are eliminated, but the production of inflammatoxic molecules is sustained, and over the long-term, contributes to neuronal death and cognitive decline. As a result, it is imperative that strategies by which microglia can be restored, or “reset” to non-activated states be investigated.

E. Microglial Elimination and Repopulation

The CSF1R is a Target for Microglial Elimination

It is well established that chronic microglia-derived inflammation is detrimental to neuronal health and cognition, but by what mechanisms, and to what degree, are not entirely known. Our lab has discovered that microglia are dependent upon signaling through the colony-stimulating factor 1 receptor in the adult brain, and that the treatment of mice with a small molecule inhibitor of CSF1R eliminates microglia throughout the central nervous system (Elmore et al., 2014). Importantly, multiple groups have since confirmed this finding (De et al., 2014; Valdearcos et al., 2014). Going forward, we will exploit this discovery in order to manipulate the microglial cellular compartment. In doing so, we hope to gain a deeper understanding of how microglia contribute to cognitive deficits, and to ultimately develop therapeutics aimed at improving functional outcomes in many human conditions, including neurodegeneration and severe brain injuries.

CSF1R is a receptor tyrosine kinase, expressed by cells of myeloid origin in the periphery, including monocytes, tissue macrophages, and Langerhans cells (Hamilton et al., 2008; Wang et al., 2012). Microglia are the only cell type in the CNS to express this receptor under homeostatic conditions, and so inhibition of CSF1R in the brain represents a directed and specific approach to studying microglial functions (Erblich et al., 2011). CSF1R is critical for the expansion and differentiation of many hematopoietic precursor cells, including microglia. Mutations in this gene result in hereditary diffuse leukoencephalopathy with spheroids (HDLS), a rare neurological condition in humans that causes white matter lesions, personality changes, and severe cognitive and motor

deficits (Hamilton et al., 2008; Rademakers et al., 2012). Mice homozygous null for CSF1R are almost entirely devoid of microglia during embryonic development and the postnatal period, with many dying by six weeks of age and almost none reaching adulthood (Dai et al., 2002; Erblich et al., 2011). These mice are small, underweight, toothless, and exhibit skeletal abnormalities, as well as strongly reduced fertility (Dai et al., 2002). Moreover, they have lower numbers of monocytes and lymphocytes in circulating blood, as well as reduced tissue macrophages, compared to WT mice (Dai et al., 2002). Colony-stimulating factor 1 (CSF1) and the more recently discovered IL-34 (Lin et al., 2008) are the two known ligands for CSF1R, and mice entirely deficient for either of these ligands exhibit reduced microglial densities, rather than a complete absence of microglia, as found in CSF1R KO mice (Wiktor-Jedrzejczak et al., 1990; Wang et al., 2012). Conversely, overexpression of CSF1 in the glial fibrillary acidic protein (GFAP)-expressing cellular compartment of mice increases microglial numbers and proliferation rates (De et al., 2014).

PLX3397 and PLX5622 are orally bioavailable CSF1R/c-Kit and CSF1-R inhibitors, respectively, created by Plexxikon, Inc. In our lab, we treated adult C57Bl/6 mice with 290 mg/kg PLX3397 for 21 days to deplete microglia, and found that this treatment eliminated >99% of cells, as quantified by immunohistochemical staining with the IBA1 microglial marker and subsequent computer analysis (Elmore et al., 2014). Furthermore, we can treat mice for longer periods of time—days, weeks, or months—and microglia remain eliminated for the duration of treatment. It is important to note that myeloid cells in the periphery are not depleted with PLX3397 treatment (Chitu et al., 2012; Coniglio et al., 2012; He et al., 2012; Prada et al., 2013; Abou-Khalil et al., 2014;

Mok et al., 2014). Additionally, a recent study using PLX5622, an analog of PLX3397, demonstrated that circulating leukocyte cell numbers are unchanged with treatment (Valdearcos et al., 2014).

Microglia Repopulate as a Result of CSF1R Inhibitor Withdrawal

Remarkably, we also found that withdrawal of treatment stimulates brain-wide repopulation with microglial progenitors that appear as $Ki67^{+}$, $nestin^{+}$, $IBA1^{-}$ cells that divide rapidly 1-2 days after treatment cessation (Elmore et al., 2014). These newly repopulating cells stop expressing Ki67 and nestin within a few days, and instead, begin expressing typical microglial markers including CX3CR1, IBA1, Tmem119, Siglech, and TREM2 (Elmore et al., 2014). Critically, these repopulating cells respond to LPS by upregulating a variety of inflammation-related genes, just as resident microglia do (Elmore, 2015). Finally, repopulated microglia achieve numbers and morphology identical to that of untreated mouse brains within 21 days of inhibitor withdrawal, highlighting the ability of the brain to tightly and accurately regulate microglial numbers and spacing (Elmore, 2015). Representative pictures of mouse brains that have been depleted of, and repopulated with, microglia are shown in Figure 4. Microglia were identified by their immunoreactivity for the IBA1 marker, as indicated by white dots in A-C and by green immunofluorescence in D-F.

Surprisingly, we have depleted healthy mice of microglia for up to three months, and found no negative effects on behavior or cognition. In fact, mice treated with PLX3397 for two months performed significantly better on the Barnes maze, a measure of learning and memory, compared to microglia-intact mice (Figure 5) (Elmore et al., 2014). Having determined that microglial elimination is not deleterious, but can even be

beneficial for behavior and cognition, we sought to determine if microglia in disease/injury settings are also dependent on CSF1R signaling, and if so, if microglial elimination or repopulation, particularly following severe neuronal insult, could improve functional recovery and inform us about the roles of this cellular population in the brain. The results of these studies, as described in my dissertation, can inform us if microglial manipulation represents a viable therapeutic option in the treatment of many neurological insults.

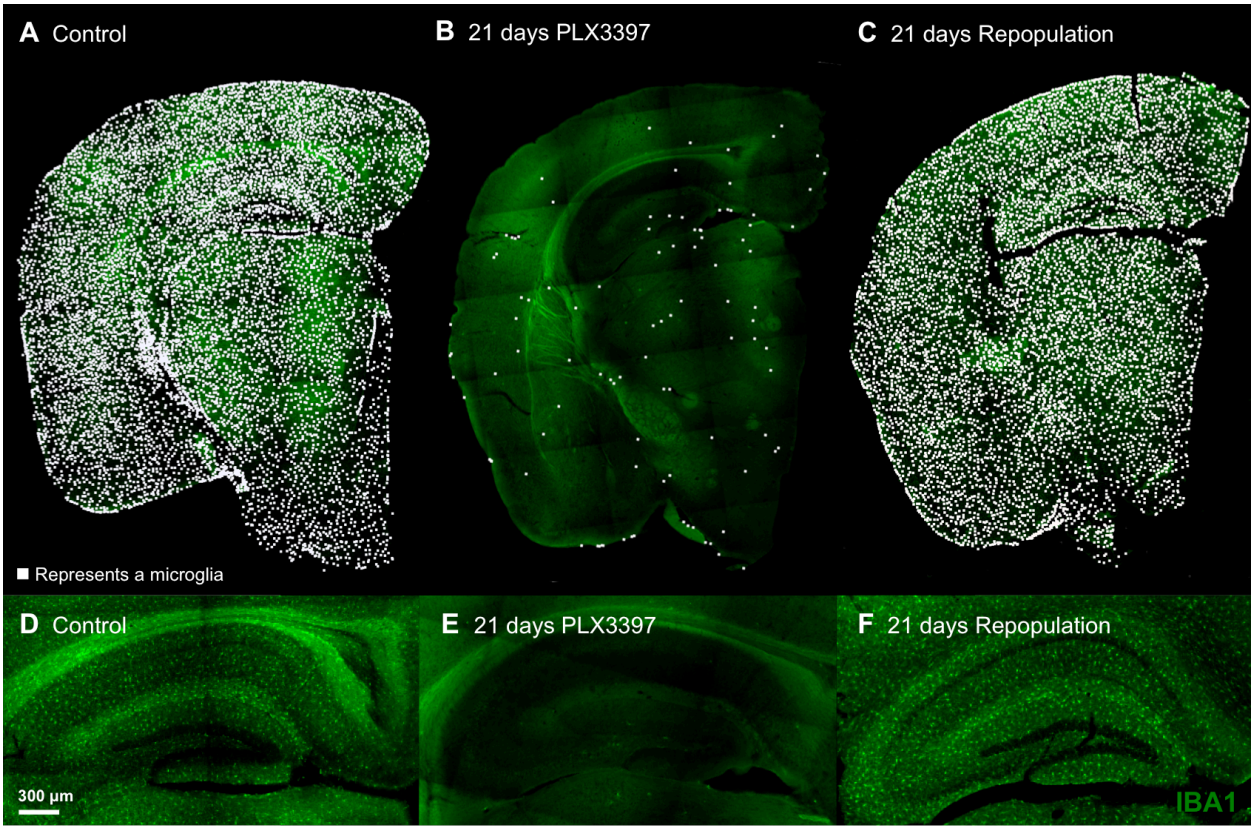

Figure 4 "Elimination of Microglia in the Adult CNS Using CSF1R Inhibition, Followed by Repopulation with New Cells" from Elmore *et al*., Copyright 2015.

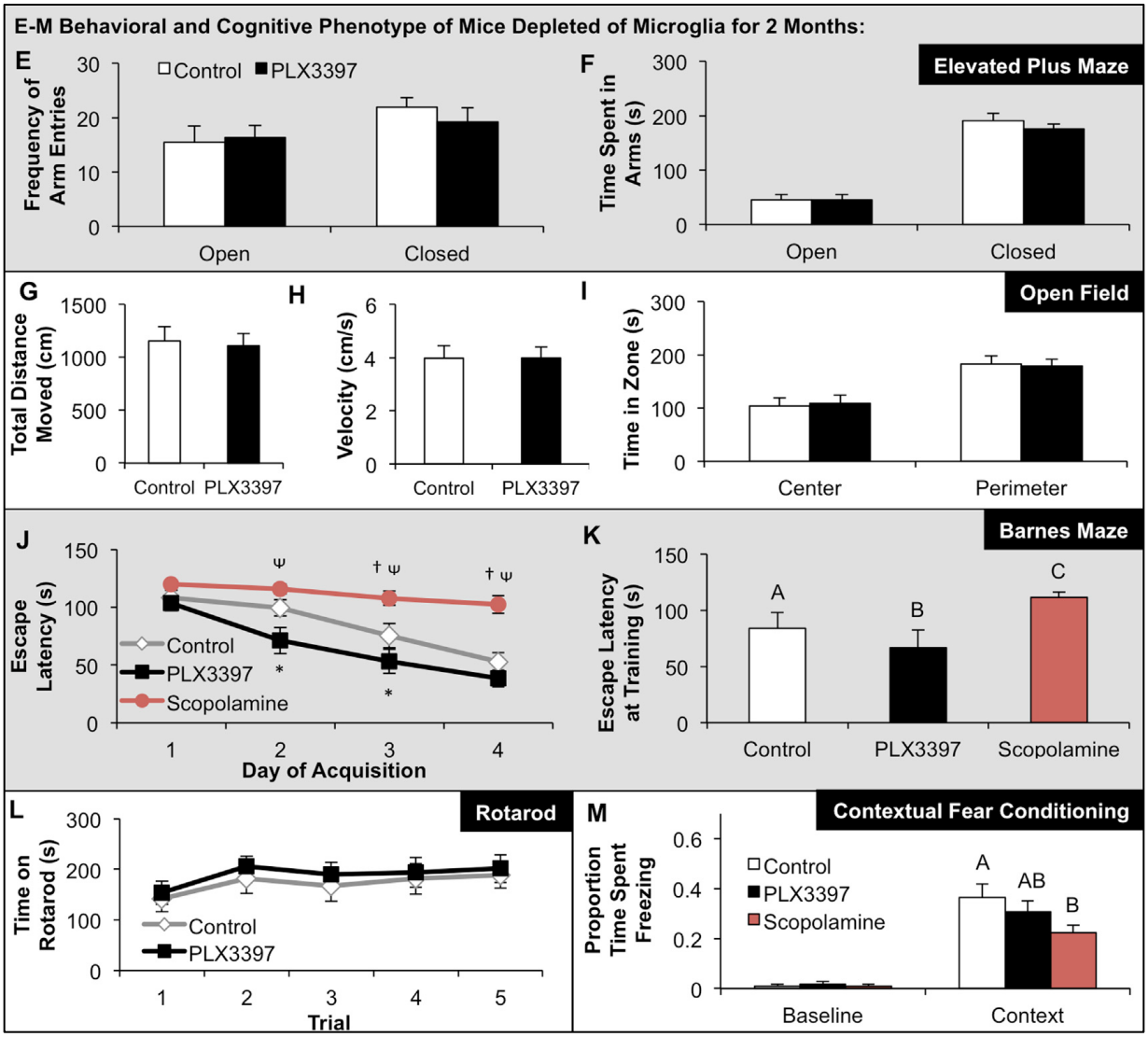

Figure 5 "CSF1R Inhibition Reduces Microglial Markers and Numbers, but Does Not Affect Brain Volume, Cognition, or Motor Function" from Elmore *et al.*, Copyright 2014. Available at: http://www.sciencedirect.com/science/article/pii/S0896627314001718

CHAPTER ONE

MICROGLIAL ELIMINATION IMPROVES FUNCTIONAL RECOVERY FOLLOWING EXTENSIVE NEURONAL LOSS

INTRODUCTION

Microglia are the primary immune cell of the central nervous system (CNS) and represent the first line of defense against pathogens, comprising about 10% of cells in the brain (Pessac et al., 2001). They exist in a quiescent state, whereby they constantly survey the local environment for any infectious agents or cellular debris (Nimmerjahn et al., 2005). The presence of such initiates a cascade of events culminating in the physical and chemical remodeling of microglia into a spectrum of "activated" states designed to attack pathogens and clear debris, through the production of pro-inflammatory cytokines such as TNF-α, IL-1β, and IL-6 (Renno et al., 1995; Liu et al., 1998). Finally, microglia take on an anti-inflammatory role, secreting molecules such as IL-4 and IL-10 as part of the resolution and repair process, before returning to a surveillant state (Colton and Wilcock, 2010).

We have recently shown that microglia in the healthy adult brain are fully and uniquely dependent upon signaling through the colony-stimulating factor 1 receptor (CSF1R), and that administration of the CSF1R/c-kit inhibitor PLX3397 leads to the rapid elimination of >95% of all microglia within 7-21 days (Elmore et al., 2014). This approach provides us with a useful tool to directly study microglial functions, as microglia are the only cell type to express CSF1R under normal conditions in the adult brain (Erblich et al., 2011). Microglia are negatively implicated in most neurodegenerative disorders and brain injuries, where they mount neuroinflammatory

responses that are never, or poorly, resolved. As an example, it has been shown that patients who suffered a traumatic brain injury (TBI) have substantially activated microglia 17 years later (Ramlackhansingh et al., 2011). Moreover, the targeting of certain pro-inflammatory molecules alone, such as IL-1β or TNF-α, can improve cognitive deficits associated with Alzheimer's disease (Tobinick and Gross, 2008; Kitazawa et al., 2011). Thus, it is essential to determine if chronically activated microglia are also dependent upon CSF1R signaling, and so can be eliminated with CSF1R inhibitors, allowing for the direct roles of microglia in disease and injury states to be explored.

MATERIALS AND METHODS

Compounds

PLX3397 was provided by Plexxikon, Inc. and formulated in standard chow by Research Diets Inc. at 290 mg/kg. Doxycycline was provided in standard chow by Research Diets Inc. at 2000 mg/kg, or by researchers in deionized drinking water at 2 mg/ml (Sigma-Aldrich, St. Louis, MO) with 5% sucrose. Kainic acid (Sigma-Aldrich) was solubilized in PBS and delivered via intraperitoneal (IP) injection at 10 mg/kg.

Animal Treatments

All rodent experiments were performed in accordance with animal protocols approved by the Institutional Animal Care and Use Committee at the University of California, Irvine. The CaM/Tet-DT_A mouse model of inducible neuronal loss was employed for functional studies, and has been previously described (Yamasaki et al.). Triple transgenic GFP-CaM/Tet mice were used for experiments involving dendritic spine

analyses, and have been previously described (Castello et al., 2014). 5-8 month-old male and female mice were maintained from birth on doxycycline chow. Upon induction of the 25-day lesion period, doxycycline chow was replaced with standard chow. To cease expression of DT_A, doxycycline was provided in drinking water, and control or PLX3397 chow was provided for the final four weeks. Behavioral tasks were performed during the final week of the study. At the conclusion of experiments, mice were sacrificed via lethal IP injection of Euthasol and perfused transcardially with 1X phosphate-buffered saline (PBS). Brains were extracted and dissected down the midline, with one half flash-frozen on dry ice for subsequent RNA and protein analyses, and the other half drop-fixed in 4% paraformaldehyde (PFA) in 1X PBS. Fixed brains were cryopreserved in a 30% sucrose solution, frozen, and sectioned at 40 μm on a Leica SM2000 R sliding microtome for subsequent immunohistochemical analyses.

For kainic acid (KA) experiments, 7-9 month-old Thy1-GFP-M mice (Jackson Laboratories) were fed either control chow or PLX3397-formulated chow for 21 days and then administered either 100 μl sterile PBS or 10 mg/kg of kainic acid dissolved in 100 μl sterile PBS via IP injection and monitored until behavior returned to normal (n=5).

Immunohistochemistry

Fluorescent immunolabeling followed a standard indirect technique (primary antibody followed by fluorescent secondary antibody), as previously described (Neely et al., 2011). Primary antibodies used include NeuN (1:1000; Abcam, Cambridge, MA), IBA1 (1:1000; Wako, Richmond, VA), GFAP (1:10,000; Abcam), 4D4 (1:5000; gifted by Dr. Oleg Butovsky), synaptophysin (1:500; Sigma-Aldrich), PSD95 (1:1000; Cell Signaling, Danvers, MA). The size of microglia cell bodies, PSD95 puncta, and synaptophysin

puncta was determined using the surface module in Imaris 7.5 software. Numbers of microglia, astrocytes, PSD95 puncta, and synaptophysin puncta were determined using the spots module in Imaris 7.5 software.

Evans Blue Analysis

Doxycycline was withdrawn from the diet of mice for 25 days to induce a neuronal lesion. Evans Blue analysis was performed as previously described (Elmore et al., 2014). Total Evans blue content was measured by absorbance at 595 nm, with an uninjected animal serving as a blank control.

Stereology

Cresyl Violet staining was performed on fixed tissue and neurons in the CA1 region were counted via stereological analysis, as previously described (Myczek et al., 2014).

Behavioral testing

Mouse cognition and behavior were evaluated on open field test (Elmore et al., 2014), elevated plus maze (Elmore et al., 2014), and Morris water maze (Baglietto-Vargas et al., 2013), in that order, as previously described. For kainic acid experiments, mice were scored on a scale from 0-7, with 0 being normal and 7 being death (Morrison et al., 1996). Scores were made every 5 minutes for 90 minutes by two blinded experimenters, and averaged between them.

mRNA Extraction and qPCR

RNA was extracted and purified from microdissected hippocampi of frozen half brains, then real-time PCR performed with Taqman Array Mouse Immune Panel cards (Thermo Fisher Scientific, USA), as per manufacturers instructions. Values were calculated as delta-delta-Ct, as previously described (Elmore et al., 2014).

Dendritic Spine Analyses

For all mice harboring Thy1-GFP-M, five non-primary apical dendrites in the CA1 of the hippocampus were imaged on a Leica DM2500 confocal microscope with 63X oil-objective and 5X digital zoom. Dendrites were also imaged in Layer 5 of cortical area V1 in CaM/Tet-GFP mice. Z-stacks of equal depth were obtained for each dendrite, deconvolved using Huygens deconvolution software, and max projections created. From the max projections, two researchers independently counted and classified spines using the Cell Counter plug-in in ImageJ software. Spine classification was based on previous literature in the field employing head-to-neck ratio (Peters and Kaiserman-Abramof, 1970). Finally, the total number of each type of spine was calculated per 10 μm of dendrite length.

Electrophysiological Analyses

Electrophysiological recordings and photostimulation were performed as in references (Xu and Callaway, 2009; Xu et al., 2010; Olivas et al., 2012; Kuhlman et al., 2013). Three-week old mice were treated for 4 weeks with control chow or PLX3397-formulated chow to deplete microglia and mice were sacrificed (n=3-4). Vehicle- and drug-treated animals were deeply anesthetized using pentobarbital sodium (100 mg/kg, IP) and transcardially perfused with chilled oxygenated artificial cerebrospinal fluid (ACSF) with the broad-spectrum excitatory amino acid antagonist kynurenic acid (KYA, 0.3 mM). Brains were extracted; visual cortical sections of 400 μm were made with a vibratome (VT1200S, Leica Systems) using the KYA-containing ACSF. Slices were rinsed with KYA with normal ACSF before being transferred into slice recording chambers. Whole-cell recordings were performed under a DIC/fluorescent Olympus

microscope (BX51WI). Slices were examined under a 4X objective for proper targeting of Layer 5 V1 neurons. To perform whole-cell recording, individual neurons were visualized at high magnification (60X objective), and patched with glass electrodes of 4–6 MΩ resistance filled with K^+ containing internal solution. Electrodes also contain 0.1% biocytin for post-hoc cell labeling and further morphological identification. Once stable, whole-cell recordings were achieved with good access resistance (< 30 MΩ), and basic electrophysiological properties were examined through hyperpolarizing and depolarizing current injections. Resting membrane potentials, input resistance, and membrane capacitance, as well as spiking patterns, were all measured. To measure spontaneous EPSC inputs, the recorded neuron was held at -70 mV in voltage clamp mode and the data of spontaneous traces was acquired over 10 minutes. During laser scanning photostimulation (LSPS) experiments, the microscope objective was switched from 60X to 4X. Stock solution of MNI-caged-l-glutamate (Tocris Bioscience, Ellisville, MO) was added to 20 ml of ACSF for a concentration of 0.2 mM caged glutamate. The cortical slice image was acquired by a high resolution digital CCD camera, which in turn was used for guiding and registering photostimulation sites. Focal laser spots approximate a Gaussian profile with a lateral width of 100 μm. Under our experimental conditions, LSPS-evoked action potentials were recorded from stimulation locations within ~100 μm of targeted somata in mouse V1 and occurred within 150 ms after photostimulation. Synaptic currents in patched neurons were detected under voltage clamp. By systematically surveying synaptic inputs from hundreds of different sites across a large cortical region, aggregate synaptic input maps were generated for individual neurons.

Statistics

Unless otherwise specified, two-way ANOVAs were employed to analyze differences between all four groups of mice. Holm-Sidak or Tukey-Kramer post-hoc analyses yielded multiple comparisons and are shown if $p<0.05$, regardless of the p value of the interaction, as determined by two-way ANOVA. Results are presented as average± standard error of the mean (SEM). Significance is defined as $p<0.05$. The following symbols are used to denote significant differences between groups, as obtained by post-hoc analyses: † Control vs. PLX3397; * Control vs. Lesion; ϕ PLX3397 vs. Lesion + PLX3397; # Lesion vs. Lesion + PLX3397.

For the kainic acid experiment, data were log transformed and repeated measures ANOVA was employed compare Control and PLX3397 groups.

For photostimulation data analysis, the amplitudes, frequencies and onset latencies of EPSCs or IPSCs from the recorded cells were measured for each stimulation site using custom-developed Matlab software (Shi et al., 2010). Laminar input patterns and source distributions were quantified. Averaged maps were analyzed using the 4X DIC image to bin responses according to laminar cytoarchitectonic landmarks. Synaptic events were binned from locations spanning ± 200 μm tangential to the targeted soma location and from the top of layer 2/3 to the bottom of layer 6 across the radial vector. Data were plotted as either the average integrated EPSCs amplitude per pixel location or the number of EPSCs detected per pixel location. Statistical comparisons of the measurements across age groups were made using Kruskal–Wallis test (nonparametric one-way ANOVA) and the Mann–Whitney U test for group comparisons. Alpha levels of $p \leq 0.05$ were considered significant.

RESULTS

Activated microglia are dependent upon signaling through the CSF1R

We first set out to determine if chronically activated microglia are dependent upon CSF1R signaling, as these cells are in the healthy brain (Elmore et al., 2014). To make this disease- and injury- relevant, we utilized a tetracycline-off inducible double transgenic system, in which we can control the expression of DT_A in forebrain neurons (CaM/Tet-DT_A mice; (Yamasaki et al., 2007)), as shown in Figure 1.1 A, and chose to treat animals with PLX3397, a CSF1R/c-kit antagonist, after the lesioning period. Withdrawal of doxycycline from the diet of adult mice induces expression of DT_A, a potent cytotoxin for eukaryotic cells (Kochi and Collier, 1993), resulting in neuronal death, initially within the CA1 region (Yamasaki et al., 2007). Readministration of doxycycline 25 days later prevents any further neuronal loss, and results in a robust loss of CA1 neurons (as previously quantified by stereological methods) and marked behavioral deficits (Yamasaki et al., 2007).

Double transgenic mice (CaM/Tet-DT_A) were established by crossing TRE-DT_A mice (Lee et al., 1998) with CaMKIIα-tTA mice (Mayford et al., 1996). In this paradigm, single transgenic TRE-DT_A mice were generated to serve as nonlesioning controls, as they lack the CaMKIIα-tTA transgene and therefore cannot produce DT_A. Adult CaM/Tet-DT_A mice were divided into four age- and sex-balanced experimental groups: 1) Nonlesioned mice that received control chow (“Control”; n=8 mice/group); 2) Nonlesioned mice that received PLX3397 chow (“PLX3397”; n=8 mice/group); 3) Lesioned mice that received control chow (“Lesion”; n=10 mice/group); and 4) Lesioned mice that received PLX3397 chow (“Lesion + PLX3397”; n=10 mice/group) (Figure 1.1 A-B). Mice that underwent

lesioning had significant neuronal loss in the CA1 and stratum radiatum, as measured by layer thickness after staining for NeuN (Figure 1.1 E).

Four weeks post-lesion, immunostaining for microglia with the marker IBA1 revealed robust increases in microglial densities with lesion alone – numbers in the hippocampal region were 207% that of control animals (Figure 1.1 C and F). Both nonlesioned and lesioned mice treated with the CSF1R inhibitor PLX3397 for 4 weeks had 70-80% of $IBA1^+$ cells eliminated compared to control mice (Figures 1.1 C and F), consistent with our previous findings. Additionally, the body size of $IBA1^+$ cells was increased by approximately 80% in both PLX3397 treated groups of mice, consistent with our previous observations (Elmore et al., 2014), while astrocyte number was significantly increased only in the Lesion + PLX3397 group (Figures 1.1 G-J).

Figure 1.1 Lesion-induced activation does not affect dependence on CSF1R signaling for survival of microglia: 5-8 month-old CaM/Tet mice (C57Bl/6-CBA mix) underwent a 25-day neuronal lesion and subsequent microglial elimination via treatment with 290 mg/kg PLX3397. ***A, B,*** Schematics of CaM/Tet mouse model of inducible neuronal loss and experimental design. ***C-D,*** Thickness of the CA1 layer significantly decreased with lesion (via two-way ANOVA, main effect of lesion, $p<0.0001$, interaction, $p=0.0151$). ***F,*** Number of microglia increases more than 200% with lesion, but subsequent PLX3397 treatment eliminates >85% of all cells. ***G, H,*** Representative 63X IBA1 immunofluorescent staining from the hippocampal region reveals increased cell body size with lesion. ***I, J,*** 10X GFAP immunofluorescent staining of CA1 and dentate gyrus reveals increase in $GFAP^+$ cells in Lesion + PLX3397. Symbols denote significant differences between groups ($p<0.05$): † Control vs. PLX3397; * Control vs. Lesion; ϕ PLX3397 vs. Lesion + PLX3397; # Lesion vs. Lesion + PLX3397. Error bars indicate SEM, (n=7-10). S. oriens, stratum oriens; CA, cornus ammonis; S. Rad., stratum radiatum; S. l-m, stratum lacunosum moleculare; L. mol., molecular layer; GC, granule cell; DG, dentate gyrus.

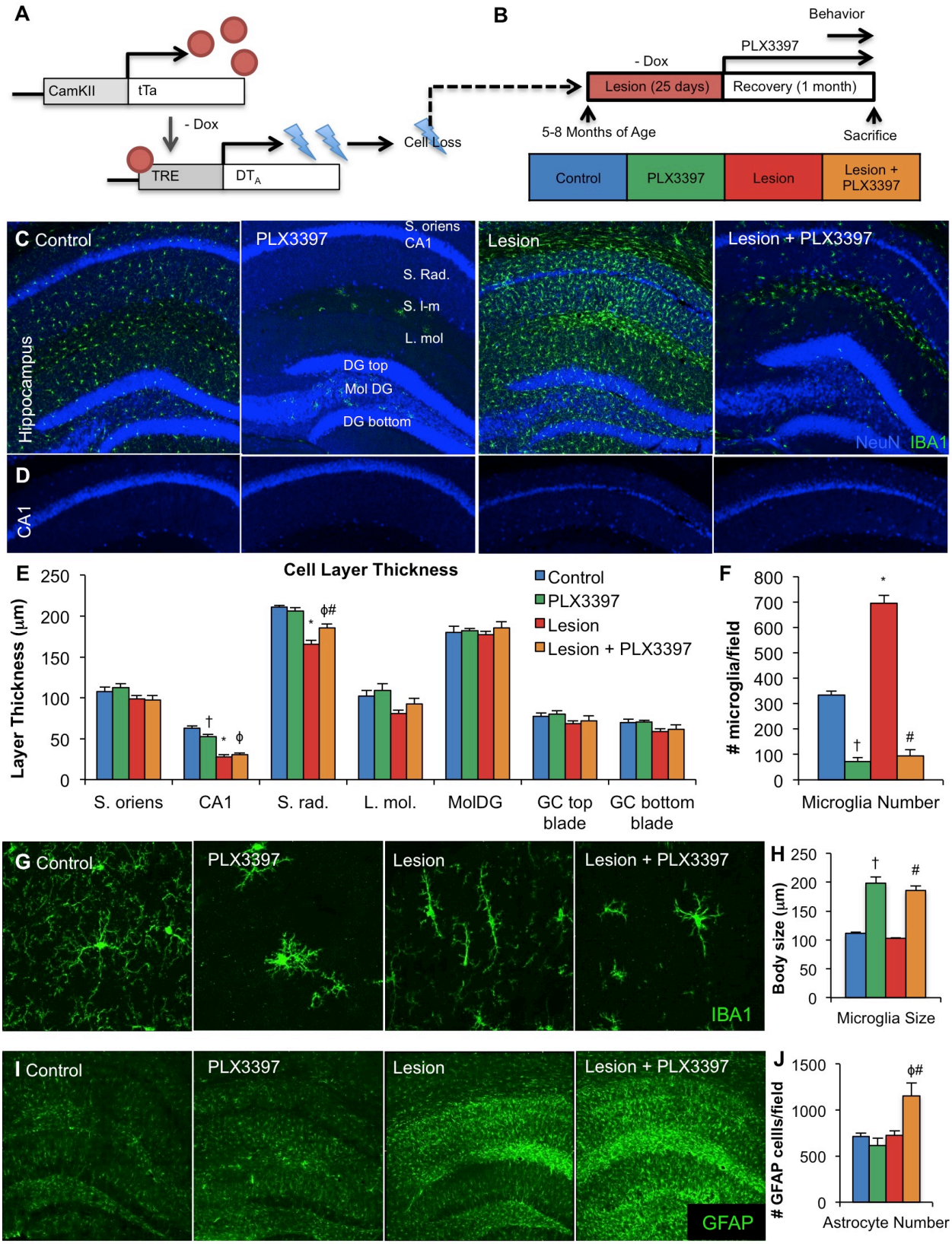
A
CamKII
tTa
- Dox
TRE
DT A
Cell Loss
B
Behavior
PLX3397
- Dox
Lesion (25 days)
Recovery (1 month)
5-8 Months of Age
Sacrifice
Control
PLX3397
Lesion
Lesion + PLX3397
C Control
PLX3397
Lesion
Lesion + PLX3397
S. oriens
CA1
S. Rad.
S. l-m
L. mol
DG top
Mol DG
DG bottom
Hippocampus
NeuN IBA1
D
CA1
E
Cell Layer Thickness
Layer Thickness (µm)
Control
PLX3397
Lesion
Lesion + PLX3397
S. oriens
CA1
S. rad.
L. mol.
MolDG
GC top blade
GC bottom blade
F
microglia/field
Microglia Number
G Control
PLX3397
Lesion
Lesion + PLX3397
IBA1
H
Body size (µm)
Microglia Size
I Control
PLX3397
Lesion
Lesion + PLX3397
GFAP
J
GFAP cellls/field
Astrocyte Number

The blood brain barrier is not compromised by neuronal lesioning

Brain insults such as multiple sclerosis, TBI, and stroke are known to compromise the blood brain barrier, resulting in the infiltration of peripheral cells (Minagar and Alexander, 2003; Chodobski et al., 2011; Yang and Rosenberg, 2011). We therefore wanted to determine if our lesion induced such changes. We withdrew doxycycline from the diet of mice harboring only the Tet-DT_A transgene (n=3) or mice harboring both the CaMKIIα and Tet-DT_A transgenes (n=4) for 25 days to induce a lesion in the bitransgenic mice. The single transgenic mice served as non-lesioning controls. On the 25^{th} day of lesioning, all but one bitransgenic mouse were injected with a solution of Evans Blue dye to probe for blood brain barrier permeability. By visual determination, none of the brains appeared to exhibit leakage of Evans Blue (Figure 1.2). Further quantification was made by homogenizing the brain, spleen, and liver tissue to extract the dye and measuring absorbance at 595 nm. Again, no detectable Evans Blue was found in any of the brains, although the peripheral organs displayed high levels of absorbance, as would be expected (Figure 1.2). Moreover, there were no statistical differences in Evans Blue content in peripheral tissues between the Control and Lesion mice. From this result, we conclude that this 25-day neuronal lesion does not compromise the blood brain barrier. Despite this finding that the blood brain barrier remained intact, we still wanted to determine if the larger $IBA1^+$ cells we observed were microglia or circulating monocytes/macrophages. To do so, we analyzed immunoreactivity for 4D4, an antibody that binds only to microglia of CNS origin, regardless of inflammation state (Butovsky et al., 2012). We found virtually all $IBA1^+$ cells to also be $4D4^+$ in all four groups of mice (Figure 1.3). Thus, the majority of $IBA1^+$

cells depend on CSF1R signaling for survival following a hippocampal lesion, and these remaining cells appear to be microglia that have escaped elimination, and not monocytes or macrophages.

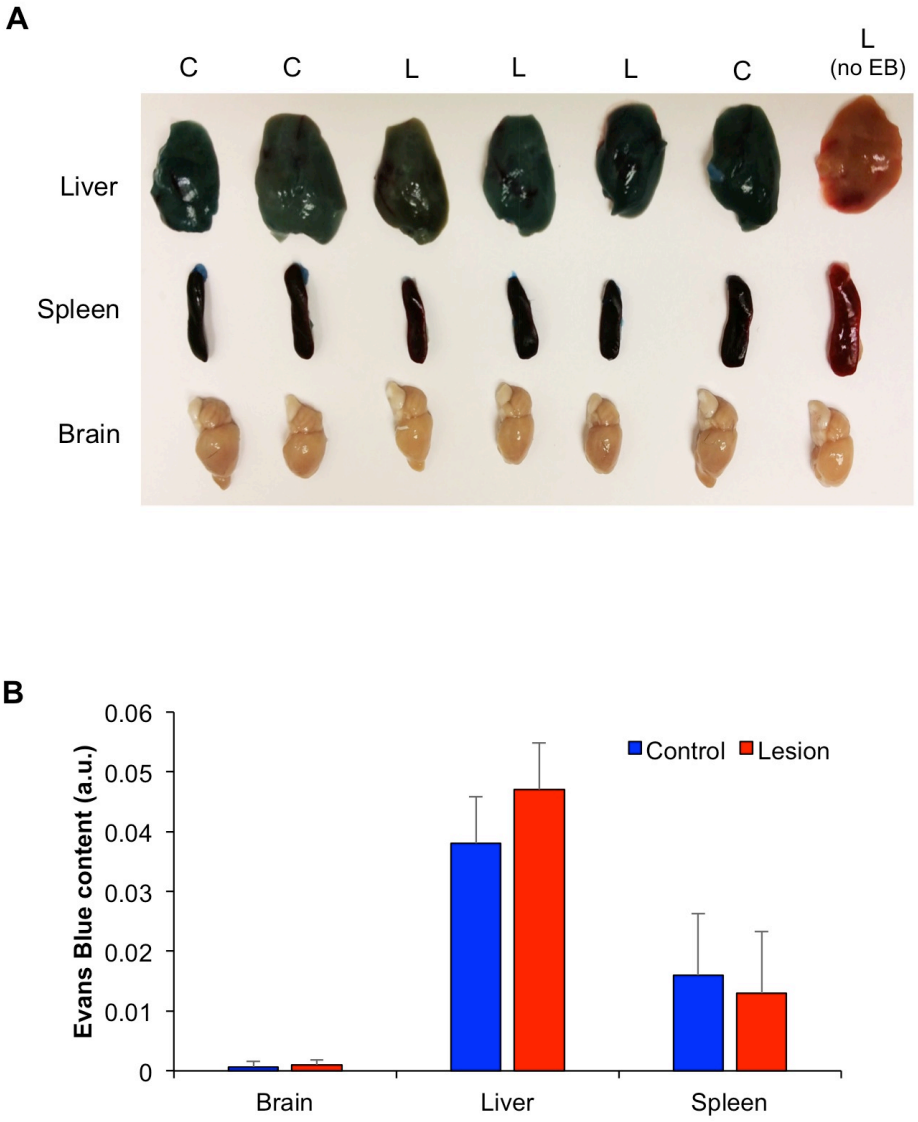

Figure 1.2 Neuronal lesioning does not compromise the blood brain barrier: ***A,*** Pictures of brain, spleen, and liver from Control mice (C) and Lesion mice (M). ***B,*** Evans Blue content was measured by absorbance at 595 nm and found only to be present in liver and spleen samples.

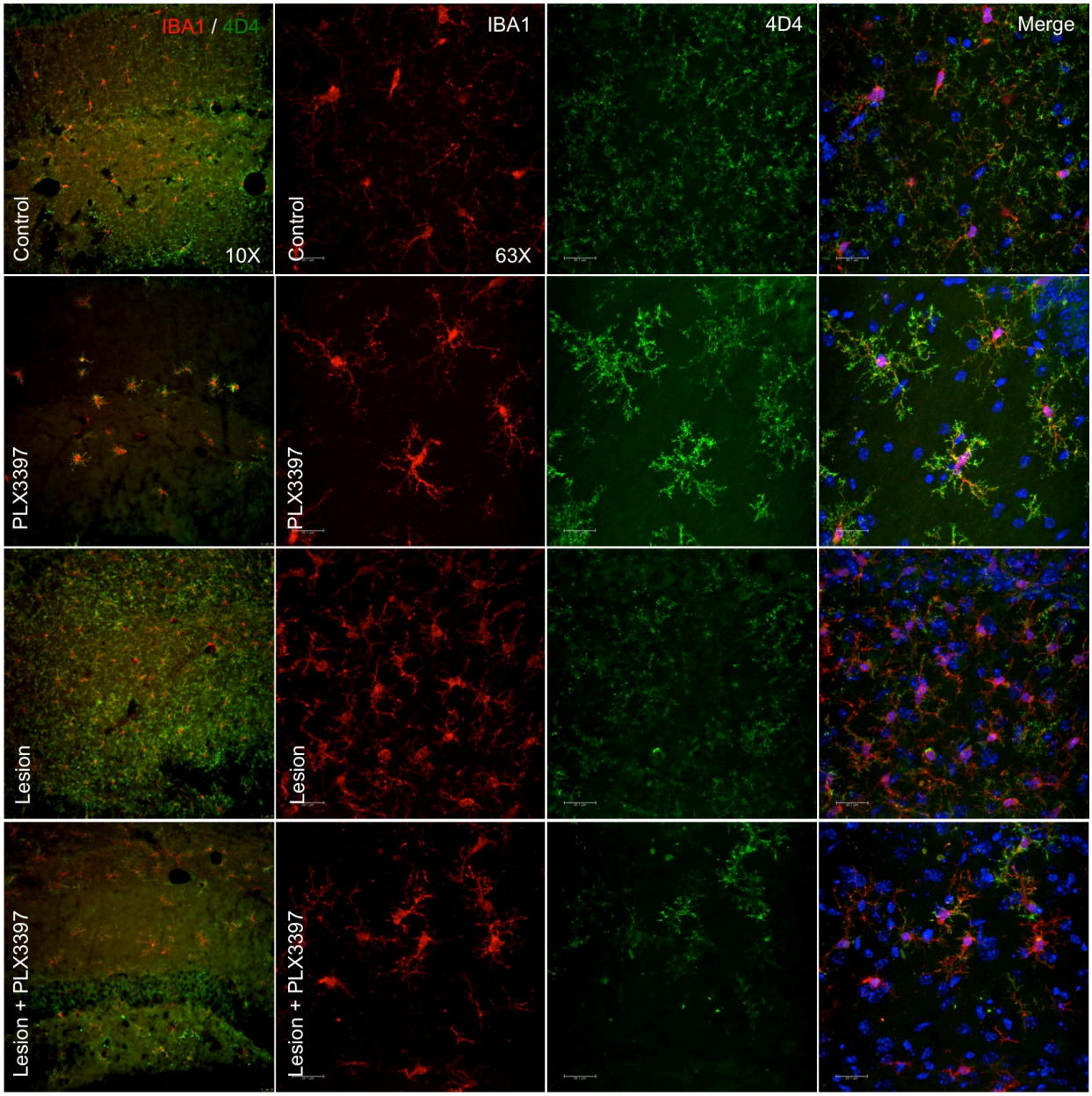

Figure 1.3 IBA1^{+} cells stain positive for CNS-derived microglia marker 4D4: ***A,*** 10X representative images of staining for IBA1 (red), 4D4 (green), and DAPI (far-red) in the hippocampus of mice. ***B,*** 63X representative images of IBA1 (red) immunoreactivity in the hippocampus. ***C,*** 63X representative images of 4D4 (green) immunoreactivity in the hippocampus. ***D,*** 63X representative, merged images of immunoreactivity for IBA1 (red), 4D4 (green), and DAPI (far-red). Co-localization of IBA1 and 4D4 immunoreactivity reveals IBA1^{+} cells to be indigenous microglia.

Immune profiling of the lesioned and microglia-depleted brain

In order to explore how microglial elimination affects the brain post-lesion, mRNA was extracted from frozen microdissected hippocampi from four mice from each group, converted to cDNA, and then analyzed against a panel of 86 immune-related genes (Figures 1.5 A-F). Of the 86 immune-related genes, 60 reached detection threshold levels and are reported here. Lesioned mice had significant increases in mRNA expression levels for cytokine-related molecules IL15, IL1α, and SOCS1, pro-inflammatory molecules B2M and BAX, the chemokine CCL19, as well as microglia/monocyte-related genes CCR2, CD80, CD86, H2EB1, and PTPRC. Critically, microglial elimination after lesioning (Lesion + PLX3397) significantly reduced levels of each of these transcripts to that of control (as indicated by the dashed line at 100%), or lower. Levels for TNFα were below threshold detection levels for all groups.

Figure 1.4 Hippocampal RNA profiling reveals lesion-induced inflammation: ***A,*** *Il-15*, *Il-1a*, and *Socs1* were significantly increased in Lesion, compared to Control. *Il-15*, *Il-18*, *Il-1a*, *Il-6*, and *Socs1* are reduced in Lesion + PLX3397, compared to Lesion. *Il-12a*, *Stat3*, and *Stat6* are significantly decreased in Lesion, compared to Control. ***B,*** *B2m*, *Bcl2*, *Bcl2l1*, *Ece1*, *Fn1*, *Ski*, *Smad3*, and *Vcam* are significantly decreased in PLX3397, compared to Control. *B2m* and *Bax* levels are increased with Lesion and restored in Lesion + PLX3397, whereas *Cd34*, *Ece1*, *Ski*, *Smad3*, *Tfrc*, and *Vegf-a* are all decreased in Lesion, compared to Control. ***C,*** *Ccl19* was increased in Lesion, compared to Control, but restored in Lesion + PLX3397. ***D,*** *Col4a5*, *Nfkb2*, and *Ptgs2* are decreased in Lesion, while *Nfkb2* and *Ptgs2* levels are also decreased in PLX3397. ***E,*** *Ccr2*, *Cd80*, *Cd86*, *H2eb1*, and *Ptprc* are increased in Lesion, compared to Control, but restored in Lesion + PLX3397. *Cd4*, *Cd86*, and *H2eb1* are all significantly decreased in PLX3397. ***F,*** *Cd34* is reduced in PLX3397 and Lesion, compared to Control mice. Symbols denote significant differences between groups ($p<0.05$): † Control vs. PLX3397; * Control vs. Lesion; ϕ PLX3397 vs. Lesion + PLX3397; # Lesion vs. Lesion + PLX3397. Error bars indicate SEM, (n=4).

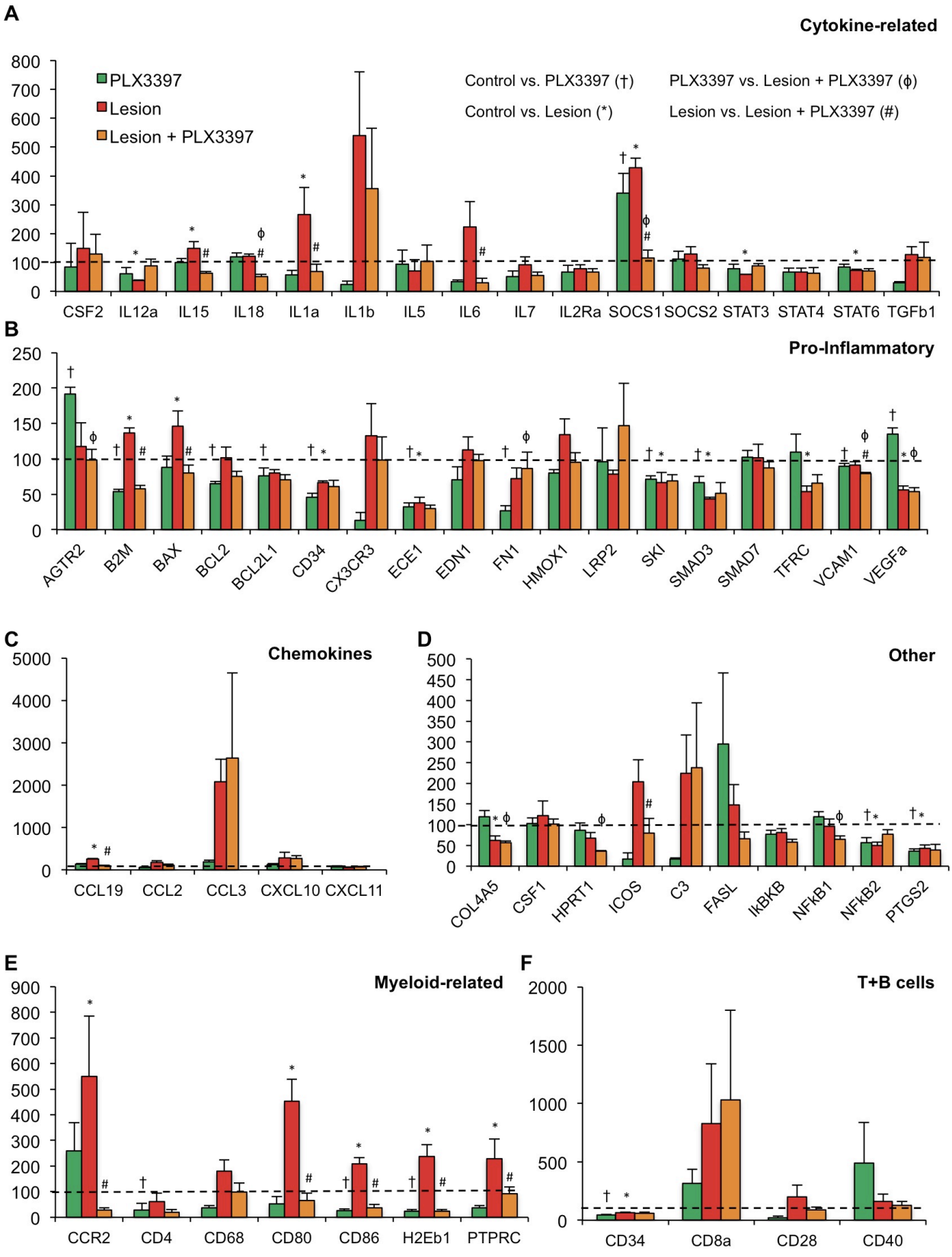
A
Cytokine-related
PLX3397
Lesion
Lesion + PLX3397
Control vs. PLX3397 (†)
Control vs. Lesion (*)
PLX3397 vs. Lesion + PLX3397 (ϕ)
Lesion vs. Lesion + PLX3397 (#)
CSF2 IL12a IL15 IL18 IL1a IL1b IL5 IL6 IL7 IL2Ra SOCS1 SOCS2 STAT3 STAT4 STAT6 TGFb1
B
Pro-Inflammatory
AGTR2 B2M BAX BCL2 BCL2L1 CD34 CX3CR3 ECE1 EDN1 FN1 HMOX1 LRP2 SKI SMAD3 SMAD7 TFRC VCAM1 VEGFa
C
Chemokines
CCL19 CCL2 CCL3 CXCL10 CXCL11
D
Other
COL4A5 CSF1 HPRT1 ICOS C3 FASL IkBKB NFkB1 NFkB2 PTGS2
E
Myeloid-related
CCR2 CD4 CD68 CD80 CD86 H2Eb1 PTPRC
F
T+B cells
CD34 CD8a CD28 CD40

Microglia elimination normalizes effects of lesion on synaptic markers

Activated microglia are implicated in synaptic surveillance and stripping following ischemia (Wake et al., 2009). Given the robust and chronic neuroinflammatory response to neuronal lesioning in our model, we wished to determine the effects of both neuronal lesioning and microglial elimination on synaptic surrogates. As microdissected hippocampi were allocated for mRNA analyses, we analyzed immunoreactivity of the pre-synaptic marker synaptophysin and the post-synaptic marker PSD95 in PFA-fixed tissue. Analyses were performed in the CA1 and stratum radiatum of the hippocampus, as these two regions demonstrated significantly thinner cell layers as a result of DT_A expression (n=7-10 mice/group). We found that PSD95 puncta number was largely decreased in the CA1 with lesion compared to Control mice, but that the elimination of microglia following lesion, via PLX3397 treatment, dampened this effect (Figure 1.5 B). Additionally, in both the CA1 and stratum radiatum, PSD95 puncta size was increased in Lesion mice. However, treatment with PLX3397 normalized puncta size in Lesion mice in both of these hippocampal regions (Figures 1.5 C and J). Lesioning also greatly increased synaptophysin puncta size and intensity in the CA1 and stratum radiatum. But again, microglial elimination in combination with lesioning normalized this effect, with size and intensity levels of synaptophysin puncta in Lesion + PLX3397 mice matching that of controls (Figures 1.5 F,G,M,N). On the whole, lesion-induced changes in both PSD95 and synaptophysin puncta were ameliorated with microglial elimination.

Figure 1.5 Neuronal lesioning induces synaptic alterations that are restored with subsequent microglial elimination: ***A,*** Representative 10X images of PSD95 and synaptophysin immunoreactivity in the CA1 region display alterations in puncta area and size. ***B-D,*** Quantification of PSD95 puncta number, area, and intensity in the CA1 shows that microglial elimination restores most lesion-induced alterations. ***E-G,*** Quantification of synaptophysin puncta number, area, and intensity in the CA1 shows lesion-induced alterations are reversed with PLX3397 treatment. **H,** Representative 10X images of PSD95 and synaptophysin immunoreactivity in the straum radiatum. ***I-K,*** Quantification of PSD95 puncta number, area, and intensity in the stratum radiatum reveals increases in puncta number with microglial elimination. ***E-G,*** Quantification of synaptophysin puncta number, area, and intensity in stratum radiatum reveal changes in puncta area and intensity with PLX3397 and/or Lesion. Symbols denote significant differences between groups ($p<0.05$): † Control vs. PLX3397; * Control vs. Lesion; ϕ PLX3397 vs. Lesion + PLX3397; # Lesion vs. Lesion + PLX3397. Error bars indicate SEM, (n=7-10).

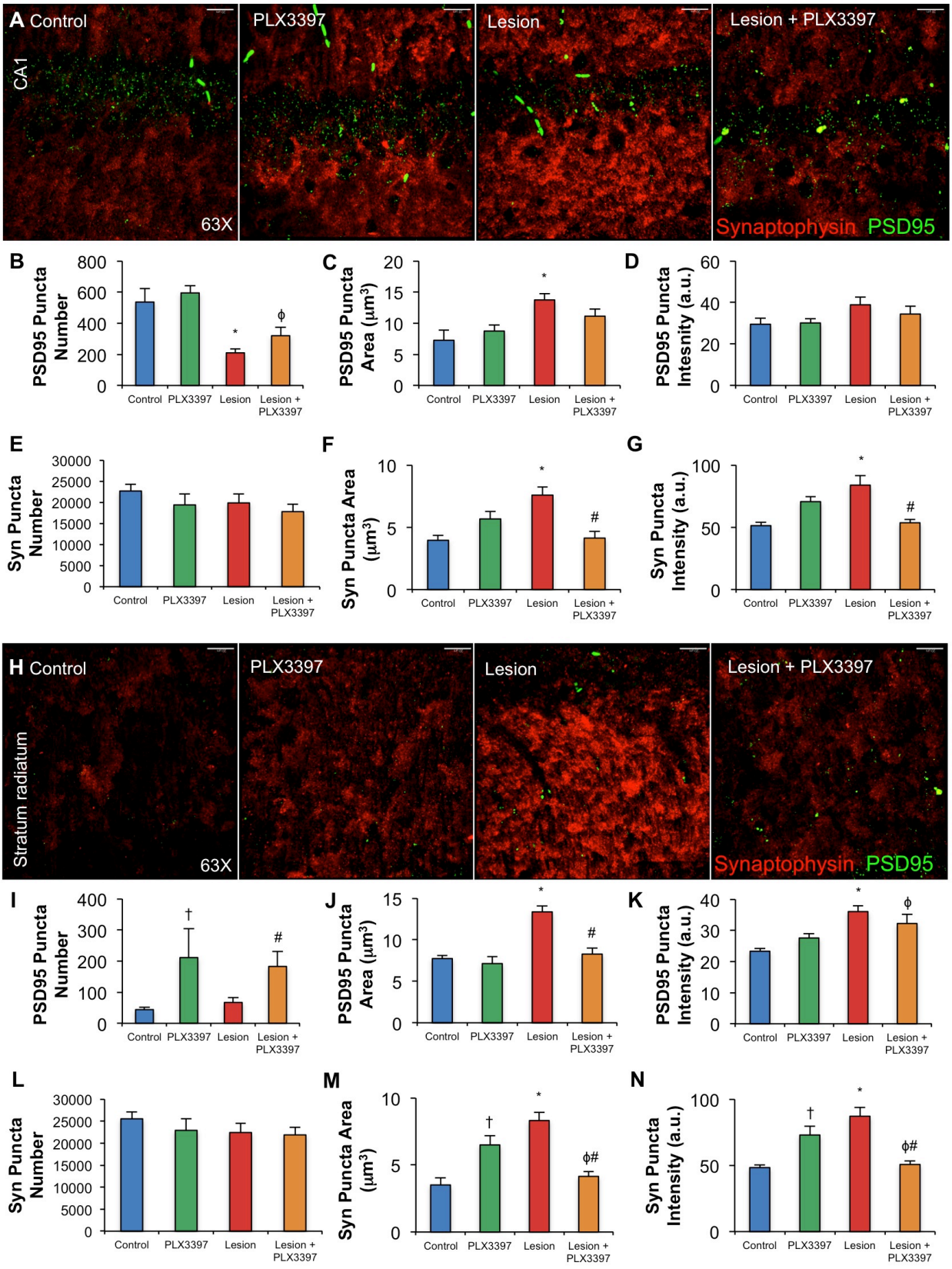
A Control
PLX3397
Lesion
Lesion + PLX3397
CA1
63X
Synaptophysin PSD95
B
PSD95 Puncta Number
C
PSD95 Puncta Area (μm³)
D
PSD95 Puncta Intesnity (a.u.)
E
Syn Puncta Number
F
Syn Puncta Area (μm³)
G
Syn Puncta Intensity (a.u.)
Control
PLX3397
Lesion
Lesion + PLX3397
H Control
PLX3397
Lesion
Lesion + PLX3397
Stratum radiatum
63X
Synaptophysin PSD95
I
PSD95 Puncta Number
J
PSD95 Puncta Area (μm³)
K
PSD95 Puncta Intensity (a.u.)
L
Syn Puncta Number
M
Syn Puncta Area (μm³)
N
Syn Puncta Intensity (a.u.)

Microglial elimination following neuronal lesion improves functional recovery

Our data show that treatment of lesioned mice with PLX3397 led to the elimination of most microglia, and was coupled with the restoration of both inflammatory signals and synaptic puncta. To evaluate the functional consequences of microglial elimination *after* neuronal injury/lesion we performed behavioral testing in these groups of mice during the last week of the study. Performance on elevated plus maze revealed that compared to Control mice, mice in the Lesion group spent significantly more time in the open arms and significantly less time in the closed arms. However, mice that were treated with PLX3397 for four weeks following the lesion (Lesion + PLX3397) performed similarly to the Control and PLX3397 groups (Figure 1.6 A). Importantly, PLX3397 treatment alone did not affect performance on this task, while the total number of arm entries was similar for all groups (Figure 1.6 B), indicating a reversal of lesion-induced deficits with elimination of microglia. Mice were next tested in open field, but no differences in behavior were observed among any of the groups (Figure 1.6 C; time in middle of open field shown). Finally, we tested mice on the Morris water maze to assess both learning and memory abilities, as well as to probe for possible motor deficits. Over the five training days of Morris water maze, all four groups learned at a similar rate, though the Lesion group (microglia-intact) trended to an increased latency to find the platform on Day 5, while the Lesion + PLX3397 did not and performed similarly to Control and PLX3397 groups (Figure 1. 6 D). Surprisingly, lesioning had no effect on latency to find the platform location during the probe trial, although both groups of mice treated with PLX3397 demonstrated significantly shorter latencies compared to microglia-intact groups (Figure 1.6 E). No significant differences were found among any of the groups in

swim speed or total distance traveled during the probe trial (Figures 1.6 F-G). Collectively, these results show that microglia impede recovery following neuronal injury and that this may be mediated through production of inflammatory signals as well as remodeling of synapses.

Figure 1.6 Elimination of microglia following extensive neuronal loss improves functional recovery: ***A,*** Lesion mice spent less time in closed arms and more time in open arms on the elevated plus maze test, compared to Control mice (via two-way ANOVA, main effect of lesion, p= 0.0006). Lesion + PLX3397 mice performed similarly to Control and PLX3397 groups in both closed and exposed arms. B) All four groups of mice had comparable numbers of arm entries. C) All four groups of mice spent similar amounts of time in the middle arena of open field testing apparatus. D) All mice learned over the 5-day training period, though the Lesion group trended to a longer latency to find platform on Day 5, compared to Lesion + PLX3397 group (p=0.0882). E) Treatment with PLX3397 increased performance on the probe trial (via two-way ANOVA, main effect of treatment, p=0.0007). F-G) All four groups of mice demonstrated comparable swim speeds and distance traveled during the probe trial. Symbols denote significant differences between groups ($p<0.05$): † Control vs. PLX3397; * Control vs. Lesion; ϕ PLX3397 vs. Lesion + PLX3397; # Lesion vs. Lesion + PLX3397. Error bars indicate SEM, (n=8-10).

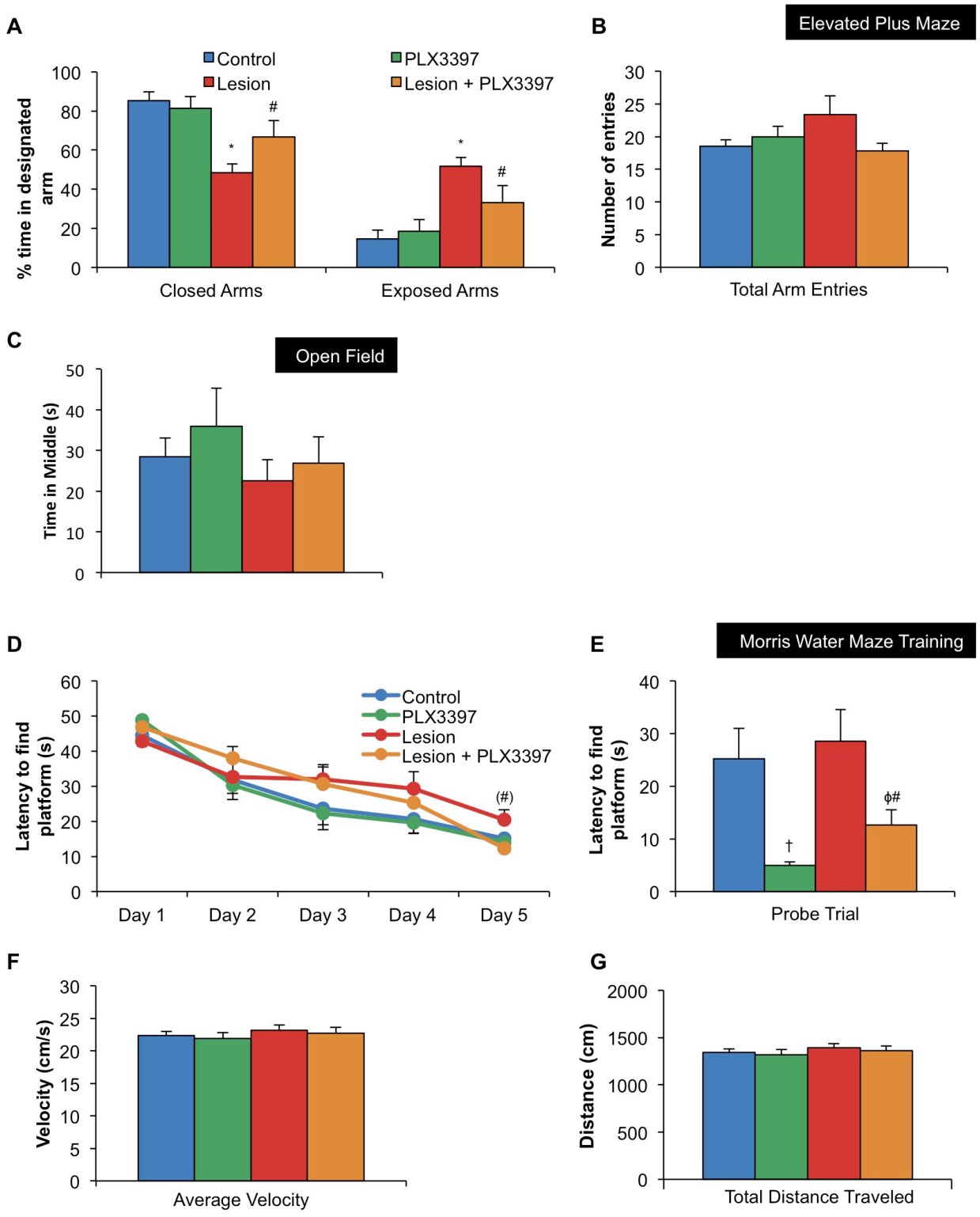
A
Control
Lesion
PLX3397
Lesion + PLX3397
% time in designated arm
100
80
60
40
20
0
*
#
*
#
Closed Arms
Exposed Arms
B
Elevated Plus Maze
Number of entries
30
25
20
15
10
5
0
Total Arm Entries
C
Open Field
Time in Middle (s)
50
40
30
20
10
0
D
Latency to find platform (s)
60
50
40
30
20
10
0
Control
PLX3397
Lesion
Lesion + PLX3397
(#)
Day 1
Day 2
Day 3
Day 4
Day 5
E
Morris Water Maze Training
Latency to find platform (s)
40
30
20
10
0
†
ϕ#
Probe Trial
F
Velocity (cm/s)
30
25
20
15
10
5
0
Average Velocity
G
Distance (cm)
2000
1500
1000
500
0
Total Distance Traveled

Microglia play a protective role *during* a lesion

Having determined that microglia play a deleterious role in the brain following neuronal injury/lesioning, we also wished to explore the roles that microglia play *during* an insult. Additionally, given the effects of microglial elimination on synaptic puncta, we designed an experiment that would allow us to also explore the effects of microglia on dendritic spines, the sites of synaptic connections, in detail. To that end we crossed bitransgenic CaM/Tet-DT_A mice with another transgenic mouse that expresses GFP under elements of the Thy1 promoter in forebrain neurons, allowing for sparse expression of GFP (Thy1-GFP-M; akin to a Golgi stain) and visualization of dendritic spines in excitatory neurons (Feng et al., 2000). We treated 5-8 month age- and sex-balanced groups of mice with control or PLX3397 chow from the start of the lesioning period (25 days), and then for an additional 4 weeks afterwards, consistent with our initial experiment, as shown in Figures 1.7 A-B (n=5-6).

As in the non-GFP cohort, microglia are dependent upon signaling through the CSF1R following lesion, with >95% of all microglia being eliminated with PLX3397 treatment (Figure 1.7 E). Of note, we found far less cell loss within the hippocampus (Figure 1.7 F) than in the non-GFP cohort, despite identical lesioning paradigms. Notably, lesion alone caused significant layer thinning only in the stratum radiatum. However, both the CA1 and stratum radiatum cell layers were further thinned in mice that lacked microglia during lesioning, suggesting that these cells play a protective role during an insult (Figure 1.7 F). For further confirmation, we performed stereological counts of neurons using a Cresyl Violet stain of the CA1 region, and found that the absence of microglia exacerbated neuronal loss (Figures 1.7 G and H), thus showing that elimination of

microglia during an insult results in greater neuronal loss. Despite a lack of overt neuronal loss we did find that lesioning induces microglia to adopt a rod-like morphology and assemble end-to-end in chains, often alongside or even wrapping around neurons in the CA1 (Figure 1.7 D). We found no lesion-induced functional deficits in these mice (Figure 1.7 I), likely as a result of only a mild lesion being achieved.

Figure 1.7 Microglial elimination in Thy1-GFP-M expressing CaM/Tet mice: 5-8 month-old GFP-CaM/Tet mice (C57Bl/6-CBA mix) had microglia eliminated for 2 months via treatment with 290 mg/kg PLX3397. A 25-day neuronal lesion was induced in half of the animals. ***A,B,*** Schematics of GFP-CaM/Tet mouse model of inducible neuronal loss and experimental design. ***C,*** Representative 10X confocal images of the hippocampal region from each group for neuronal nuclei (NeuN in blue channel), microglia (IBA1 in red channel), and GFP in the green channel. ***D,*** Representative 63X IBA1 immunofluorescent staining from the hippocampal region showing rod like morphologies with lesion. ***E,*** Quantification of microglial numbers per hippocampal subfield per group. ***F,*** Thickness of the hippocampal layers with lesion and treatment. ***G,*** Representative 20X pictures of Cresyl Violet staining in the CA1 cell layer from each group. ***H,*** Stereological quantification of neurons in the CA1 region from each group. ***I,*** Lesion mice did not display a deficit in performance on elevated plus maze. Symbols denote significant differences between groups ($p<0.05$): † Control vs. PLX3397; * Control vs. Lesion; ϕ PLX3397 vs. Lesion + PLX3397; # Lesion vs. Lesion + PLX3397. Error bars indicate SEM. (n=5-6).

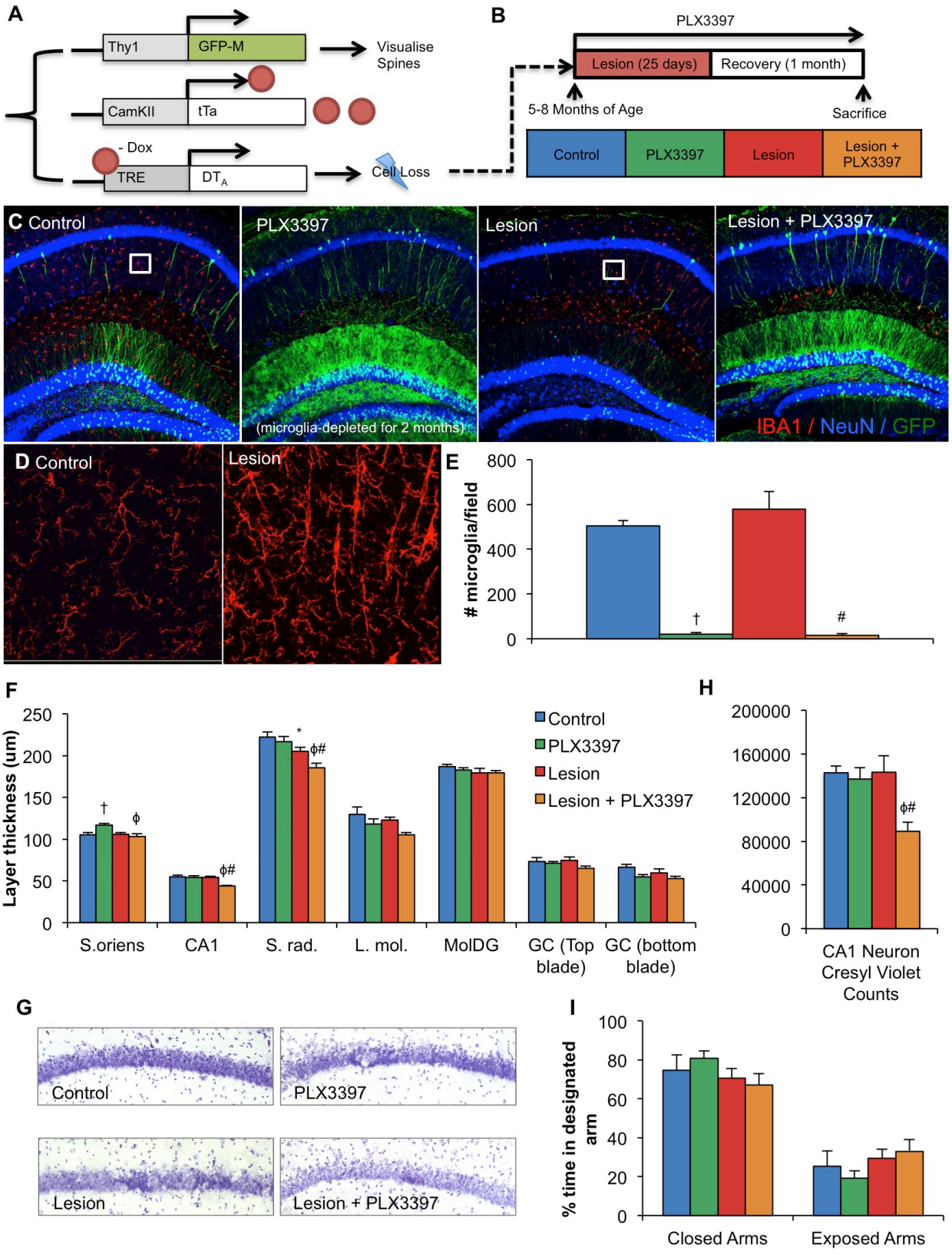
A
Thy1
GFP-M
Visualise Spines
CamKII
tTa
- Dox
TRE
DT A
Cell Loss
B
PLX3397
Lesion (25 days)
Recovery (1 month)
5-8 Months of Age
Sacrifice
Control
PLX3397
Lesion
Lesion + PLX3397
C Control
PLX3397
(microglia-depleted for 2 months)
Lesion
Lesion + PLX3397
IBA1 / NeuN / GFP
D Control
Lesion
E
microglia/field
800
600
400
200
0
†
#
F
Layer thickness (um)
250
200
150
100
50
0
Control
PLX3397
Lesion
Lesion + PLX3397
†
ϕ
ϕ#
*
ϕ#
S.oriens
CA1
S. rad.
L. mol.
MolDG
GC (Top blade)
GC (bottom blade)
H
200000
160000
120000
80000
40000
0
ϕ#
CA1 Neuron Cresyl Violet Counts
G
Control
PLX3397
Lesion
Lesion + PLX3397
I
% time in designated arm
100
80
60
40
20
0
Closed Arms
Exposed Arms

Microglia regulate dendritic spine densities in the intact brain

Due to the presence of the GFP within excitatory neurons we were able to examine dendritic spine densities and morphologies in the four groups. It has been previously reported that these CaM/Tet-DT_A/GFP mice show reactive synaptogenesis following lesioning (Castello et al., 2014), resulting in overall increases in spine densities, and therefore we were most interested in the effects of microglial elimination in the non-lesioned mice, and the combination of lesion and microglial elimination. We confirmed increases in spine densities in CA1 apical non-primary dendrites following lesioning, and found that elimination of microglia alone led to a robust 35% increase in spine density (Figure 1.8 B). Increases in dendritic spines due to microglial elimination were not indiscriminate: eight-week elimination of microglia increased mushroom spines by 44% and thin spines by 71%, while decreasing stubby spines by 55%. Interestingly, the combination of lesion and microglial elimination did not further increase overall spine numbers, though it is possible that a physiological upper threshold of this effect was reached.

To determine if the effects of microglial elimination are global, we also analyzed spine type and number in pyramidal cells in Layer 5 of the primary visual cortex (V1), a site distant from the focal point of the neuronal insult. Similar increases in dendritic spine numbers were seen with microglial elimination, though importantly, not with lesion alone (Figure 1.8 D). Again, mushroom and thin spines were increased and stubby spines decreased in PLX3397 mice compared to controls. Representative images of dendrites in the CA1 and Layer 5 of V1 are shown in Figures 1.8 A and 8 C, respectively. These

data suggest that it is the local environmental response to the lesion that produces a change in spine number, while microglial elimination globally increases spine numbers.

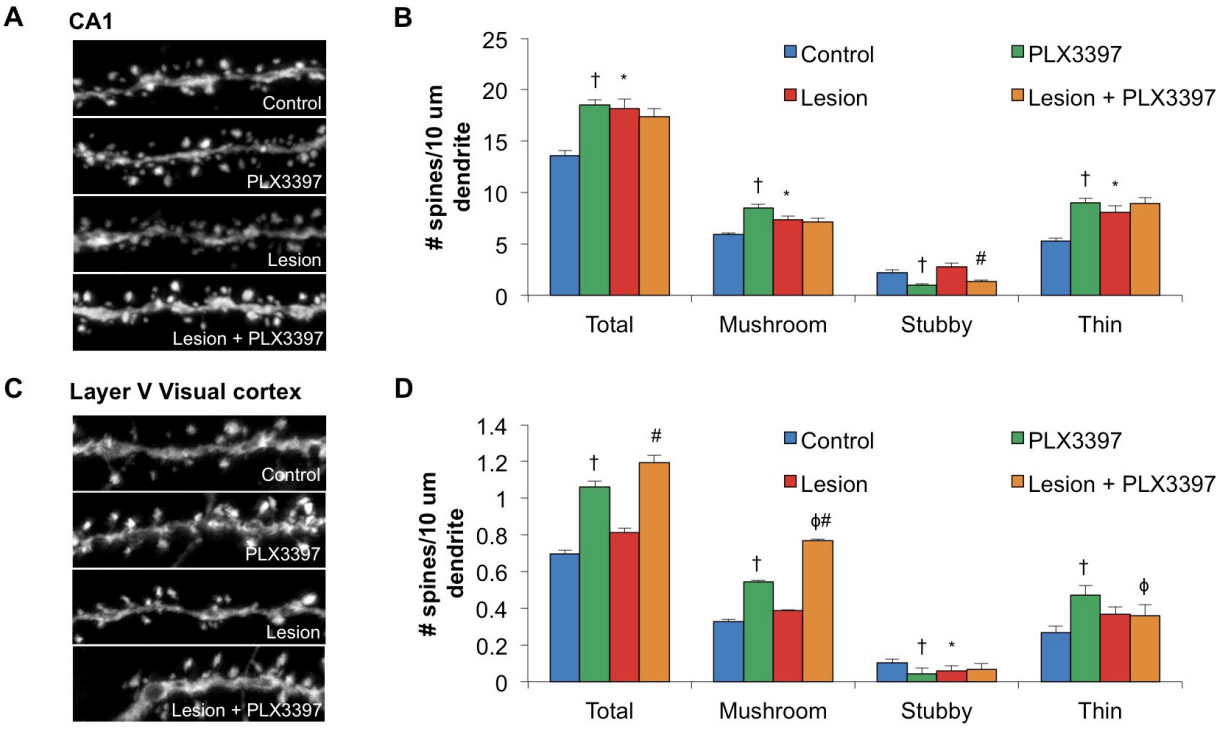

Figure 1.8 Microglial elimination increases dendritic spine densities throughout the brain: ***A,*** Representative images of dendrites from the CA1 region. ***B,*** Quantification of dendritic spines, overall and by type, in the CA1 region. ***C,*** Representative images of dendrites from Layer 5 in V1. ***D,*** Quantification of dendritic spines, overall and by type, in Layer 5 of V1. Symbols denote significant differences between groups ($p<0.05$): † Control vs. PLX3397; * Control vs. Lesion; ϕ PLX3397 vs. Lesion + PLX3397; # Lesion vs. Lesion + PLX3397. Error bars indicate SEM, (n=5).

Microglial Elimination Increases Excitatory Connectivity

Given the robust increase in spine number we found with microglial elimination, regardless of lesion, we wanted to determine if this phenomenon translated into changes in neuronal connectivity. We collaborated with the laboratory of Dr. Xiangmin

Xu to assess excitatory connectivity in Layer 5 of cortical Area V1 with microglial elimination. Due to methodological constraints, mice could not be older than three months of age at the time of testing. To this end, we treated 6 week-old mice for 4 weeks with PLX3397 to deplete microglia. Importantly, the intrinsic properties of neurons were unchanged with microglial elimination (Figure 1.9).

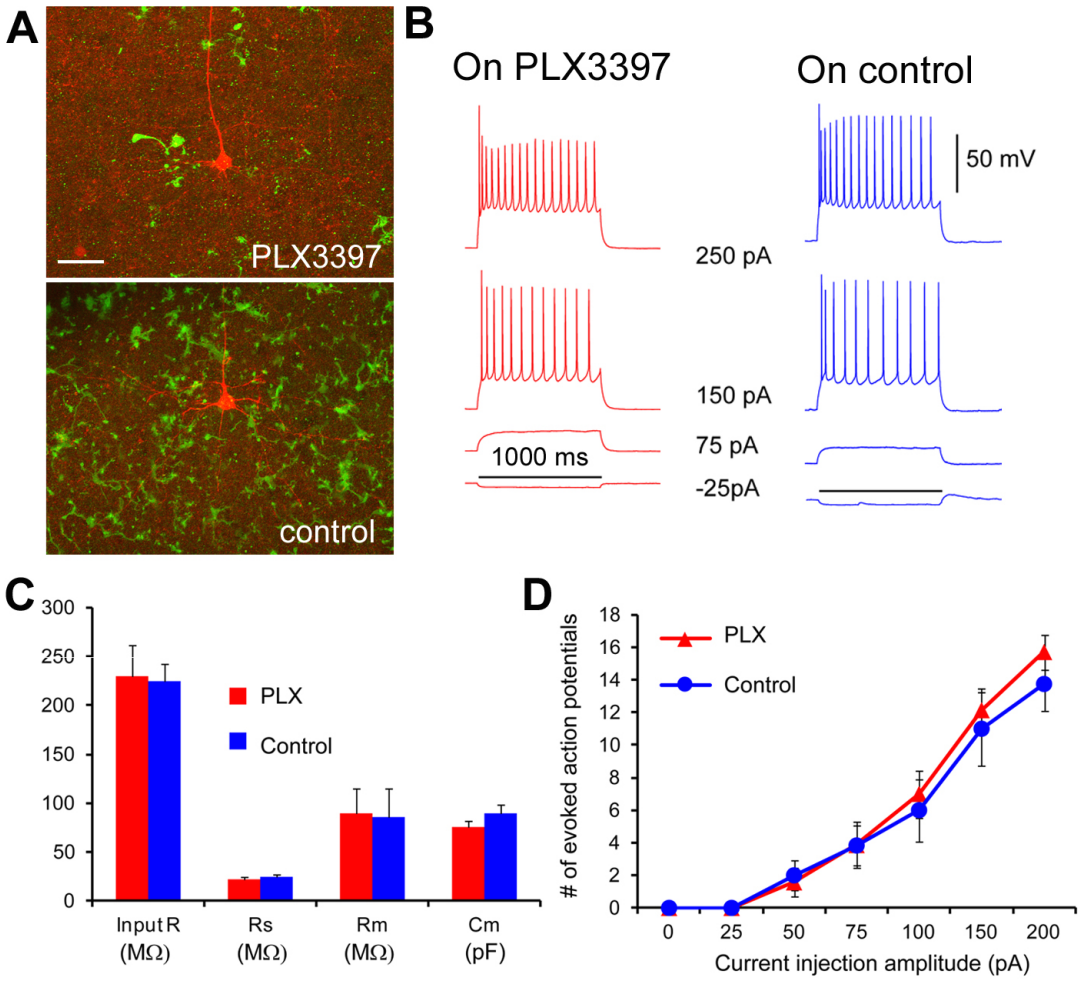

Figure 1.9 Excitatory pyramidal cells in control and microglia-depleted mice do not differ in their intrinsic electrophysiological properties: ***A,*** Example images of mice on PLX3397 showing microglial depletion, compared to control. Microglia marker IBA1, shown in green, and the recorded cell visualized with biocytin, shown in red. ***B,*** Hyperpolarized and depolarized responses of the representative cells in response to intrasomatic current injections. ***C,*** Comparison of average input resistance (R input), series resistance (Rs), membrane resistance (Rm), and membrane capacitance (Chitu et al.) between cells of mice on PLX3397 and control. ***D,*** The current injection-response function does not differ between PLX3397 and control cells. Error bars indicate SEM, (n=6-7).

Laser-scanning photostimulation was employed to determine excitatory connectivity. Using this technique, brain slices were bathed in artificial CSF with caged glutamate and a grid was super imposed over the tissue, with each square of the grid containing roughly 10 neurons. A single neuron at an arbitrary location in the grid was recorded from intracellularly, while a laser was flashed onto a different, single square of the grid, uncaging glutamate and exciting the neurons in the square. If those neurons were connected to the distant neuron being recorded from, the neuron was depolarized and excitation was detected. The experimenter continued by photostimulating squares of the grid one-by-one until, ultimately, a connectivity map of the local area was created. Figure 1.10, below, shows a single neuron in Layer 5 from which recordings were made, along with the superimposed grid.

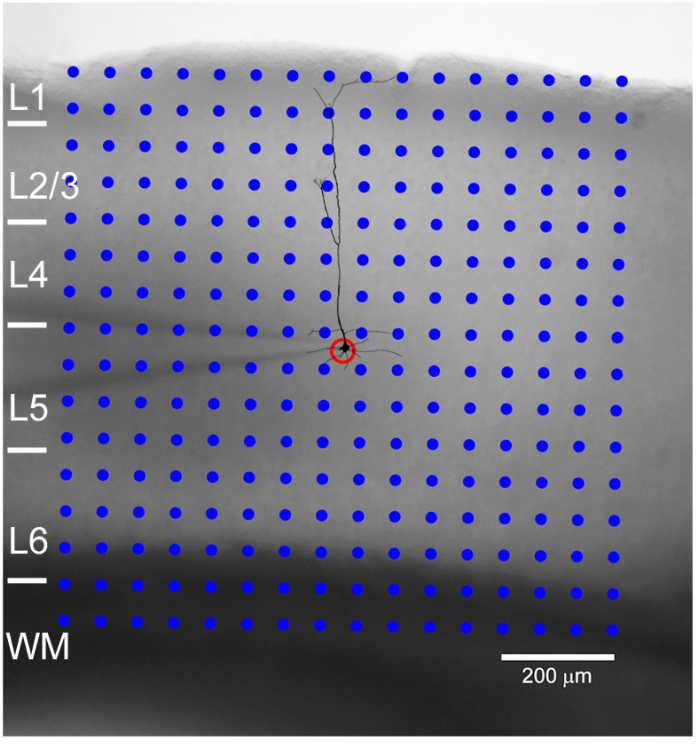

Figure 1.10 An excitatory pyramidal cell in Layer 5 of V1 (encircled in red).

Using LSPS, Xu's group observed two striking effects: 1) The total excitation arriving at recorded neurons in greatly increased in the absence of microglia and 2) The total numbers of inputs to recorded neurons is increased with microglial elimination. The results of these experiments are shown in Figure 1.11.

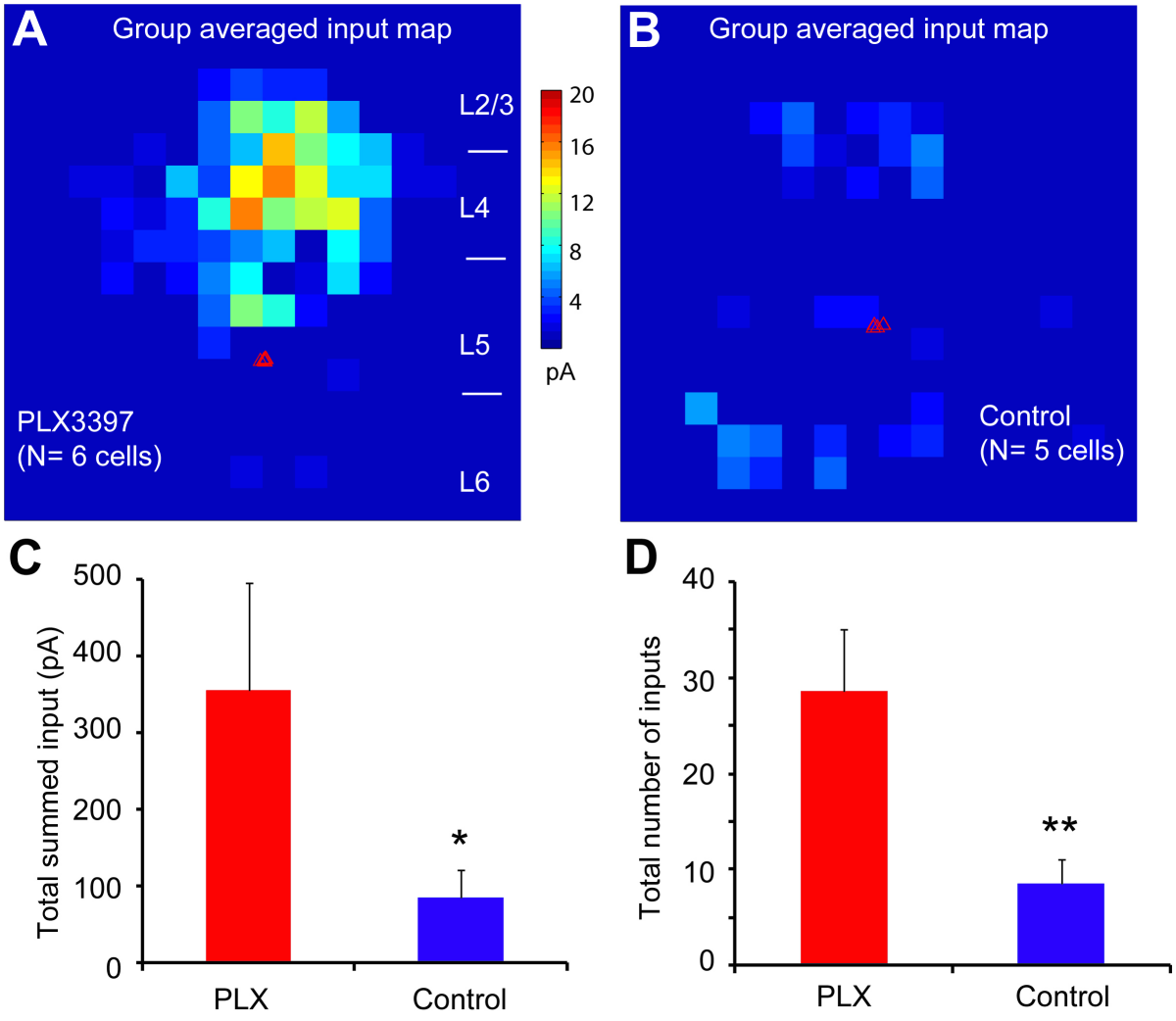

Figure 1.11 Excitatory connectivity is increased in the absence of microglia: ***A,*** An averaged connectivity map generated from recording from cells in mice treated with PLX3397. ***B,*** An averaged connectivity map generated from recording from cells in untreated mice. ***C,*** Control-treated mice have significantly less total summed input than PLX3397-treated mice. ***D,*** Control-treated mice have significantly fewer total inputs than PLX3397-treated mice. Significance denote by *p<0.05, **p<0.01. Error bars indicate SEM, (n=5-6).

Finally, we wanted to determine if such increased excitatory connectivity conferred functional differences in microglia-depleted mice. To test this, we treated adult mice for 3 weeks with control- or PLX3397-formulated chow and then injected them with a sub-convulsive dose of kainic acid (10 mg/kg) via IP injection and scored their behavior on a seizure scale, from 0-7 (shown in Table 1.1).

Table 1.1 Seizure scale, as described by Morris *et al*., 1996.

Score	Description
0	normal
1	immobility; staring off into space; cessation of typical activity such as walking, exploring, sniffing, and grooming
2	rigid posture; forelimb and/or tail extension
3	automatisms; repetitive scratching, circling, head bobbing (wet dog shakes)
4	seizure behaviors; forelimb clonus (involuntary muscular contraction and relaxation) and rearing and falling
5	repetition of seizure behaviors
6	severe, tonic-clonic whole body seizures
7	death

In accordance with our hypothesis that increased excitatory connectivity could reduce seizure threshold, we found that mice depleted of microglia had significantly higher scores on the seizure scale at multiple time points surveyed (Figure 1.12). However, we counted and categorized dendritic spines in the CA1 of these mice and found that 3-week microglial elimination did not significantly affect spine numbers (data not shown). Together, these results demonstrate that microglial elimination increases connectivity at the synaptic, neuronal, and network levels, and moreover, that microglia are critical regulators of neuronal signaling in the central nervous system.

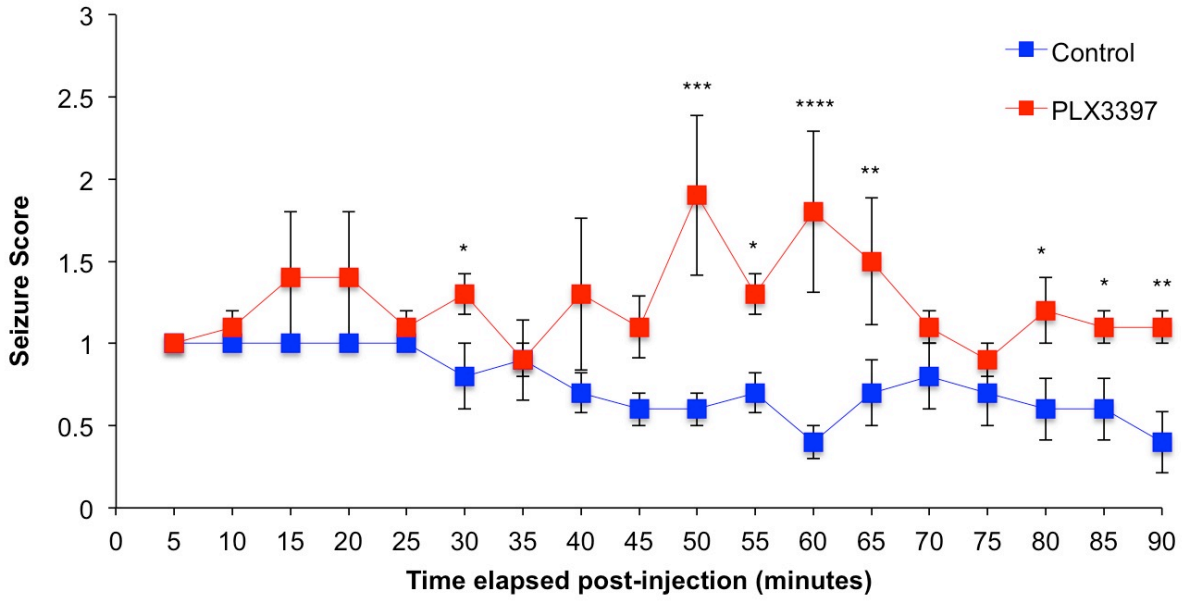

Figure 1.12 Microglial depletion leads to increased seizure score following kainic acid injection. Mice treated with PLX3397 for three weeks had significantly higher scores on the seizure scale at 45, 50, 55, 60, 85, and 90 minutes post-injection. Significance denoted by *p<0.05, **p<0.01, ***p<0.005, ****p<0.0001. Error bars indicate SEM, (n=5).

DISCUSSION

Upon neural insult or invasion by a pathogenic species, microglia become activated and secrete pro-inflammatory cytokine, but subsequently assume an anti-inflammatory role, secreting molecules such as IL-4 and IL-10 as part of the resolution and tissue repair process (Colton and Wilcock, 2010). However, with severe insults like traumatic brain injury (TBI) or chronic neurodegenerative conditions, microglia remain activated, and in this way are believed to contribute to cognitive decline. We hypothesized that

eliminating microglia after a severe neuronal lesion would partially attenuate functional deficits caused by the insult, by way of reducing pro-inflammatory signaling, as well as any harmful interactions microglia may have with the local brain environment. We previously discovered that microglia are critically dependent on signaling through the CSF1R for their survival in the adult mouse brain (Elmore et al., 2014), but had not extended these studies to look at microglia in disease/activation states. To that end, we utilized a genetic hippocampal lesion model that results in extensive neuronal loss and chronic microglia-evoked neuroinflammation, as this model has relevance to traumatic brain injuries, stroke, hippocampal sclerosis, and Alzheimer's disease. Crucially, we find that these chronically activated microglia are indeed dependent on CSF1R signaling, as we are still able to successfully eliminate the vast majority of microglia from the CNS following lesioning, through administration of the small molecule CSF1R inhibitor PLX3397. This finding allows researchers to eliminate microglia from any disease or injury state and directly determine the roles that these cells play.

By eliminating microglia either during or after lesioning, we were able to parse protective versus harmful effects that these cells exert in the brain. For example, we found that the elimination of microglia for four weeks *following* neuronal lesioning results in the recovery of lesion-induced deficits on the elevated plus maze. Surprisingly, we did not find lesion-induced deficits during the probe trial of Morris water maze testing. However, we suspect that the interim period of time between the end of lesioning and the beginning of behavioral testing could allow for the recovery of some lesion-induced deficits. Indeed, a study recently showed that lesioned CaM/Tet mice exhibit deficits one

month post-lesion, but not three months post-lesion, on the 24-hour probe trial of Barnes maze, a hippocampal-dependent measure of memory (Myczek et al., 2014).

To explore possible mechanisms by which elimination of microglia following injury might promote recovery, we performed inflammatory profiling. Microglia are immune competent cells and produce and secrete a plethora of signaling molecules, as well as cellular toxins such as reactive oxygen species, depending on their activation state (Colton and Wilcock, 2010). Of the inflammation-related genes that we measured, lesioning induced an upregulation in expression of 11 genes, but subsequent microglial elimination was able to reduce expression of all these transcripts to that of control levels, or lower. Thus, elimination of microglia also eliminates the substances that they produce, which may negatively affect the local parenchyma. For these reasons, we assessed the integrity of the BBB but found that the lesion did not have an effect. Despite our finding that the BBB was not grossly compromised, there still exists the possibility that circulating monocytes/macrophages could be present in the brain and contributing to lesion-induced inflammation. Indeed, several of the markers that were upregulated with lesion are associated with peripheral monocytes, such as CCR2 (Charo et al., 1994), CD80 (Dilioglou et al., 2003), CD86 (Dilioglou et al., 2003), and CD45 (Pardo-Manuel de Villena et al., 1996), all of which were reduced with PLX3397 treatment. However, despite lesion-induced increases in monocyte markers, we found that all cells positive for IBA1 were also positive for 4D4, an antibody that only detects indigenous microglia, regardless of experimental condition (Butovsky et al., 2012). These results are in agreement with previous literature indicating that infiltrated cells do not contribute to injury-induced microgliosis, nor are they long-lived in the CNS (Ajami et

al., 2007; Mildner et al., 2007). For these reasons, we do not believe that IBA1$^+$ cells represent infiltrated or circulating monocytes/macrophages.

It is also important to consider the physical interactions that microglia have with their local environment. It is known that microglia also have roles as synaptic architects, at least in the developing brain (Paolicelli et al., 2011; Schafer et al., 2012). Microglia are highly branched and motile, forming frequent physical interactions with synapses (Perry and O'Connor, 2010; Yirmiya and Goshen, 2011). In addition, they possess phagocytic activity, and are therefore ideally suited to regulate the synaptic landscape. In this study we explored the effects of both lesioning and microglial elimination on the pre-synaptic protein synaptophysin, as well as the post-synaptic protein PSD95. We focused on the CA1 and stratum radiatum of the hippocampus, where significant neuronal loss occurred. With microglial elimination, we observed reversals of lesion-induced alterations in the size and number of synaptic puncta. The loss of puncta number is not surprising given the lesion, and it is plausible that remaining puncta increase in size to compensate for the loss in overall number. In parallel with these data, another group found that systemic administration of LPS decreased the number, but increased the volume, of PSD95 puncta in wild-type mice (Valero et al., 2014).

In contrast to the harmful effects that microglia exert following lesion, microglial elimination *during* the lesion period promoted hippocampal neuronal loss of more than 35% as measured by stereology. Thus, the presence of microglia during an insult appears to support neuronal survival, revealing divergent roles for these cells depending upon the insult phase.

Using CaM/Tet-GFP mice, we were able to explore the effects of microglial elimination on dendritic spine densities and morphologies. In the developing brain, microglia are involved in activity- and complement-dependent pruning by phagocytosing pre-synaptic inputs (Schafer et al., 2012), as well as in a CX3CL1-CX3CR1-dependent fashion (Paolicelli et al., 2011; Zhan et al., 2014). *Ex-vivo* evidence suggests that microglia can shape glutamatergic signaling at both pre- and post-synaptic sites, resulting in changes in the electrophysiological properties of primary P3-P7 neurons (Schafer et al., 2012; Ji et al., 2013). Additionally, short-term elimination of microglia from P30 mice demonstrated marked changes in dendritic spine dynamics, due to a lack of microglia-derived BDNF signaling (Parkhurst et al., 2013). Crucially, we find that eight weeks, but not three weeks, of microglial elimination leads to large increases in spine number in all brain regions surveyed, indicating that microglia play substantial roles in the maintenance of dendritic spine densities in the adult brain, in addition to the roles described in the developing brain. Excitingly, these increases in spine number translate to increases in local neuronal connectivity, as well as reduced seizure threshold. Such an opportunity to manipulate dendritic spine number and excitatory connectivity in the adult brain merits further research by the field, and could have far-ranging implications for conditions in which aberrant spine and neuronal networks are present, including neurodegenerative diseases, autism, and multiple forms of mental retardation.

Overall, our data reveal that elimination of microglia facilitates functional recovery following neuronal lesioning. Thus, microglia are harmful to the CNS following injury, and we can negate these effects through their elimination with CSF1R inhibitors. While the elimination of an entire cell type has broad effects, it is likely a combination of a

reduction in the inflammotoxic substances normally produced by microglia, as well as the removal of their physical interactions with other cells types, such as neurons, that underlies these functional benefits.

CHAPTER TWO

MICROGLIAL REPOPULATION DAMPENS INFLAMMATION IN THE INJURED ADULT BRAIN

INTRODUCTION

Microglia are the primary immune cell of the central nervous system and are responsible for responding to insults involving cellular harm and death. They quickly proliferate and migrate to the site of injury upon detection of such an event. There, they secrete a plethora of inflammatory signaling molecules, ultimately allowing them to support neuronal health and/or eliminate dead or dying neurons.

Despite the protective and beneficial roles that microglia play in the brain, they are negatively implicated in many CNS disorders and injuries. During normal inflammatory responses to pathogens or dead cells, microglia undergo a phenotypic shift that allows them to respond appropriately to the event, and then subsequently revert to a quiescent state, at which point the inflammatory response is effectively resolved. However, after extensive injury, such as TBI or stroke, as well as during neurodegenerative diseases, microglia become remodeled in response to the insult but fail to resolve their activated state. This results in a chronic neuroinflammatory process that can last for decades, harming the local brain environment.Therefore, finding ways to manipulate and resolve microglial responses is a high priority.

We have determined that microglia in both the healthy and injured/diseased brain are dependent upon signaling through the colony-stimulating factor 1 receptor (CSF1R) for their survival (Elmore et al., 2014). Administration of small molecule inhibitors of the

CSF1R cross the blood brain barrier (BBB) and rapidly cause all microglia to undergo cell death within days. Treated mice then lack microglia for the duration of treatment, be it days, weeks, or months (Elmore et al., 2014).

In addition to the finding that we can eliminate microglia from healthy, diseased, and injured brains, we also discovered that we can induce rapid repopulation of the entire microglia-depleted CNS through the withdrawal of the CSF1R inhibitor. Upon inhibitor withdrawal, microglia progenitors resident within the CNS are stimulated to proliferate and then differentiate into new microglia (Elmore et al., 2014). This process takes up to 21 days, by which time the repopulated microglia are phenotypically indistinguishable from normal microglia in the healthy brain (Elmore, 2015).

The ability to eliminate microglia at will and then replenish this cellular compartment begs many important questions, with regard to the resolution of chronic neuroinflammatory events. If we eliminate harmful microglia in disease or injury conditions, and then allow for new progenitor-derived microglia to repopulate the brain, what effects will this have? Will the new microglia inherit the activation state of the old microglia, or will they present as ramified, quiescent cells? Likewise, could the act of repopulation have any further beneficial effects on the brain? For example, repopulating microglia resemble microglia during the developmental period (Orlowski et al., 2003), and as such, these new microglia may help to refine neuronal circuitry in ways that that could be useful following injury, such as promoting neuronal plasticity.

This study investigates the effects of microglial repopulation, following neuronal injury, on subsequent inflammatory signaling, as well as functional recovery. In doing so, we can address crucial questions about how the environment dictates cell behavior, and

vice versa. Furthermore, the act of short-term microglial elimination followed by repopulation is potentially translatable to humans, unlike indefinite microglial elimination. Thus, our findings could direct an entirely novel approach to 1) resolve chronic neuroinflammatory states and 2) facilitate brain repair.

MATERIALS AND METHODS

Compounds

PLX5622 was provided by Plexxikon, Inc. and formulated in standard chow by Research Diets Inc. at 1200 mg/kg. Doxycycline was provided in standard chow by Research Diets Inc. at 2000 mg/kg, or by researchers in deionized drinking water at 2 mg/ml (Sigma-Aldrich, St. Louis, MO) with 5% sucrose.

Animal Treatments

All rodent experiments were performed in accordance with animal protocols approved by the Institutional Animal Care and Use Committee at the University of California, Irvine. The CaM/Tet-DT_A mouse model of inducible neuronal loss was employed for functional studies, and has been previously described (Yamasaki et al.). 5-8 month-old male and female mice were maintained since birth on doxycycline chow. Upon induction of the 30-day lesion period, doxycycline chow was replaced with standard chow. To cease expression of DT_A, doxycycline was provided in drinking water, and after 7 days, control or PLX5622 chow was provided for 14 days. Finally, PLX5622 treatment was withdrawn for 21 days, allowing microglia to fully repopulate. Behavioral tasks were performed during the final week of the study. At the conclusion of experiments, mice were sacrificed via lethal IP injection of Euthasol and perfused transcardially with 1X phosphate-buffered saline (PBS). Brains were extracted and dissected down the

midline, with one half flash-frozen on dry ice for subsequent RNA and protein analyses, and the other half drop-fixed in 4% paraformaldehyde (PFA) in 1X PBS. Fixed brains were cryopreserved in a 30% sucrose solution, frozen, and sectioned at 40 μm on a Leica SM2000 R sliding microtome for subsequent immunohistochemical analyses.

Confocal microscopy

Fluorescent immunolabeling followed a standard indirect technique (primary antibody followed by fluorescent secondary antibody), as previously described (Neely et al., 2011). Primary antibodies used include NeuN (1:1000; Abcam, Cambridge, MA), IBA1 (1:1000; Wako, Richmond, VA), GFAP (1:10,000; Abcam), S100β (1:1000, Abcam). Numbers of microglia were determined using the spots module in Imaris 7.5 software.

Behavioral testing

Mouse cognition and behavior were evaluated on open field test (Elmore et al., 2014), elevated plus maze (Elmore et al., 2014), accelerating rotarod (Elmore et al., 2014), Morris water maze (Baglietto-Vargas et al., 2013), and novel place (Baglietto-Vargas et al., 2013), in the order as presented, and as previously described.

RNA Extraction and Analysis

RNA was extracted and purified from microdissected hippocampi of frozen half brains using Qiagen RNEasy Mini Kit (Hilden, Germany). A custom CodeSet of 182 transcripts was created by NanoString Technologies (Seattle, Washington). Total RNA was diluted to 20 ng/μl with nuclease-free water and protocols were carried out per manufacturer instructions.

Dendritic Spine Analyses

Five to seven non-primary apical dendrites in the CA1 of the hippocampus per animal were imaged on a Leica DM2500 confocal microscope with a 63X oil-objective and 5X digital zoom. Z-stacks of equal depth were obtained for each dendrite and deconvoluted using Huygens deconvolution software, and max projections created. From the max projections, researchers counted and classified spines using the Cell Counter plug-in in ImageJ software. Spine classification was based on previous literature in the field employing head-to-neck ratio (Peters and Kaiserman-Abramof, 1970). Finally, the total number of each type of spine was calculated per 10 μm of dendrite length.

Statistics

Two-way ANOVAs were employed to analyze differences between all four groups of mice. For Nanostring analyses specifically, Tukey-Kramer post-hoc values are reported when $p<0.05$, regardless of the the p value for the interaction, as determined via two-way ANOVA. For all other two-way ANOVA analyses, Holm-Sidak post-hoc values are reported when $p<0.05$, regardless of the p value for the interaction, as determined via two-way ANOVA. For dendritic spine analyses, a one-way nonparametric ANOVA adjusted for multiple comparisons was employed and p values were determined using Dunn test. Results are presented as average± standard error of the mean (SEM). Significance is defined as $p<0.05$. The following symbols are used to denote significant differences between groups, as obtained by post-hoc analyses: † Control vs. Repopulation; * Control vs. Lesion; ϕ Repopulation vs. Lesion + Repopulation; # Lesion vs. Lesion + Repopulation.

RESULTS

Microglial elimination and repopulation following neuronal lesion

To make our studies relevant to both disease and injury, we utilized the tetracycline-off inducible transgenic CaM/Tet-DT_A mouse, in which diphtheria toxin A chain (DT_A) is expressed in forebrain excitatory neurons upon withdrawal of doxycycline from the diet. The hippocampal region, specifically the CA1 subfield, is affected most strongly in these mice, just as it is in humans with AD (West et al., 1994). Additionally, we sought to examine the effects of microglial repopulation on the synaptic landscape, as microglia are known to carry out dendritic spine pruning in development, and we believe that the birth of these new microglia could potentially recapitulate such a period. To most easily do so, we again crossed the CaM/Tet-DT_A mice to the Thy1-GFP-M mouse line, yielding CaM/Tet-GFP mice.

We allowed CaM/Tet-GFP mice to age to 5-8 months old and then withdrew doxycycline from their diet for 30 days, inducing a neuronal lesion (control mice do not harbor the CaM transgene, and therefore do not lesion upon doxycycline withdrawal). We then readministered doxycycline into the diet for the duration of the study. We waited 7 days after doxycycline withdrawal for expression of DT_A to fully cease, and then treated mice with control chow or chow that was formulated with 1200 mg/kg of the CSF1R antagonist PLX5622, to eliminate microglia, for 14 days. Finally, we withdrew PLX5622 treatment and allowed microglia to repopulate from a progenitor source for 21 days, as this is the time point at which repopulating microglia are identical in number and

morphology to that of untreated brains (Elmore, 2015). Our experimental paradigm effectively yields 4 experimental groups of mice, as seen in Figure 2.1 A-B: 1) nonlesioned mice with resident microglia (Control); 2) nonlesioned mice with repopulated microglia (Repopulation); 2) lesioned mice with resident microglia (Lesion); and 4) lesioned mice with repopulated microglia (Lesion + Repopulation). Importantly, we also sacrificed mice after 14 days of treatment with PLX5622 and confirmed that microglia depletion did occur prior to repopulation, via staining for the microglia marker IBA1 (Figure 2.1 D). Consistent with our previous experiments, lesioning dramatically increased the number of microglia within the brain, even 10 weeks after lesioning began (Figure 2.1C, E). Microglial repopulation in the non-lesioned mice had returned microglial numbers precisely back to that of control levels, while microglia numbers remained elevated in the Lesion + Repopulation group. To show the dramatic effects of the lesion, we measured neuronal layer thickness via immunoreactivity for the neuronal nuclei marker NeuN and found that both Lesion and Lesion + Repopulation displayed significantly reduced layer thicknesses across most of the hippocampus (Fig 2.1 F). Overall, hippocampi appeared shrunken in both Lesioned groups, indicating extensive neuronal loss. Indeed, prior studies have shown this loss to occur at the level of ~85% within the CA1 (Yamasaki et al., 2007). It is important to point out that the neuronal loss occurred prior to microglial elimination and repopulation, and thus we would not expect the treatment (Repopulation) to affect the amount of neurons lost.

Figure 2.1 Neuronal lesioning followed by subsequent microglial repopulation in CaM/Tet-GFP mice. Experimental paradigm: ***A,*** Schematic depicting the mouse transgenes. ***B,*** Schematic depicting the treatment paradigm and resulting experimental groups. ***C,*** 10X representative images of hippocampal regions. ***D,*** 10X representative image of mice sacrificed after 14 days of treatment with PLX5622, revealing microglial depletion did occur. ***E,*** Quantification of neuronal layer thickness, via NeuN immunoreactivity. Error bars represent SEM, (n=9-11). $p<0.05$; † Control vs. Repopulation; * Control vs. Lesion; ϕ Repopulation vs. Lesion + Repopulation; # Lesion vs. Lesion + Repopulation.

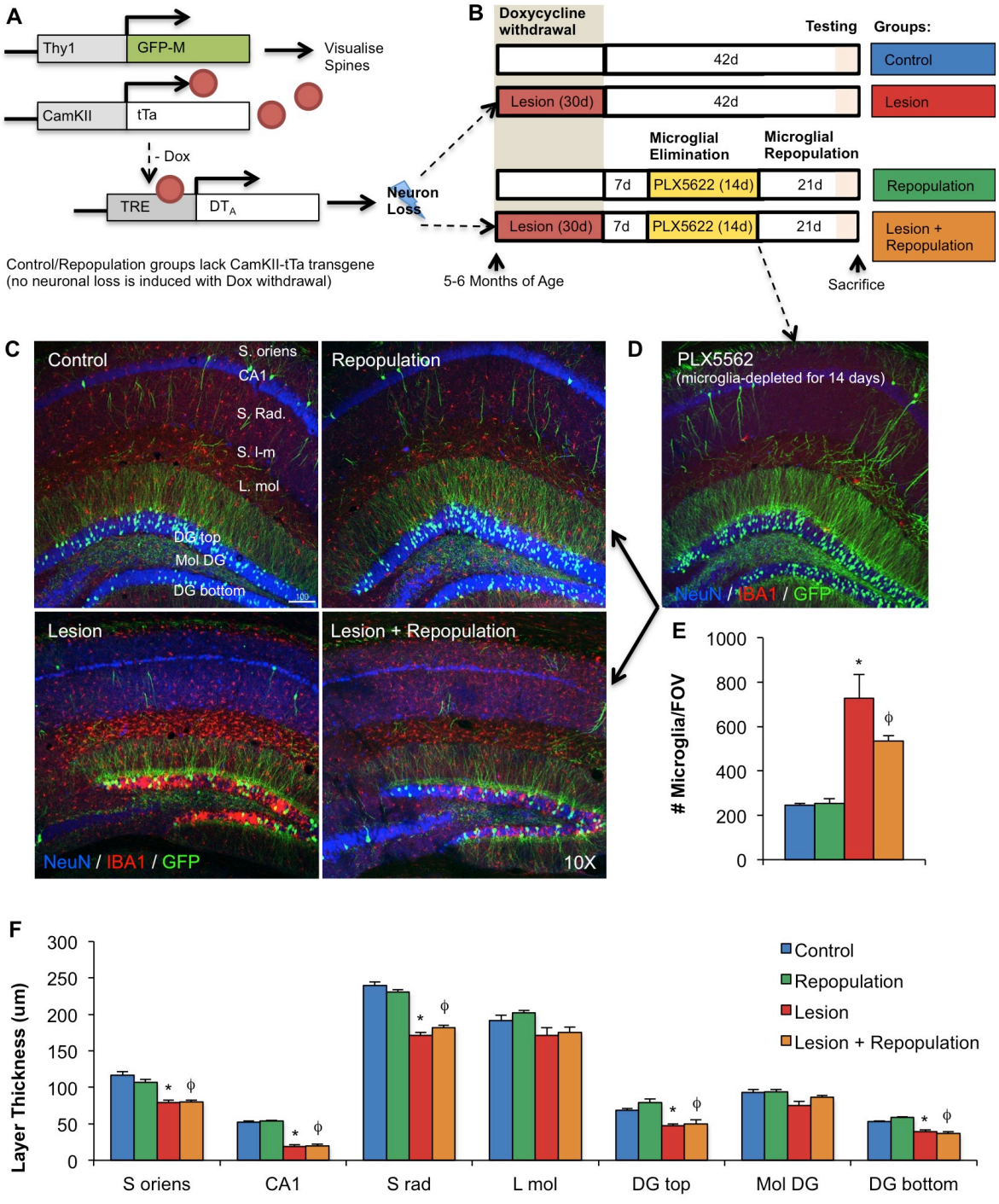
A
Thy1
GFP-M
Visualise Spines
CamKII
tTa
- Dox
TRE
DT A
Neuron Loss
Control/Repopulation groups lack CamKII-tTa transgene (no neuronal loss is induced with Dox withdrawal)
B
Doxycycline withdrawal
Testing
Groups:
42d
Control
Lesion (30d)
42d
Lesion
Microglial Elimination
Microglial Repopulation
7d
PLX5622 (14d)
21d
Repopulation
Lesion (30d)
7d
PLX5622 (14d)
21d
Lesion + Repopulation
5-6 Months of Age
Sacrifice
C
Control
S. oriens
CA1
S. Rad.
S. l-m
L. mol
DG top
Mol DG
DG bottom
Repopulation
Lesion
Lesion + Repopulation
NeuN / IBA1 / GFP
10X
D
PLX5562
(microglia-depleted for 14 days)
NeuN / IBA1 / GFP
E
Microglia/FOV
1000
800
600
400
200
0
F
Layer Thickness (um)
300
250
200
150
100
50
0
S oriens
CA1
S rad
L mol
DG top
Mol DG
DG bottom
Control
Repopulation
Lesion
Lesion + Repopulation

Repopulating microglia appear morphologically naïve

While we did not find a statistical difference in the number of microglia between the Lesion and Lesion + Repopulation groups of mice, there was an obvious difference in the appearance of repopulating microglia. In Lesion mice, microglia displayed highly swollen cell bodies, particularly in the dentate gyrus and in the cortex. Furthermore they stained more brightly for IBA1 and possessed short stubby processes, indicative of an activated state. It is important to note that these microglial changes are 10 weeks after the onset of lesioning and 6 weeks since its end, and in this way represent chronically unresolved microglia, such as those implicated in human diseases. Furthermore, we know that these microglia impair functional recovery as their chronic elimination in this model improves recovery (Chapter 1). However, stark differences can be seen in the Lesion + Repoulation mice, where the majority of microglia do not display altered morphologies, but resemble normal ramified microglia, with smaller somas and long, fine processes. Representative images are shown in Figures 2.2 A-C. Thus, these findings indicate that microglial repopulation has highly robust effects on microglial morphologies, appearing to resolve the classically activated morphological phenotype of these cells.

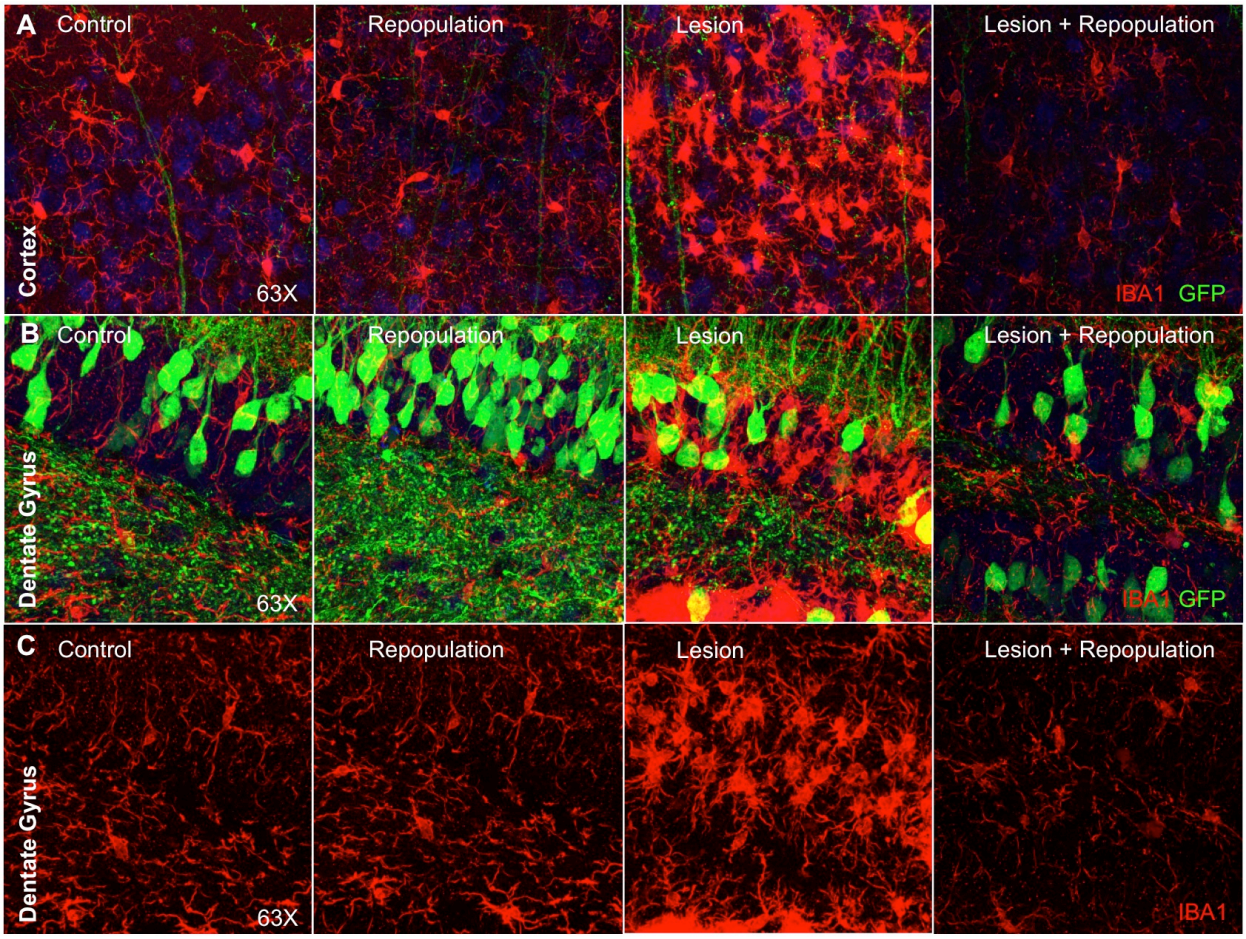

Figure 2.2 Repopulating microglia appear morphologically naïve***. A,*** 63X representative images of the cortex. ***B,*** 63X representative images of the dentate gyrus. ***C,*** Same images as in ***B***, but with the green channel removed for ease of IBA1 visualization. GFP^{+} neurons in green, IBA1 in red.

Lesion-induced increases in GFAP are normalized with microglial repopulation

Besides microglia, astrocytes are also capable of modulating inflammatory events in the CNS and are critical to neuronal health (Min et al., 2006; Saijo et al., 2009). We wanted to determine the effects of both lesioning and microglial repopulation on astrocyte populations. To do so, we probed fixed tissue with antibodies against GFAP and S100β, two canonical markers of astrocytes. We quantified the number of $GFAP^+$ cells and found that the number was greatly increased in the Lesion group of mice. Interestingly, the increase in $GFAP^+$ cells was attenuated in the Lesion + Repopulation group (Figure 2.3). Of note, the effects of lesioning and repopulation on GFAP immunoreactivity are identical to the effects found at the RNA level, described in the next section. Additionally, we observed a shift in the expression pattern of the S100β signal, whereby immunoreactivity was found intracellularly in non-lesioned groups of mice, and extracellularly in lesioned groups of mice. Therefore, we performed overall signal intensity measurements (arbitrary units) instead of S100β-positive cell counts, but found no differences in intensity among the groups. The noted change in expression pattern is in accordance with previous literature indicating that S100β can be secreted, and in doing so, acts as a trophic factor, during neuronal stress (Marshak, 1990; Kleindienst et al., 2005; Kleindienst and Ross Bullock, 2006).

Figure 2.3 Lesion-induced increases in GFAP are normalized with microglial repopulation: ***A,*** 10X representative images of S100β labeling (blue) and GFAP labeling (red). ***B,*** Quantification of GFAP-positive cells reveals an increase in Lesion mice that is not found in Lesion + Repopulation mice. ***C,*** Quantification of S100β intensity reveals no difference among groups. Error bars represent SEM, (n=5-6). $p<0.05$; † Control vs. Repopulation; * Control vs. Lesion; ϕ Repopulation vs. Lesion + Repopulation; # Lesion vs. Lesion + Repopulation.

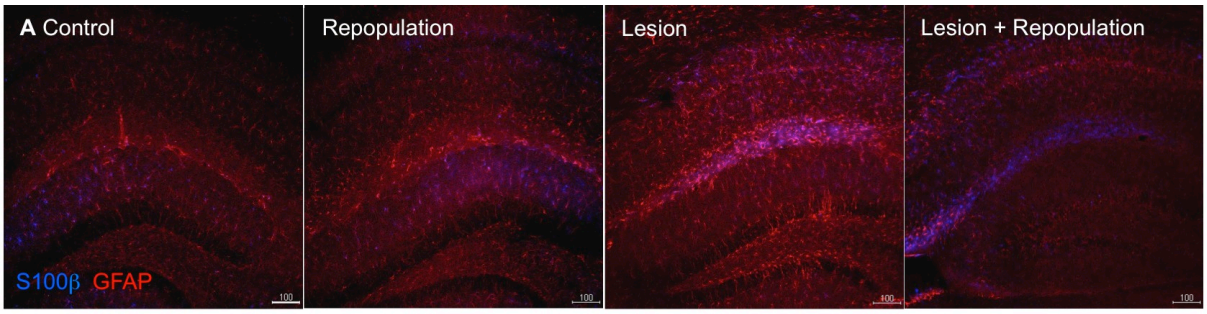

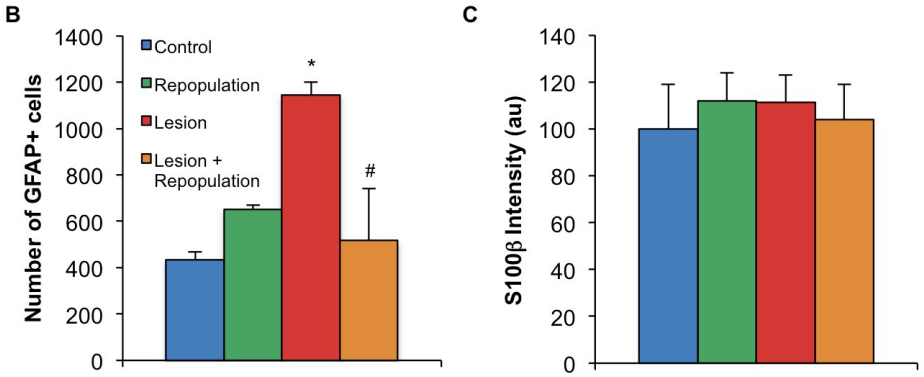

Microglial repopulation dampens lesion-induced inflammation

Having shown that microglial repopulation following extensive neuronal injury has dramatic effects on the localization and morphology of reactive microglia, we sought to determine the neuroinflammatory states of the brains by directly analyzing mRNA levels for 81 inflammatory-related genes, using Nanostring technology. We created a custom gene set encompassing an additional 101 genes related to neurodegeneration, synaptic plasticity, and learning and memory.

Among the AD-related genes, apolipoprotein E, and Cathepsin B, C, and D were all significantly increased in Lesion, compared to control, but this effect was attenuated in Lesion + Repopulation brains (Figure 2.4). Cathepsin proteins are involved in apoptosis, indicating that signaling through these cell death pathways is dampened with microglial

repopulation. Of the aging-related genes, annexin A5, cyclin-dependent kinase 2 and, and cycline-depedent kinase inhibitor 1C are significantly lowered in Lesion + Repopulation, compared to Lesion alone. Annexin A5 is involved in blood coagulation, while the cycline-dependent kinase proteins are involved in cell-cycle regulation and proliferation. Looking at plasticity-related genes, transcript levels of four are decreased with lesion, and three are increased with lesion. However, none of these effects are abrogated with post-lesion microglial repopulation. Finally, five neurotransmission-related genes are decreased with lesioning, while four are increased. Of these, only two lesion-associated increases are rescued by microglial repopulation—fibroblast growth factor 2 and the related fibroblast growth factor receptor 1, both of which are known to be upregulated by astrocytes with brain lesion (Clarke et al., 2001). While many of the lesion-induced changes in these genes are sustained even with microglial repopulation, a different pattern emerges when looking at inflammation-related genes.

Transcript levels of 26 inflammation-related genes are significantly increased in the Lesion group, but restored to control levels in the Lesion + Repopulation group (Figure 2.4). These genes encode proteins involved in complement and other immune response pathways, monocyte chemoattraction, leukocyte endothelial transmigration, microglia proliferation and survival, microglia-mediated phagocytosis, and apoptotic cell death pathways. Thus, microglial elimination followed by repopulation appears to mostly resolve chronic neuroinflammatory events in the CNS, and demonstrates that repopulating cells do not inherit the activation state of the replaced cells. Thus, chronic microglial responses are not simply due to the environmental cues, but are inherit within the cells themselves, explaining why indigenous microglia often fail to resolve insults.

Figure 2.4 Microglial repopulation dampens inflammatory signaling following neuronal lesion: Nanostring technology was employed to assess RNA transcript levels of 182 ***A,*** AD-, ***B,*** aging-, ***C,*** plasticity-, ***D,*** neurotramission-, and ***E,*** inflammation-related genes. Levels have been normalized to control, set at 100%. Error bars represent SEM, (n=4). $p<0.05$; † Control vs. Repopulation; * Control vs. Lesion; ϕ Repopulation vs. Lesion + Repopulation; # Lesion vs. Lesion + Repopulation.

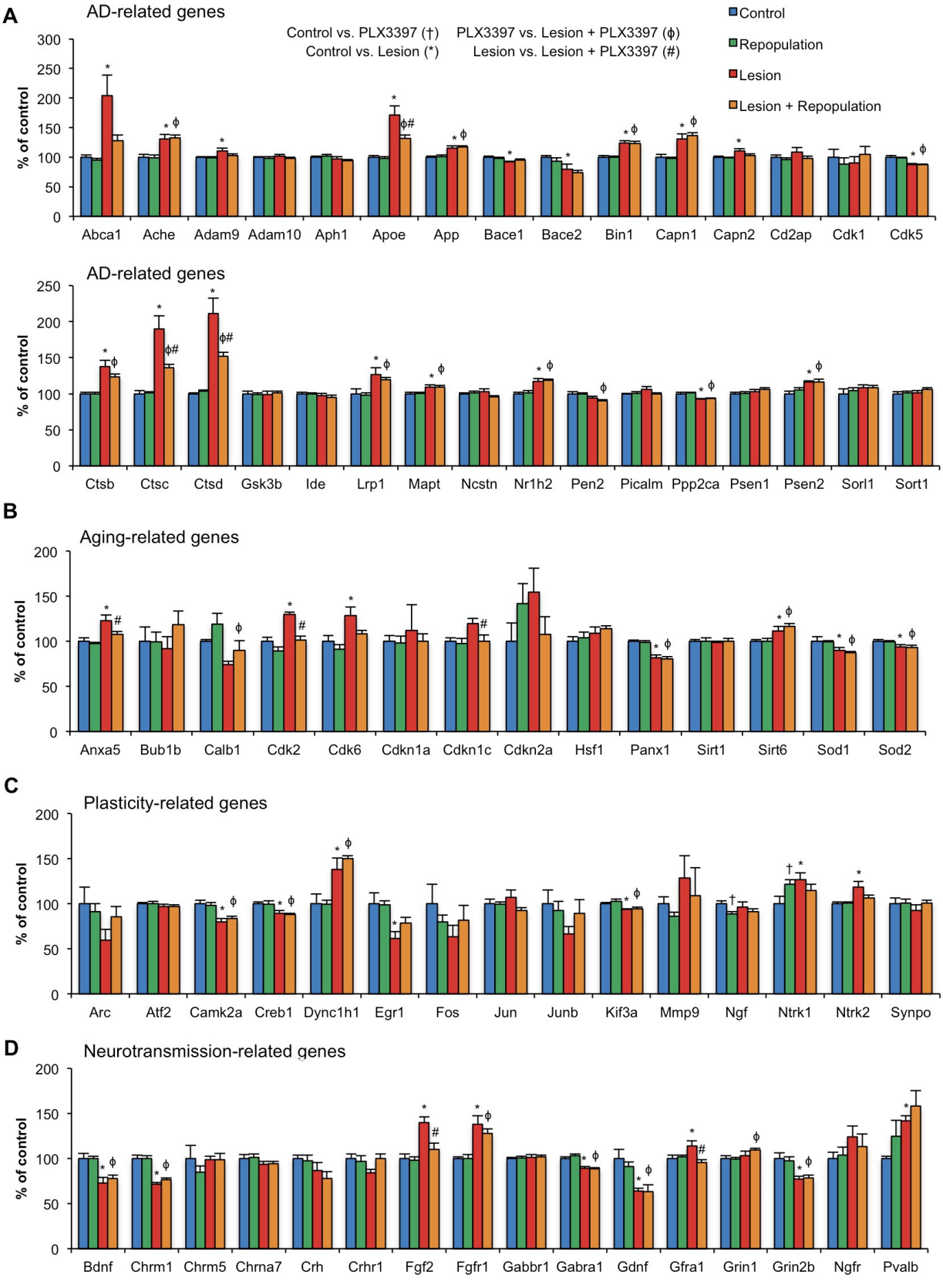
A
AD-related genes
Control vs. PLX3397 (†)
Control vs. Lesion (*)
PLX3397 vs. Lesion + PLX3397 (ϕ)
Lesion vs. Lesion + PLX3397 (#)
Control
Repopulation
Lesion
Lesion + Repopulation
% of control
Abca1 Ache Adam9 Adam10 Aph1 Apoe App Bace1 Bace2 Bin1 Capn1 Capn2 Cd2ap Cdk1 Cdk5
AD-related genes
Ctsb Ctsc Ctsd Gsk3b Ide Lrp1 Mapt Ncstn Nr1h2 Pen2 Picalm Ppp2ca Psen1 Psen2 Sorl1 Sort1
B
Aging-related genes
Anxa5 Bub1b Calb1 Cdk2 Cdk6 Cdkn1a Cdkn1c Cdkn2a Hsf1 Panx1 Sirt1 Sirt6 Sod1 Sod2
C
Plasticity-related genes
Arc Atf2 Camk2a Creb1 Dync1h1 Egr1 Fos Jun Junb Kif3a Mmp9 Ngf Ntrk1 Ntrk2 Synpo
D
Neurotransmission-related genes
Bdnf Chrm1 Chrm5 Chrna7 Crh Crhr1 Fgf2 Fgfr1 Gabbr1 Gabra1 Gdnf Gfra1 Grin1 Grin2b Ngfr Pvalb

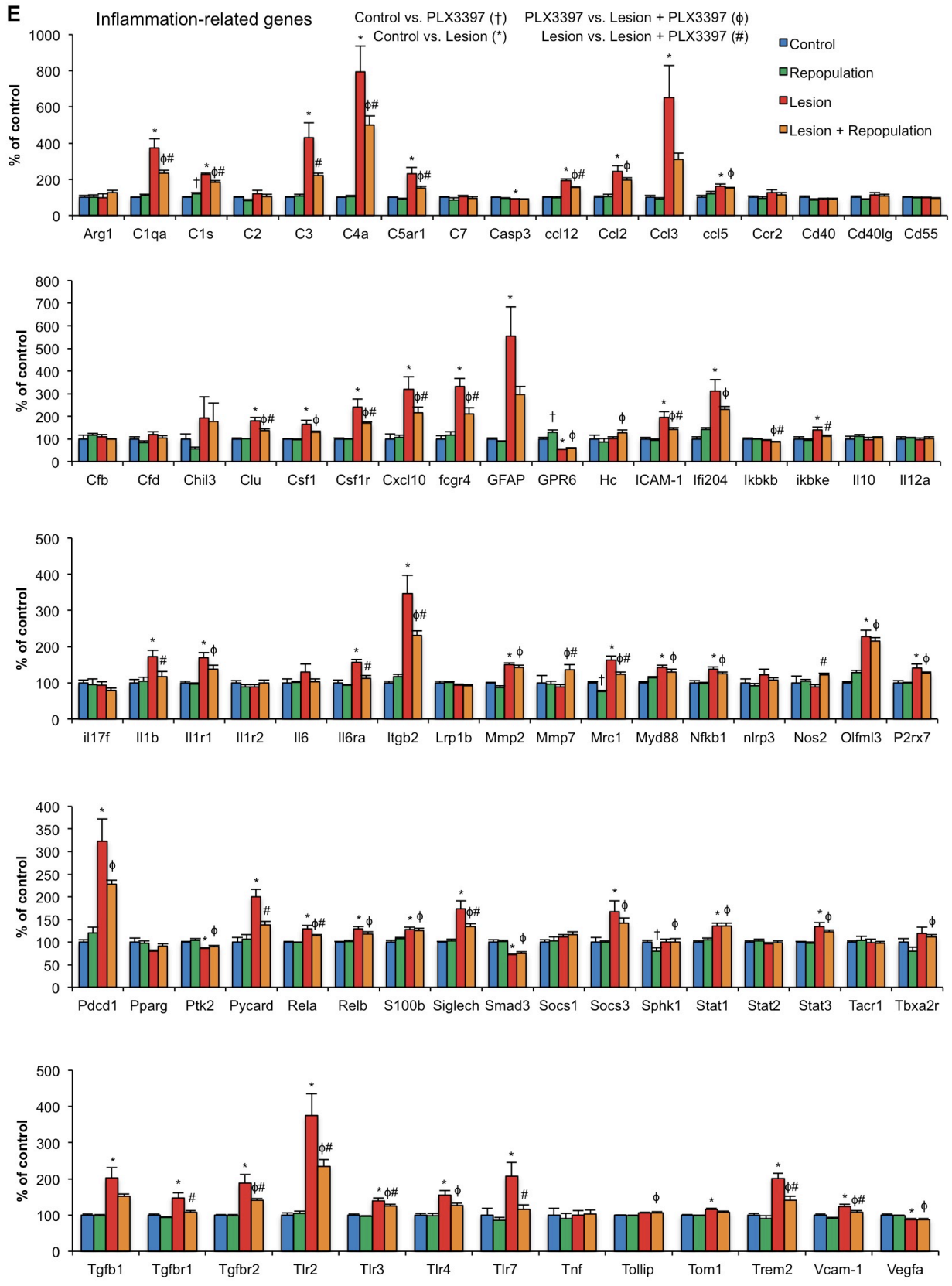
E
Inflammation-related genes
Control vs. PLX3397 (†)
Control vs. Lesion (*)
PLX3397 vs. Lesion + PLX3397 (ϕ)
Lesion vs. Lesion + PLX3397 (#)
Control
Repopulation
Lesion
Lesion + Repopulation
% of control
Arg1 C1qa C1s C2 C3 C4a C5ar1 C7 Casp3 ccl12 Ccl2 Ccl3 ccl5 Ccr2 Cd40 Cd40lg Cd55
Cfb Cfd Chil3 Clu Csf1 Csf1r Cxcl10 fcgr4 GFAP GPR6 Hc ICAM-1 Ifi204 Ikbkb ikbke Il10 Il12a
il17f Il1b Il1r1 Il1r2 Il6 Il6ra Itgb2 Lrp1b Mmp2 Mmp7 Mrc1 Myd88 Nfkb1 nlrp3 Nos2 Olfml3 P2rx7
Pdcd1 Pparg Ptk2 Pycard Rela Relb S100b Siglech Smad3 Socs1 Socs3 Sphk1 Stat1 Stat2 Stat3 Tacr1 Tbxa2r
Tgfb1 Tgfbr1 Tgfbr2 Tlr2 Tlr3 Tlr4 Tlr7 Tnf Tollip Tom1 Trem2 Vcam-1 Vegfa

Microglial repopulation increases total spine number

While microglial repopulation appears to be able to partially "reset" the inflammatory status of the inflamed/injured brain, we also hypothesized that the act of repopulation may confer additional beneficial effects on the brain. Given the similarities between repopulating microglia and microglia found during the developmental period, which are involved in synaptic sculpting and plasticity, we wondered if repopulation itself would modulate neuronal activity and morphologies. Inherent in the design of our experiment, we had included the Thy1-GFP-M transgene in order to explore how repopulation affects the synaptic landscape. Thus, we imaged non-primary apical dendrites of pyramidal neurons in the CA1 hippocampal layer of all four groups of mice. Additionally, we imaged neurons in the CA1 of mice that were sacrificed following 14 days of PLX5622 treatment in order to determined if any repopulation-related alterations in spine numbers were due to microglial repopulation itself, or due to the elimination that must precede such repopulation. Subsequent counting and classification of spines revealed that the 14 day treatment with PLX5622 greatly increased total spine number, specifically by increasing thin and mushroom spines (Figure 2.5). Importantly, these effects are maintained, but not increased, in the Repopulation and Lesion + Repopulation groups of mice.

Figure 2.5 Microglial repopulation results in increased dendritic spine density: Elimination alone increases mushroom and thin spines, though this effect is negated when repopulation occurs in combination with lesion. Spine numbers are normalized to 10 μm of dendrite length. Error bars represent SEM, (n=5-7). *p<0.05, **p<0.01, ***p<0.005, ****p<0.0001.

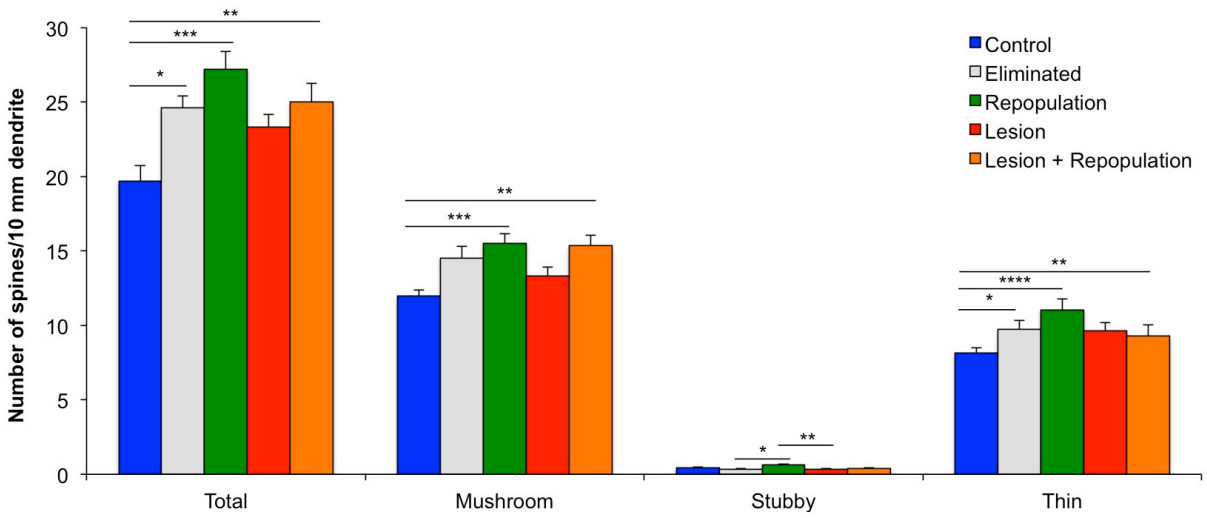

Microglial repopulation rescues behavioral deficits induced by neuronal lesion

In our experimental paradigm, we have withdrawn CSF1R inhibitor treatment to repopulate the brain with new microglia following extensive neuronal loss. Here, we find that the repopulating cells appear relatively ramified, even in the presence of a lesioned brain, and confer large reductions in inflammatory signaling. Therefore, we sought to understand if microglial repopulation could also improve functional outcomes in lesioned mice. We first tested mice on the elevated plus maze, a measure of anxiety-related behaviors. Mice in the Lesion group spent significantly more time in the exposed arms of the maze, and significantly less time in the open arms of the maze, compared to mice in the Control group (Fig 2.6 A). Importantly, mice that underwent microglial repopulation following lesion performed identically to that of control mice, indicating that the repopulation of the microglia compartment is sufficient to rescue lesion-induced deficits in this task. Mice were additionally tested by the Morris water maze task, a measure of learning and memory, commonly thought to be dependent on the hippocampus. On day 5 of training, mice in the Lesion group exhibited significantly

increased latencies to find the platform, compared to control mice (Figure 2.6 C). However, mice in the Lesion + Repopulation group displayed no such deficit. No statistically significant differences were found among any of the groups during the probe trial, although a clear tendency of the Lesion group to perform most poorly was observed. Finally, we assesses motor function, via accelerating rotarod and swim speed during the Morris water maze. Although lesioning had a significant effect on accelerating rotarod performance, mice in all four groups exhibited similar swim speeds in the water maze (Figures 2.6 B and D).

Figure 2.6 Microglial repopulation restores lesion-induced deficits on behavioral tasks ***A,*** Lesion mice spend significantly more time in open arms and less time in closed arms, but Lesion + Repopulation mice perform identically to controls. ***B,*** Lesioned mice exhibit significantly shorter times to fall during accelerating rotarod testing. ***C,*** Lesion mice take significantly more time to find the platform, compared to Control. However, Lesion + Repopulation mice perform similar to control groups. ***D,*** No significant differences in swim speed exist among groups of mice. ***E,*** Though not significant, Lesion mice cross the platform location fewer times than all other groups. ***F,*** Though not significant, Lesion mice take longer to find the platform location than all other groups. Error bars represent SEM, (n=9-11). $p<0.05$; † Control vs. Repopulation; * Control vs. Lesion; ϕ Repopulation vs. Lesion + Repopulation; # Lesion vs. Lesion + Repopulation.

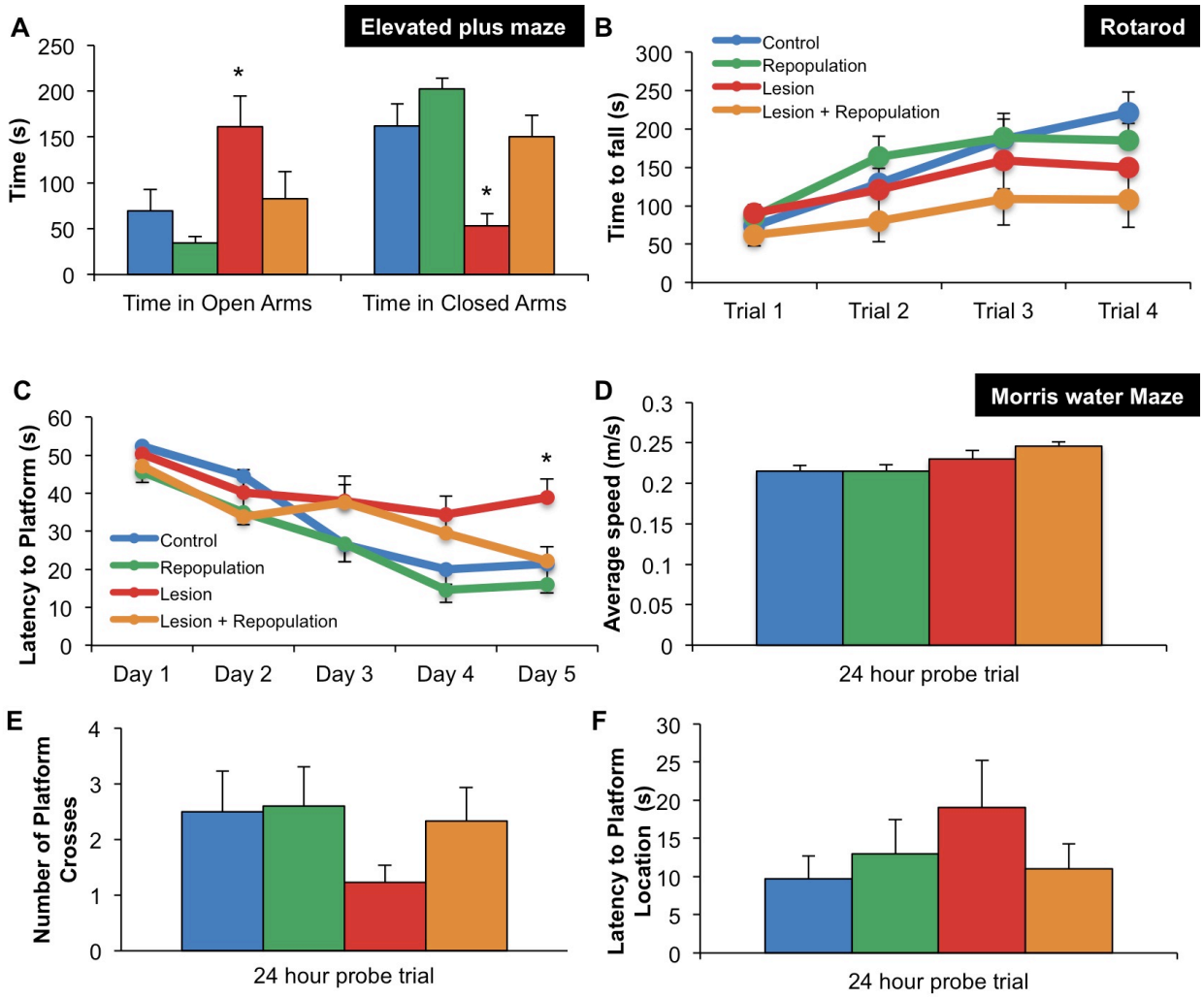
A
Elevated plus maze
Time (s)
250
200
150
100
50
0
*
*
Time in Open Arms
Time in Closed Arms
B
Rotarod
Control
Repopulation
Lesion
Lesion + Repopulation
Time to fall (s)
300
250
200
150
100
50
0
Trial 1
Trial 2
Trial 3
Trial 4
C
Latency to Platform (s)
60
50
40
30
20
10
0
*
Control
Repopulation
Lesion
Lesion + Repopulation
Day 1
Day 2
Day 3
Day 4
Day 5
D
Morris water Maze
Average speed (m/s)
0.3
0.25
0.2
0.15
0.1
0.05
0
24 hour probe trial
E
Number of Platform Crosses
4
3
2
1
0
24 hour probe trial
F
Latency to Platform Location (s)
30
25
20
15
10
5
0
24 hour probe trial

DISCUSSION

Microglia become primed with age and injury, often fail to resolve insults, and instead, remain chronically activated. Researchers have tried to attenuate age- and insult-related microglial activation using non-steroidal anti-inflammatory drugs (NSAIDS) and the microglia-specific inhibitor minocycline. Prophylactic NSAID use is likely beneficial, as lifetime use of NSAIDs is inversely correlated with risk of developing Alzheimer's disease (Stewart et al., 1997; Etminan et al., 2003). However, clinical trials have not found any disease- or behavior-modifying effects of NSAIDS in individuals already diagnosed with AD. Results of minocycline studies are mixed, even within the same experimental model (Plane et al., 2010). In one study, researchers treated rats with minocycline 30 days after a spinal cord injury to reduce microglia-mediated pain (Hains and Waxman, 2006). For the duration of treatment, the researchers were successful in deactivating microglia and reducing pain. However, as soon as researchers withdrew minocycline, the pain returned. Such results illustrate the likely futility of treating major insults with anti-inflammatories, as their effects only last as long as they are given. As in that study, microglia are likely to resort to activation following severe neuronal insult unless an NSAID or minocycline is chronically employed. Unfortunately, such a treatment regimen would risk the health of other organs. Specifically, adults over 75 years of age are advised against chronic NSAID due to the increased risks of gastrointestinal bleeding, ulcers, increased blood pressure, stroke, heart attack, heart failure, and kidney impairment (Marcum and Hanlon, 2010). For these reasons, we sought to develop a clinically feasible approach for the long-term reduction of microglial activation.

Although previous findings by our lab indicated that microglial elimination, via CSF1R inhibition, is beneficial for post-injury outcomes, we do not foresee the indefinite elimination of an entire cell population to be a realistic therapeutic approach. However, our discovery that the microglial compartment can fully repopulate itself upon withdrawal of CSF1R inhibitor treatment allows for the swift elimination and subsequent repopulation of microglia, and this, we believe, represents a clinically viable approach to resetting the inflammation state of the brain.

Critically, our data reveal that we can renew the microglial compartment, even in the face of massive inflammation. In doing so, we dampen inflammatory signaling and at least partially “reset” the microglia, as they are fewer in number and no longer displayed an activated, amoeboid morphology. Of the 81 inflammation-related gene transcripts we analyzed, 46 were significantly increased ($p<0.05$) in lesion mice that maintained their original microglia. However, 29 of the 46 lesion-induced increases in pro-inflammatory transcripts were significantly reduced when microglia were repopulated following lesion. Given that these analyses were carried out 45 days after expression of DT_A ceased, we believe these results demonstrate the long-term resolution of inflammation, and that more time between lesion cessation and analysis would only reveal a further reduction in pro-inflammatory signaling.

A reduction in dendritic spine numbers is observed in many neurological conditions, including mental retardation, schizophrenia, depression, stroke, epilepsy, substance abuse, and neurodegeneration (Calabrese et al., 2006; Penzes et al., 2011). In our studies, we find that microglial elimination, via 14-day treatment with PLX5622, is accompanied by a robust increase in dendritic spines. This effect is sustained with

microglial repopulation, both in the healthy and lesioned brain, though spine numbers are not significantly increased beyond the effect of elimination alone. Therefore, microglial repopulation by itself does not appear to increase dendritic spine numbers. However, it is critical to bear in mind that microglial repopulation cannot proceed without first eliminating microglia. Future studies will need to be carried out in order to determine if microglial elimination, followed by subsequent repopulation, can induce spine increases in other types of injury/disease models, or if our results are broadly applicable to all types of insults.

As the CSF1R inhibitors developed by Plexxikon have progressed to Phase 3 clinical trials and are well tolerated in treated individuals, we hope that microglial repopulation, via CSF1R inhibitor treatment and withdrawal, can offer a realistic and permanent solution to chronic inflammation and improve functional outcomes in individuals who have suffered a severe brain insult.

CHAPTER THREE

AGE-RELATED DOWNREGULATION OF THE $CaV_{3.1}$ T-TYPE CALCIUM CHANNEL AS A MEDIATOR OF AMYLOID BETA PRODUCTION

INTRODUCTION

As Alzheimer's disease (AD) disproportionately affects the aged population, it is imperative to understand what changes in the brain with aging to allow for the accumulation of pathology and subsequent deficits in cognition. In addition to microglia-derived inflammation, cellular calcium dyshomeostasis is an established hallmark of both aging and Alzheimer's disease (AD), and is thought to play a role in not only disease initiation, but also progression (Landfield and Pitler, 1984; Lopez et al., 2008; Green, 2009). Age- and disease-related changes in various calcium channels, receptors, and pumps have been shown to contribute to changes in processing of the amyloid precursor protein (APP), namely increases in production of the toxic beta-amyloid peptide (Aβ) (Green et al., 2008; Oules et al., 2012). Such an increase in Aβ levels can further increase calcium dyshomeostasis in a vicious, feed-forward cycle, ultimately resulting in cell death (Resende et al., 2008; Demuro et al., 2011) While discrete components of calcium signaling have been studied, a comprehensive overview of age- and AD-related changes in components of calcium signaling has not been carried out to date. We have queried a human microarray data set that demonstrate the breadth of changes in calcium-related genes between young non-demented (20-59) and aged non-demented (60-99) individuals, and aged non-demented (60-99) and demented (74-95) individuals. Moreover, we have identified a dramatic and consistent age-related reduction in the expression of the *cacna1g* gene,

which encodes the $CaV_{3.1}$ T-type calcium channel. A further reduction in expression of *cacna1g* is observed with AD, identifying this gene as a potential mediator of calcium dysregulation that contributes to cognitive decline.

Heretofore, T-type calcium channels have been largely unexplored in the context of Alzheimer's disease. While the expression and activity of high-voltage activated calcium (HVAC) channels such as L-type channels are known to change with age, and these channels have been historically implicated in AD-associated calcium dysregulation, T-type calcium channels represent a unique class of voltage-activated calcium channels (Thibault and Landfield, 1996; Anekonda et al., 2011). T-type calcium channels are expressed widely throughout the brain, as well as in other excitable cells of the body and constitute a group of low voltage-activated calcium (LVAC) channels composed of three different subtypes— $CaV_{3.1}$, $CaV_{3.2}$, and $CaV_{3.3}$, encoded by the genes *cacna1g*, *cacna1h*, and *cacna1i*, respectively. Unlike HVAC channels, T-type calcium channels require only minimal membrane depolarizations and conduct modest amounts of Ca^{2+} into the cell. As a result of their gating kinetics, a subset of T-type channels remain tonically active at resting membrane potential, allowing Ca^{2+} to flow into the cell. Because T-type calcium channels conduct small amounts of calcium into the cell near resting membrane potential and further depolarize the membrane, HVAC channels may become activated as a result (Perez-Reyes, 2003). Due to these properties, T-type calcium channels have been described as being "ideally suited for regulating neuronal excitability" (Iftinca, 2011). Currently, T-type calcium channel blockers are found to be ameliorative for a variety of conditions including epilepsy, essential tremor, and neuropathic pain, and the role the channels play in autism, vasodilation, sleep cycle

regulation, and tumor cell cycle regulation continues to be investigated (Dogrul et al., 2003; Anderson et al., 2005; Oshima et al., 2005; Splawski et al., 2006; Astori et al., 2011; Quesada et al., 2011; Brodie et al., 2012; Rim et al., 2012).

The significance of understanding the consequences of age- and AD-related T-type channel downregulation is three-fold. First, as researchers are investing effort into blocking T-type channels toward the goal of managing the previously mentioned conditions, it is critical to know if the $CaV_{3.1}$ channel is a target that disappears with age, rendering T-type calcium channel blockers less effective. Second, FDA-approved T-type channel blockers such as trimethadione and ethosuximide already exist for absence seizures and more indications in which T-type calcium channels are implicated are becoming apparent, calling for further investigation in humans. It is critical to understand if administration of T-type blockers to humans is creating a pro-amyloidogenic environment in the brain, as this could render an individual more susceptible to developing AD. Finally, if $CaV_{3.1}$ downregulation is a major initiating factor for the increased production of the toxic Aβ peptide, then the $CaV_{3.1}$ T-type calcium channel represents a novel target for preventative therapeutics in Alzheimer's disease.

MATERIALS AND METHODS

Human microarray data

Human tissue samples

Human tissue samples were obtained and RNA purified as previously described (Cribbs et al., 2012). Briefly, tissue samples were taken from 57 individuals categorized as non-demented young (20-59 years old) or non-demented aged (60-99 years old) and from

26 individuals categorized as having Alzheimer's disease (74-95 years old). Brain regions included entorhinal cortex (EC), hippocampus (HC), posterior cingulate gyrus (PCG), and superior frontal gyrus (SFG). More details on group statistics have been previously reported (Cribbs et al., 2012).

Microarray analysis

Microarray analysis and validation was carried out as previously described (Cribbs et al., 2012). A correlation test was performed with GraphPad Prism software to determine the degree of correlation between age and *cacna1g* mRNA expression level.

Immunoblot Assays

Western blot of brain homogenates

Half brains were flash frozen on dry ice following extraction from the mouse. The cerebellum was removed and the remaining brain was homogenized in 150 mg/ml Tissue Protein Extraction Reagent (Thermo Scientific) with Complete Mini Protease Inhibitor Cocktail tablets (Roche) and Phosphatase 2 Inhibitor Cocktail (Sigma-Aldrich). Homogenates were subsequently centrifuged at 44,000 rpm for one hour at 4°C, yielding soluble protein fractions. A protein quantification assay was performed to determine protein concentration of each sample (Bio-Rad). 20 μg of protein was loaded per well with reducing agent and sample buffer. For quantification of $CaV_{3.1}$ expression in nontransgenic and triple transgenic (3xTg-AD) mice, protein homogenates were run on 3-8% Tris-Acetate gels with Tris-Acetate SDS running buffer (Invitrogen). All other samples were run on 4-12% Bis-Tris gels with MES SDS running buffer (Invitrogen). Proteins were transferred to 0.02 μm nitrocellulose membranes, which were blocked in 5% nonfat milk in Tris-buffered saline supplemented with 0.2% Tween-20. Membranes

were probed with specific primary antibodies. Primary antibodies used were: rabbit anti-$CaV_{3.1}$ (1:1000, Alomone, Jerusalem, Israel), rabbit anti-CT20 APP for full length APP, C99, C89, and C83 (1:3000, Calbiochem), rabbit anti-ADAM10 (1:1000,Millipore), rabbit anti-BACE (1:1000, Millipore), mouse anti-HT7 (1:1000, Pierce), mouse anti-AT270 (1:1000, Pierce), rabbit anti-phospho Tau ser199/202 (1:1000, Millipore), rabbit anti-Cdk5 (Millipore), mouse anti-GSK-3β (BD Biosciences), rabbit anti-phospho GSK-3α/β ser21/9 (Cell Signaling), rabbit anti-p35 C-terminus, mouse anti-spectrin (Millipore), rabbit anti-calpain 1 (1:1000, Cell Signaling), rabbit anti-calpain 2 (1:1000, Cell Signaling), rabbit anti-actin (1:10,000, Sigma-Aldrich), rabbit anti-GAPDH (1:10,0000, Sigma-Aldrich). Membranes were incubated with goat anti-rabbit (1:10,000, Sigma-Aldrich) or goat anti-mouse (1:5000, Sigma-Aldrich) HRP-conjugated secondary antibodies for visualization. Steady state levels of protein expression were quantified via densitometric analysis and normalized to actin or GAPDH expression.

Western blot of cell lysates

N2a and HEK269 cells were rinsed with ice-cold PBS and lysed in Mammalian Protein Extraction Reagent (Thermo Scientific) with Complete Mini Protease Inhibitor tablet (Roche) by centrifuging at 14,000 rpm for 10 minutes at 4°C. Protein concentration of samples was determined as stated in previous section. 20 μg of protein was loaded into each well of 4-12% Bis-Tris Gels and gels were run with MES SDS running buffer (Invitrogen). Gels were transferred and probed as described above. Primary antibodies used were: rabbit anti-$CaV_{3.1}$ (above), rabbit anti-CT20 for C99, C89, and C83 (above), rabbit anti-ADAM 10 (above), mouse anti-secreted APPα (1:500, Wako), and rabbit anti-actin (above).

Immunohistochemistry Analyses

DAB Analysis

Half of each mouse brain was drop-fixed in 4% paraformaldehyde and subsequently cryopreserved in 30% sucrose. Frozen half brains were sectioned at 40 μm on a freezing microtome. Free-floating sections were incubated in 30% H_2O_2 with methanol to quench endogenous peroxidase and then treated with 70% formic acid for four minutes. Sections were blocked in Tris-buffer saline supplemented with 0.1% Triton X100 (Sigma-Aldrich) and 2% bovine serum albumen (Sigma-Aldrich). Sections were incubated in mouse anti-6E10 (1:1000, Sigma-Aldrich) overnight and incubated with anti-mouse HRP-conjugated secondary (1:10,000, Sigma-Aldrich) supplemented with normal horse serum (Vector Labs). Deposition of DAB precipitate was achieved using the VECTASTAIN Elite ABC system (Vector Labs).

Thioflavin-S Analysis

Cryopreserved tissue sections were mounted on slides and allowed to dry overnight. Mounted tissue was washed in descending ethanol concentrations (100%, 95%, 70%, 50%) and incubated in 0.5% Thioflavin S (Sigma-Aldrich) solution in 50% ethanol. Slides were coverslipped and imaged on a Leica confocal microscope using Z-stacks. These stacks were then analyzed using Bitplane Imaris 7.42, to calculate the number and volumes of plaques.

ELISA Analyses

ELISA Analysis of Brain Homogenates

Soluble protein fractions were generated from half brains as described in 2.2.1. The remaining pellet was solubilized in half the volume of the initial pellet in TPER in 70%

formic acid and centrifuged again at 44,000 rpm for one hour at 4°C to yield an insoluble protein fraction. $A\beta_{1-40}$ and $A\beta_{1-42}$ levels were measured in the soluble and insoluble fractions as described in Green *et al*., 2008.

ELISA Analysis of Media from Cell Culture

Growth medium from N2a cells treated with NNC-55-0396 for 8 or 24 hours was collected at the time of cell collection and soluble $A\beta_{1-40}$ and $A\beta_{1-42}$ levels were measured as described in Green *et al*., 2008.

Cell Culture

N2a (Neuro 2A, ATCC) and HEK269 (APP expressing) cells were maintained in Dulbecco's Modified Eagle Medium (Invitrogen) supplemented with 10% fetal bovine serum (Invitrogen) and 1% penicillin/streptomycin (Invitrogen). Cells were subcultured every 3 days at 70-80% confluency and were discarded after 20 passages. For treatment, N2a cells were plated in 6-well plates at 300,000 cells/well (8 hour treatment) or 200,000 cells/well (24 hour treatment) and treated 24 hours later with PBS or NNC-55-0396 (5mM stock solution dissolved in 1X PBS) to a final concentration of 8 μM. Media were collected from the wells at the conclusion of treatment for ELISA analysis.

Cell Transfection

HEK269 cells were transiently transfected with pcDNA or cacna1g cDNA (Origene) using Lipofectamine 2000 reagent (Invitrogen). Expression was allowed to proceed for 72 hours before cells were collected.

Statistics

Analysis of microarray data was performed as previously described (Berchtold et al., 2008). R^2 and p values for gene expression correlations were calculated using

GraphPad Prism software. Student's unpaired t-tests were employed to determine p values in different treatments groups for the 3xTg-AD mice, N2a cells, and HEK269 cells.

RESULTS

CACNA1G mRNA expression is decreased in the human brain with age

Human microarray data was analyzed for 19 different calcium related genes, with three RNA probe sets for each gene, in four different regions of the brain—the entorhinal cortex (EC), the hippocampus (HC), the posterior cingulate gyrus (PCG), and the superior frontal gyrus (SFG). Analyses collapsed across the three probe sets revealed significant changes in mRNA expression levels with age across the four brain regions. 10 out of 19 genes were significantly changed with age compared to young controls in the EC, while expression levels of 13 out of 19 genes change with age in the HC (Figures 3.1 A and B). In the PCG and SFG, the vast majority of genes showed differences in expression levels with age, with 17 of 19 in the former and 18 of 19 in the latter (Figues 3.1 C and D). Noticeably, the expression levels of most genes decreased with age, though levels of expression for genes encoding ionositol triphosphate receptors (IP_3R) and ryanodine receptors (RyR) were consistently upregulated across the brain regions surveyed. Aside from expression levels of *calb1*, which encodes calbindin D28k, a calcium binding protein whose expression is known to decrease dramatically with age and Alzheimer's, the expression of *cacna1g*, a gene encoding the $CaV_{3.1}$ T-type calcium channel, was most conspicuously decreased in all four brain areas (Sequier et al., 1990; Riascos et al., 2011).

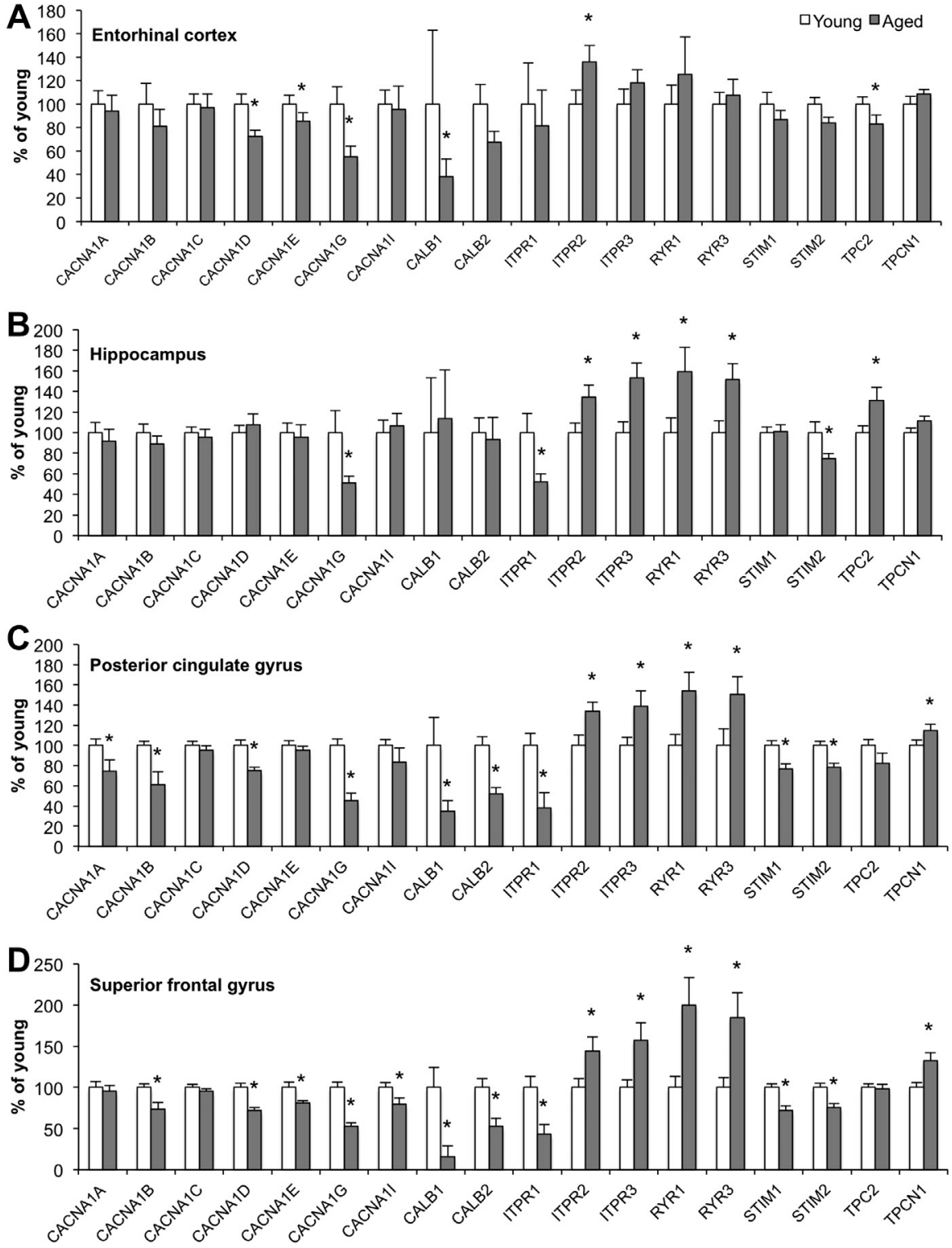

Figure 3.1 Human microarray data analysis of calcium-related genes as a function of age. Human microarray database included samples from young nondemented (20–59) and aged nondemented (74–95) individuals. Gene expression values for a single probe set for each gene are normalized to young controls in 4 different areas of the brain: entorhinal cortex (A; n = 21 young, 9 aged), hippocampus (B; n = 18 young, 16 aged), posterior cingulate gyrus (C; n = 18 young, 15 aged), and superior frontal gyrus (D; n = 22 young, 16 aged). Errors bars represent standard error of the mean.
* $p < 0.05$.

mRNA expression levels of this channel were reduced by 41%, 49%, 45% and 46% in the EC, HC, PCG, and SFG, respectively, when probe sets were collapsed across regions. Moreover, expanded data for all three RNA probe sets for *cacna1g* revealed consistent reductions in expression (Table 3.1).

Table 3.1 Expression levels of human cacna1g as a function of age. Expanded data with all 3 probes reveal significant decreases in cacna1g expression in all four brain areas. Key: EC, entorhinal cortex; HC, hippocampus; PCG, posterior cingulate gyrus; SFG, superior frontal gyrus. a: $p<0.05$; b: $p<0.01$; c: $p<0.001$.

Probe	211315_s_at	210380_s_at	207869_s_at
EC			
Young	100.00	100.00	100.00
Aged	52.38[a]	42.54[b]	47.88[a]
HC			
Young	100.00	100.00	100.00
Aged	75.46[a]	54.02[a]	48.54 (p = 0.058)
PCG			
Young	100.00	100.00	100.00
Aged	62.10[c]	55.81[c]	54.45[c]
SFG			
Young	100.00	100.00	100.00
Aged	62.86[c]	55.23[c]	50.31[c]

As age-related changes in this channel in the brain have not previously been reported or suggested, we sought to determine if such dramatic changes were further exaggerated in the presence of Alzheimer's disease. Analysis revealed significant and inverse correlations between age and *cacna1g* expression.Importantly, this age-related downregulation held true when tissue from individuals with AD were also included (Figures 3.2 A-D). Moreover, two of three probes revealed *cacna1g* expression to be significantly decreased in the AD brain compared to aged, non-demented controls in the HC, a region critical for learning and memory that degenerates relatively early in the course of Alzheimer's disease (Figure 3.2 E) (de Leon et al., 1989).

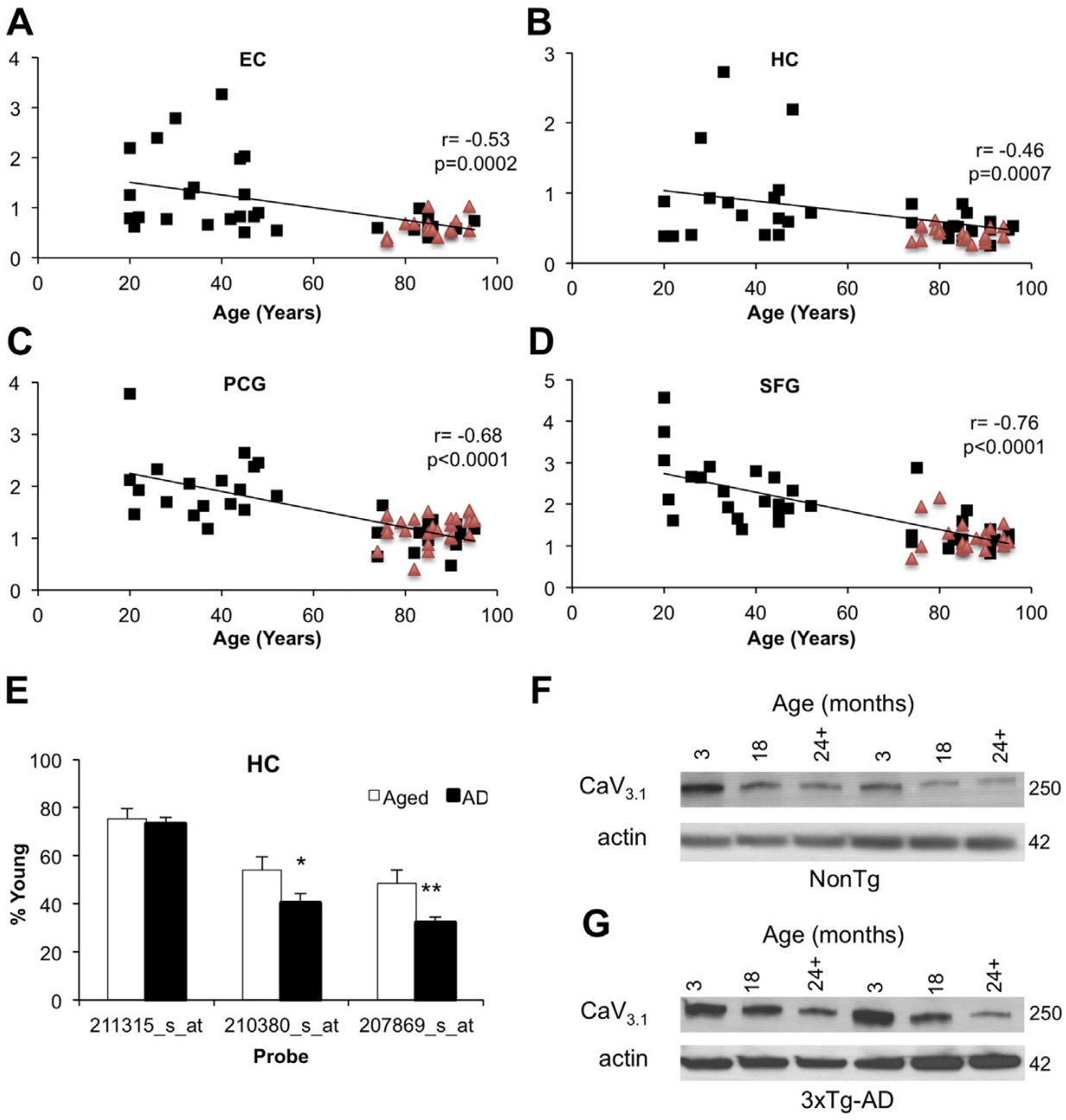

Figure 3.2 Correlation between cacna1g expression and age and Alzheimer's disease (AD). Significant and inverse relationships exist between age and cacna1g expression in the entorhinal cortex (n = 45, p = 0.0002), hippocampus (n = 52, p = 0.0007), posterior cingulate gyrus (n = 57, p < 0.0001), and then superior frontal gyrus (n = 59, p < 0.0001) (A–D). Two of 3 probe sets in the hippocampus reveal significant age-related decreases in AD brains compared with aged brains (E; n = 18 AD, n = 16 aged). Steady state levels of the $CaV_{3.1}$ T-type calcium channel are decreased with age in nontransgenic (top) and 3xTg-AD mice (bottom) (F). * p < 0.05, ** p < 0.01. Abbreviation: AD, Alzheimer's disease.

Steady state levels of $CaV_{3.1}$ decrease with age in brains of WT and 3xTg-AD mice

We wanted to determine if the downregulation of T-type channel mRNA expression held true at the protein level, and going forward, we aimed to manipulate this channel in mice. We therefore assessed steady state levels of $CaV_{3.1}$ by Western blot analysis in the 3xTg-AD transgenic mouse model of AD and nontransgenic controls (NTg) for these mice. We found a robust, age-related decrease in expression of this channel in both NTg and 3xTg-AD mice (Figure 3.2 F and G), confirming the age-related decline of this channel is maintained at both the mRNA and protein level.

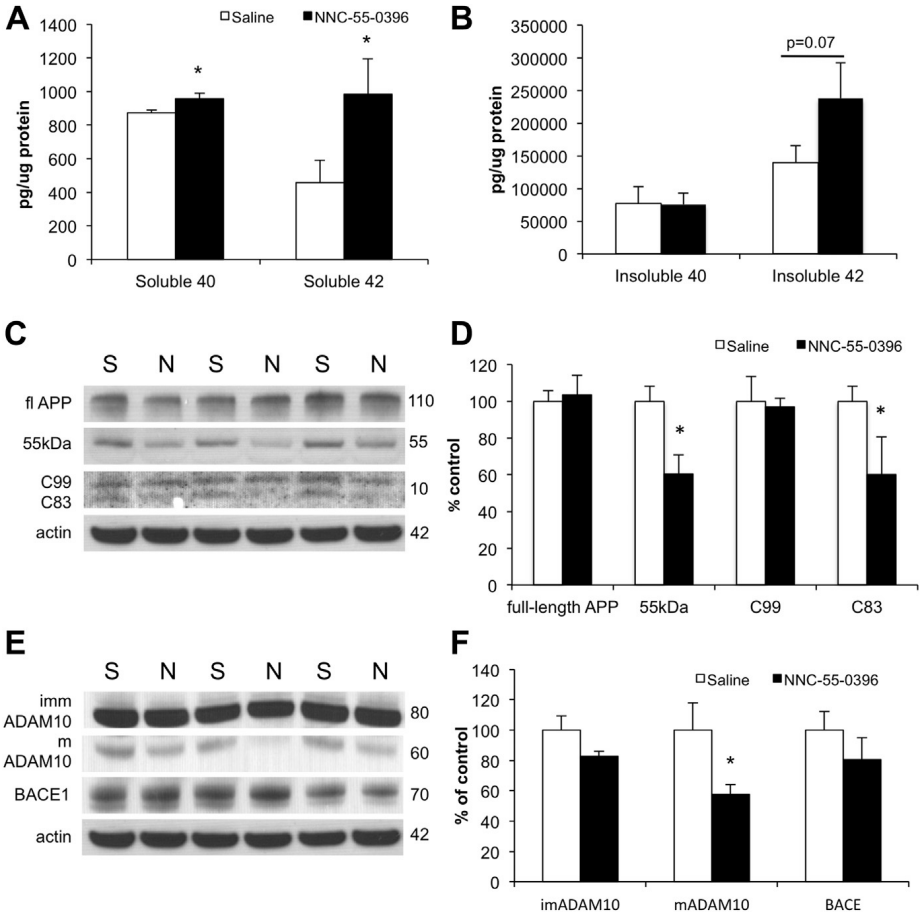

Figure 3.3 NNC-55-0396 decreases non-amyloidogenic processing, resulting in increased Aβ production. Treatment with NNC-55-0396 increased soluble levels of $A\beta_{1\text{-}40}$ and $A\beta_{1\text{-}42}$ in 3xTg-AD mice, while levels of insoluble $A\beta_{1\text{-}42}$ trended toward an increase (A–B). Western blot showed levels of full length amyloid precursor protein (APP) were unchanged with treatment, but a 55kDa C-terminal fragment and C83 were both significantly decreased (C, quantified in D). T-type channel inhibition decreased levels of mature ADAM10, though no changes in immature ADAM10 or BACE1 were found (E, quantified in F). * $p < 0.05$. Abbreviation: APP, amyloid precursor protein.

$CaV_{3.1}$ blockade results in increased Aβ production

To explore the consequences of T-type channel reductions with age, we next used pharmacological inhibitors of the channels to mimic the aged brain. 14-16 month-old female 3xTg-AD mice were injected intraperitoneally every other day for two weeks with 20 mg/kg NNC-55-0396 dissolved in PBS and controls were injected with an equal volume of PBS (Saline n=9; NNC-55-0396 n=8). NNC-55-0396 in a highly selective T-type calcium channel blocker (7 uM vs. >100uM IC_{50} for $CaV_{3.1}$ T-type vs. L-type calcium channels, respectively). Importantly, NNC-55-0396 is not readily processed by cells to create an active metabolite capable of inhibiting L-type calcium channels, unlike its analog Mibefradil (Huang et al., 2004). The dose was chosen based on previous literature demonstrating efficacy of NNC-55-0396 in a mouse model of essential tremor (Quesada et al., 2011). Despite a relatively short treatment, ELISA analysis revealed significant increases in both $A\beta_{1-40}$ and $A\beta_{1-42}$ in the TPER-soluble fraction of the brain homogenates, and a trend toward an increase (p=0.07) in $A\beta_{1-42}$ in the 70% formic acid-soluble (insoluble) fraction of the brain homogenates (Figures 3.3 A and B). This increase in Aβ production was accompanied by decreases in the C83 C-terminal fragment of APP, a product of non-amyloidogenic processing, and a 55kDa C-terminal fragment of APP (Figures 3.3 C and D). Furthermore, the mature proteolytically active form of the α-secretase ADAM10 was decreased with T-type channel blockade, while no changes in steady state levels of the β–secretase BACE1 were observed with treatment (Figures 3.3 E and F). It is likely the decrease in mature ADAM10 that underlies the decrease in C83 production. Together, these data demonstrate the T-type channel blockade reduces non-amyloidogenic processing, shifting the equilibrium

toward the amyloidogenic processing pathway, and in turn, produces higher levels of the Aβ peptide.

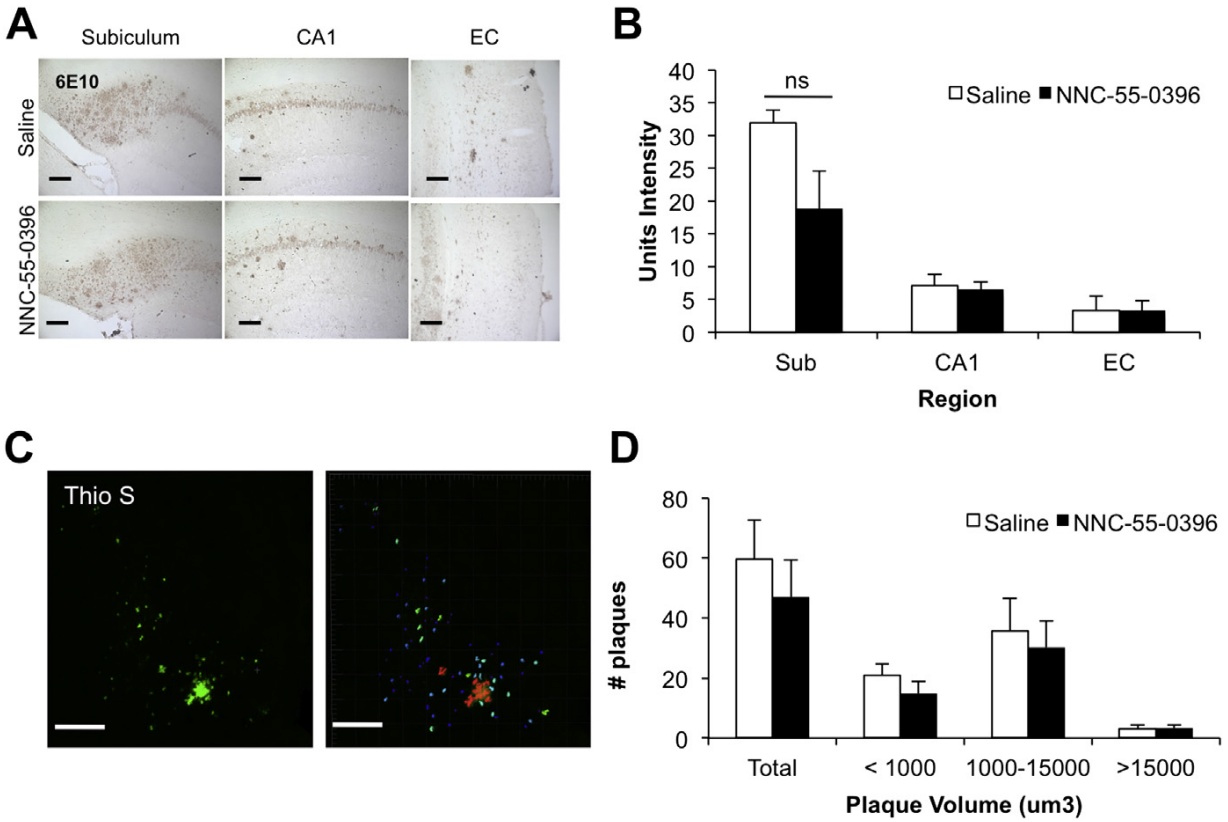

Figure 3.4 T-type channel inhibition does not affect plaque load in 3xTg-AD mice. Plaque load as assessed by 6E10 staining in the subiculum (Hsieh et al.), CA1, and entorhinal cortex (EC) revealed no significant differences between untreated and treated animals (A–B). A representative picture of thioflavin-S staining for dense core plaques on the left, categorized by plaque volume using Imaris BitPlane software on right revealed no significant changes between groups (C–D). Abbreviations: EC, entorhinal cortex; Sub, subiculum.

T-type channel blockade does not alter plaque load in 3xTg-AD mice

We looked by immunohistochemistry to determine if plaque load was altered in mice treated with NNC-55-0396. Probing with 6E10, we did not detect any differences in plaque number in the subiculum, CA1, or entorhinal cortex. We further investigated the number of dense core plaques between saline and NNC-55-0396 treated mice by staining with Thioflavin-S and using BitPlane Imaris software to segregate and color

code plaques by volume (Figure 3.4 C is a representative image of a brain slice stained for Thio-S and subsequently processed with Imaris). Figure 3.4 D reveals no significant differences in plaque number between groups, regardless of plaque volume categorization.

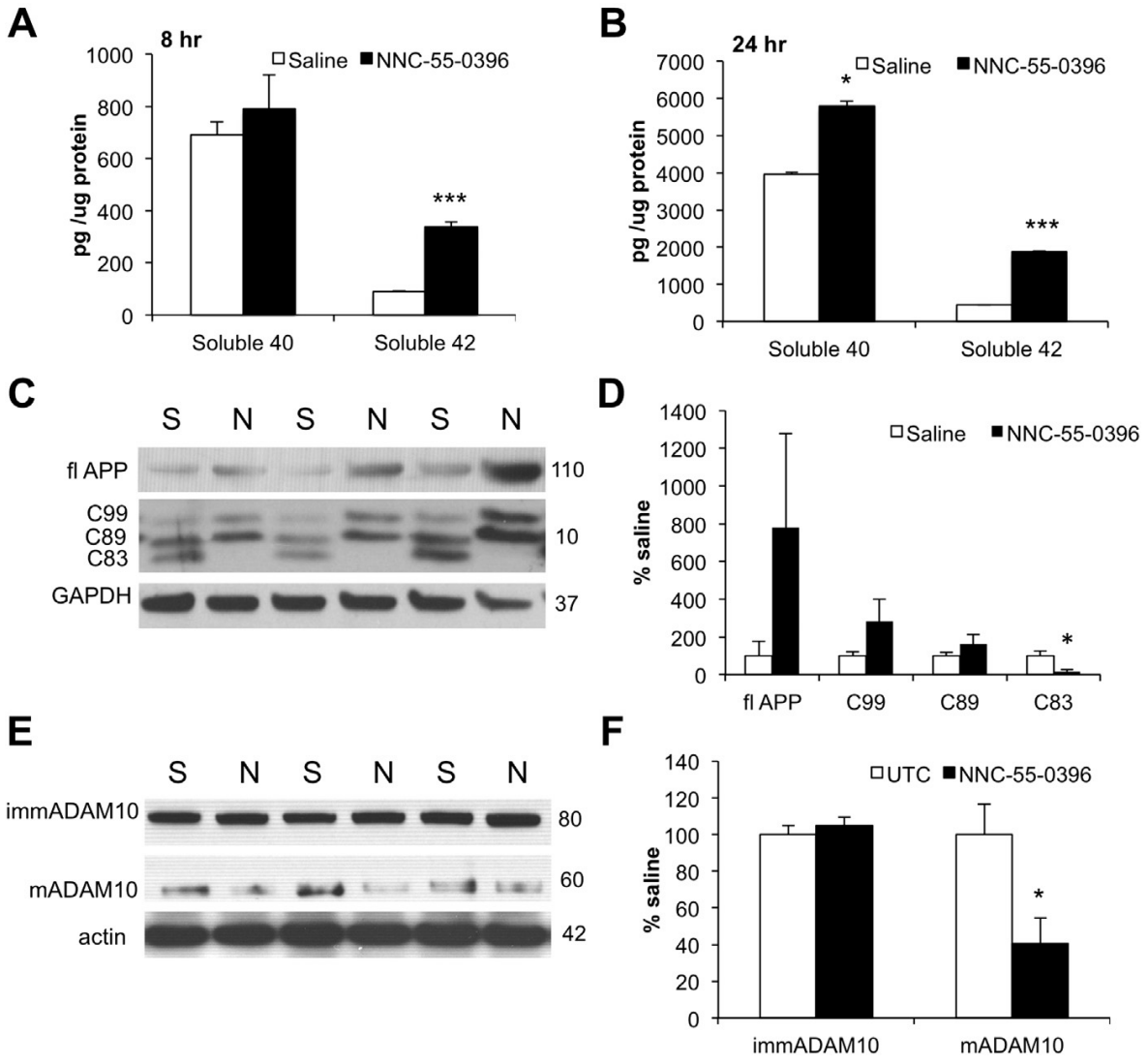

Figure 3.5 The effects of NNC-55-0396 are recapitulated in N2a cells. N2a cells treated with 8 μM NNC-55-0396 for 8 hours secrete significantly more Aβ1-42, while 24 hour treatment results in significant increases in both Aβ1-40 and Aβ1-42 (A–B). Eight hours of T-type channel inhibition insignificantly increases full-length amyloid precursor protein (APP) levels and significantly decreases levels of C83 (C–D). As in the 3xTg-AD mice, decreases in C83 were accompanied by decreases in mature ADAM10, without changes in BACE1 levels with 8 hours of treatment (E–F). * $p < 0.05$, *** $p < 0.001$. Abbreviation: APP, amyloid precursor protein.

The effects of T-type channel blockade on APP processing are recapitulated in a murine neuroblastoma cell line

To confirm the changes in APP processing *in vitro*, we treated the murine N2a cell line with 8 μM NNC-55-0396 for 8 and 24 hours. With 8 hours of treatment, soluble $A\beta_{1-42}$ was significantly increased, as determined by a sandwich ELISA (Figure 3.5 A). By 24 hours, levels of both soluble $A\beta_{1-40}$ and $A\beta_{1-42}$ were significantly increased in cells treated with the T-type channel inhibitor compared to those treated with saline (Figure 3.5 B). While steady state levels of full-length APP (fl APP) were increased, levels of the C83 C-terminal fragment of APP were dramatically reduced with just 8 hours of treatment with NNC-55-0396 (Figure 3.5 C). We speculate that the increase in fl APP is due to reduced cleavage by α-secretase, thereby leaving a larger pool of APP unprocessed. Given that T-type channel inhibition increased Aβ levels and decreased C83 in both the 3xTg-AD mice and the N2a cell line, we sought to determine if the underlying changes in APP processing were maintained *in vivo*. Indeed, we observed a decrease in mature ADAM10 in cells treated with the blocker, confirming the inhibitory nature of T-type channel blockade on ADAM10 maturation both *in vitro* and *in vivo*.

$CaV_{3.1}$ overexpression increases non-amyloidogenic processing in HEK269 cells

We next wanted to ensure that the effects of NNC-55-0396 on APP processing are due to the effects on the T-type calcium channels and not an off-target effect of the compound. To determine this, we overexpressed pcDNA or *cacna1g* cDNA in HEK cells expressing APP for 72 hours. We achieved a 74% increase in $CaV_{3.1}$ expression, which coincided with an almost three-fold increase in secreted APP-alpha (sAPPα), as measured from media collected at 72 hours (Figure 3.6 A). As sAPPα is a product of α-

secretase processing, this suggests that overexpression of the T-type calcium channel increases non-amyloidogenic processing, opposite the effects seen with inhibition. Moreover, a trend toward an increase in mature ADAM10 was also seen with $CaV_{3.1}$ overexpression (Figures 3.6 A and B). While this change is not statistically significant, it is not entirely surprising, as NNC-55-0396 blocks all three T-type calcium channels—$CaV_{3.1}$, $CaV_{3.2}$, and $CaV_{3.3}$—and therefore indicates the $CaV_{3.1}$ is likely not the sole T-type channel mediating the effects on APP processing. We attempted both siRNA and shRNA knockdown of *cacna1g* in N2a and HEK269 cells, but were unable to achieve robust reductions in steady state levels of the channel, perhaps due to a long half-life or numerous alternative splice variants (Emerick et al., 2006).

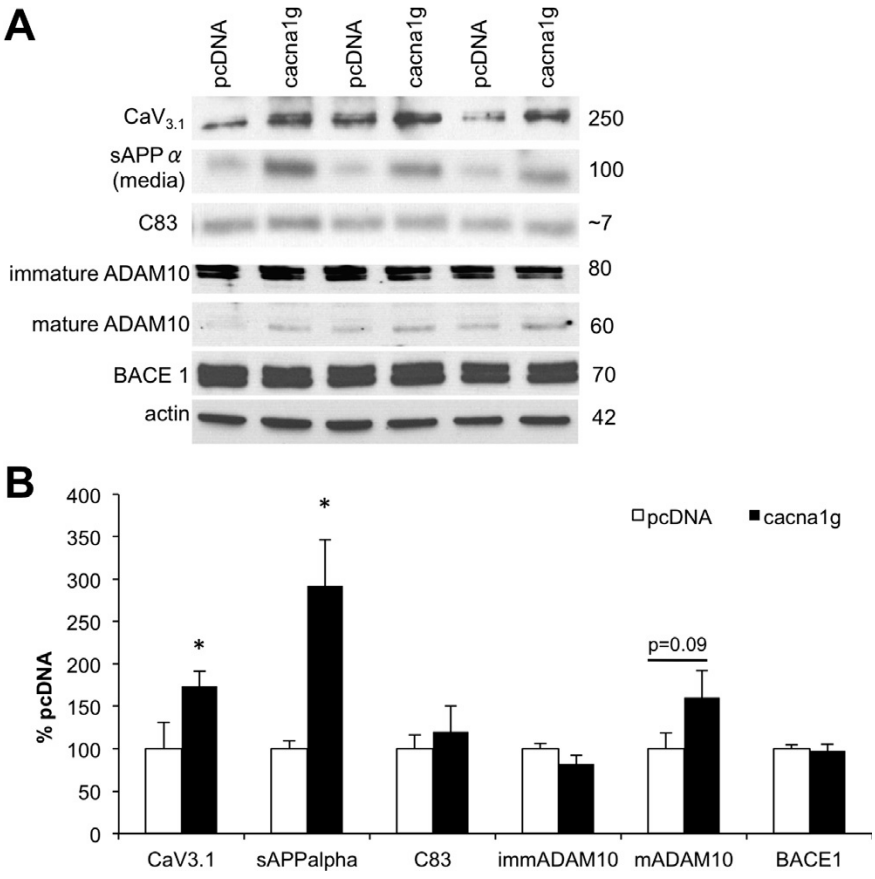

Figure 3.6 Overexpression of cacna1g produces complementary effects to NNC-55-0396 in HEK69 cells. We achieved a 74% overexpression of the $CaV_{3.1}$ T-type channel in HEK269 cells, which coincided with a significant increase in secreted APPα and a trend toward an increase in mature ADAM10 levels, while BACE1 levels remained unchanged (A, quantified in [B]). * $p \leq 0.05$.

Short-term T-type channel inhibition does not alter tau phosphorylation, despite decreasing p25

Despite dramatic changes in APP processing seen in 3xTg-AD mice with NNC-55-0396 treatment, there were no observable changes to total or phosphorylated levels of tau. Indeed, no differences were noted when probing with HT7 for total tau. Likewise, no changes were found when probing with AT270, an antibody recognizing tau phosphorylated at threonine 181, a marker of paired helical filaments (PHF). Finally, tau can be phosphorylated at serine 199 by GSK3β and serine 202 by GSK3β, as well as Cdk5, two putative tau kinases (Morioka et al., 2006). An antibody detecting these phosphorylation sites again demonstrated no differences. Finally, levels of GSK3 phosphorylated at serines 9 and 21, an AKT-mediated event that can inhibit GSK3 activity, were unchanged (Figure 3.7 A) (Cross et al., 1995).

Although we did not find changes in total or phosphorylated levels of tau, nor in total or phosphorylated levels of Cdk5 or GSK3β, we found a striking downregulation in p25 production (Figure 3.7 B). Typically, p35, a short-lived protein, associates with Cdk5 to limit its activity and location in the cell (Patrick et al., 1998). However, with age and neurodegeneration, increased calpain activity leads to increased cleavage of p35 to p25, a degradation-resistant and promiscuous regulator of Cdk5 that allows for its extended activity and aberrant cellular localization as a kinase, ultimately resulting in tau hyperphosphorylation and neuronal death (Patrick et al., 1999; Cruz et al., 2003). To confirm that this decrease in p25 production was a result of a reduction in calpain activity, we probed for α-spectrin, a 250 kDa protein in the brain that yields a 150 kDa calpain-specific cleavage fragment (Veeranna et al., 2004). We found an 80% reduction

in the spectrin breakdown product (SBDP150), indicating a downregulation of calpain-mediated cleavage. In probing for steady state levels of calpains, we found a trending reduction in calpain 1 (p=0.08) and a significant reduction in calpain 2, distinguished by calcium concentrations required for activity (micromolar and millimolar, respectively).

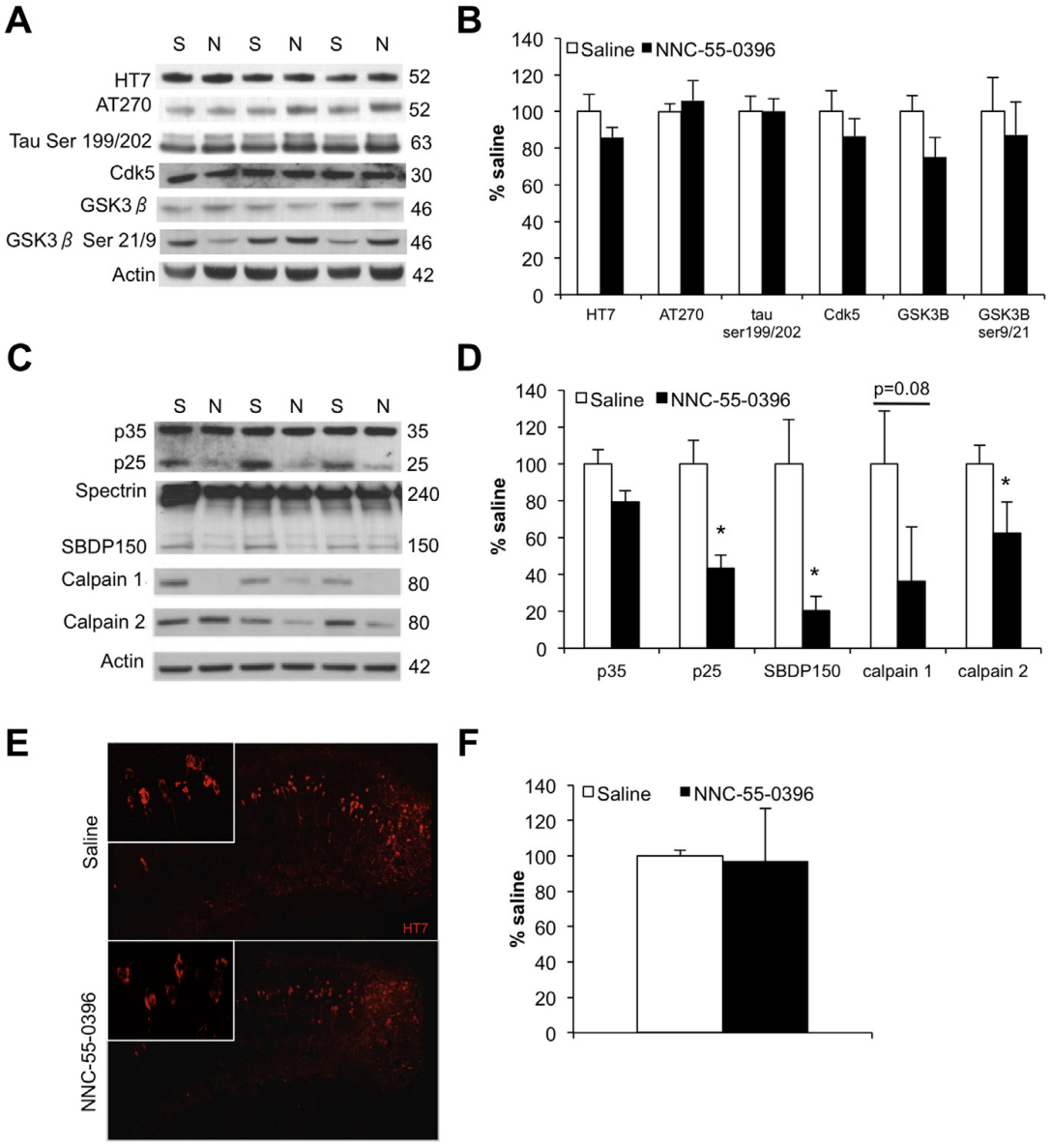

Figure 3.7 T-type channel inhibition reduces calpain-mediated cleavage, does not change tau pathology in 3xTg-AD mice. T-type channel inhibition had no effect on total or phosphorylated levels of tau, or total or phosphorylated levels of Cdk5 or GSK3β, as determined by western blotting (A, quantified in [B]). Immunofluorescent staining for HT7 in the hippocampus also revealed no differences (E, quantified in [F]). Levels of p25 and the calpain-specific spectrin breakdown product (SBDP150) were significantly decreased with NNC-55-0396 treatment, likely because of a trend toward a decrease in calpain 1 levels and a significant decrease in calpain 2 levels (C, quantified in [D])

This finding is in line with previous literature reporting that treatment with the T-type channel blocker Mibefradil attenuates calpain 2 transcription at all time points surveyed (1, 3, 7, and 14 days) in the heart following a myocardial infarction, and reduces calpain 1 transcription at two of four time points (Sandmann et al., 2002).

DISCUSSION

We report age-related changes in expression levels in most of the 18 calcium-related genes surveyed across 4 brain regions. In terms of calcium-related proteins that have already been extensively studied, such as IP_3 and ryanodine receptors and calbindin d28K, our findings from human microarray data are relatively congruent with previously published findings. Expression profiles for genes encoding both IP_3Rs and ryanodine receptors revealed consistent age-related increases, which is in agreement with literature suggesting that augmentations in calcium signaling through both types of endoplasmic reticulum-bound calcium receptors contribute greatly to the calcium dyshomeostasis seen with age and Alzheimer's disease (Brodie et al., 2012). It is of note that age-related decreases in IP_3R density have been found in the cerebral cortex, albeit in rats (Martini et al., 1994). Of all gene expression levels surveyed, the gene encoding calbindin D28k was most significantly changed. Levels were decreased by between 65% and 79% in the EC, PCG, and SFG. Additionally, both probes for calbindin revealed significant decreases (85% and 86%) in hippocampal tissue from AD brains compared with tissue from aged controls brains (data not shown). These findings are in accordance with the idea that calbindin immunoreactivity is reduced in the hippocampus with AD and correlates with pathology, and cognitive impairment (Palop et

al., 2003; Lopez et al., 2008; Iftinca, 2011). On the whole, our results underscore the extent of age-related changes in calcium handling and lend credence to the calcium hypothesis of Alzheimer's disease.

Focusing more narrowly, our findings inform us that the age-related decreases in $CaV_{3.1}$ expression in the brain, and the use of pharmacologic agents that block this channel, could mediate increases in amyloid production that initiate a cascade of toxic cellular events in the brain. Despite the potentially positive outcomes of T-type blockade for tau pathogenesis, it is widely accepted that Aβ production precedes tau hyperphosphorylation, leading us to postulate that the use of T-type channel inhibitors in the middle-aged adult could produce a highly amyloidogenic environment in the brain that initiates pathogenesis and could not be offset by a concurrent reduction in tau phosphorylation, as this appears to be a downstream event.

Beyond these data serving as a cautionary tale for the use of T-type channel blockers, our findings related specifically to cacna1g represent the discovery of another gene capable of mediating age- and AD-related Aβ production, and is a novel opportunity to intervene in the course of aberrant aging processes. Going forward, we aim to identify ways by which expression of the cacna1g gene is downregulated with age in the brain, and how we may be able to upregulate expression or activity. Literature from the cancer field identifies cacna1g as a tumor suppressor gene and implicates age-related cacna1g promoter hypermethylation and the resulting decrease in expression in a variety of peripheral cancers (Toyota et al., 1999; Dogrul et al., 2003; Garcia-Baquero et al., 2013). Interestingly, a novel compound ST101 was found to inhibit Aβ generation and improve cognition in 3xTg-AD mice, and its mechanism of action was recently revealed

to be through enhancement of T-type calcium channels (Green et al., 2011).

Troublingly, support has recently emerged for clinical trials using T-type channel blockers to treat Alzheimer's, after some successes with L-type blockers in animal models of AD, despite disappointing results in human clinical trials (Lopez-Arrieta and Birks, 2000). Moreover, the belief that antihypertensive use reduces the risk dementia remains controversial, and a recent database study of antihypertensives found that while angiotensin converting enzyme inhibitor and beta-blocker use was inversely associated with incident dementia, calcium channel blocker use was positively associated with cognitive deficits (Wagner et al., 2012).

In summary, the efficacy of calcium channel blockers for the prevention or treatment of Alzheimer's disease is not convincing, and more importantly, they may actually lead to deleterious results, including an increased risk of cancer and dementia. Our results suggest that age- and disease-related downregulation of the $Ca_V3.1$ T-type calcium channel is conducive to amyloid production and that the use of T-type channel blockers should be critically reviewed for its potential as a pro-amyloidogenic agent, at least in patients of middle or older age. Further efforts to understand both what causes the downregulation of and how to enhance the activity of T-type channels in the aged brain may yield novel therapeutic strategies for the prevention of Alzheimer's disease.

DISSERTATION CONCLUDING REMARKS

Microglia are the immunocompetent cells of the central nervous system and represent the first line of defense against pathogens, comprising ~12% of cells in the brain. At rest, microglia survey the entire brain parenchyma each hour (Nimmerjahn et al., 2005). Upon neural insult or invasion by a pathogenic species, microglia become activated, assuming an amoeboid morphology and favoring secretion of pro-inflammatory cytokines such as TNF-α, IL-1β, and IL-6. Ultimately, microglia take on an anti-inflammatory role, secreting molecules such as IL-4 and IL-10, as part of the resolution and repair process (Colton and Wilcock, 2010). Unfortunately, following severe insults such as traumatic brain injuries, and over the course of neurodegenerative conditions, microglia are unable to resolve these neuroinflammatory events and instead remain chronically activated, secreting neurotoxic molecules that likely inhibit cognitive processes.

While microglia are well known for their role as the resident immune cells of the brain, another role as synaptic architects has more recently emerged. In the developing brain, microglia are involved in activity-dependent pruning by phagocytosing pre-synaptic inputs (Schafer et al., 2012). *Ex-vivo* evidence suggests that microglia can shape glutamatergic signaling at both pre- and post-synaptic sites, resulting in changes in the electrophysiological properties of primary P3-P7 neurons (Schafer et al., 2012; Ji et al., 2013). At a clinical level, aberrant numbers, signaling, and activation of microglia are found in neurodevelopment disorders such as Rett Syndrome and autism (ASD), and a single prenatal injection of LPS in a pregnant rat leads to communication and cognitive deficits in pups (Maezawa and Jin, 2010; Kirsten et al., 2012; Tetreault et al., 2012;

Suzuki et al., 2013). Although the effects of microglia on synaptic modeling in the developing brain are striking, it was previously unknown if microglia continue to serve the same role under homeostatic conditions in the adult brain.

Together, my dissertation aims to determine if microglia-mediated mechanisms contribute to functional deficits associated with extensive neuronal loss, such as is experienced with Alzheimer's disease, stroke, and TBI. Paramount to this line of inquiry, our lab discovered that microglia are physiologically dependent upon colony stimulating factor 1 receptor (CSF1R) signaling for their survival (Elmore et al., 2014). We can take advantage of this dependency through administration of CSF1R inhibitors for 7-21 days, which results in the elimination of virtually all microglia from the entire CNS. Microglia remain eliminated for the duration of treatment, be it days or months. Critically, withdrawal of CSF1R inhibitor treatment leads to brain-wide repopulation of microglia from a CNS-derived progenitor pool within 21 days (Elmore et al., 2014).

I first wanted to determine if microglia contribute to functional decline following a neuronal lesion, and so employed the CaM/Tet mouse model. Adult CaM/Tet mice inducibly express diphtheria toxin in forebrain excitatory neurons upon withdrawal of doxycycline from the diet, resulting in ~85% death of CA1 neurons. We then eliminated microglia for four weeks following doxycycline readministration, at which time the lesion ceased, in an effort to ameliorate lesion-induced deficits at both the molecular and behavioral levels. We found that lesioned mice performed poorly on elevated plus maze testing and on Day 5 of Morris water maze training, compared to non-lesioned mice. However, mice that were lesioned and subsequently had their microglia eliminated performed at the level of control mice. Moreover, lesioning increased the transcript

levels of many pro-inflammatory signaling molecules and altered the size and number of both synaptophysin and PSD-95 puncta. Again, microglial elimination following lesioning rescued these effects. These results indicate that microglia are involved in increased inflammatory signaling, as well as synaptic alterations associated with neuronal lesion.

Given the changes in synaptic surrogates, I performed further testing to determine if microglia continue to modulate dendritic spine numbers in the adult brain, as they do in development. I treated adult mice with PLX3397 for eight weeks to eliminate microglia and found a 35% global increase in dendritic spines. In another experiment, mice that underwent microglial repopulation boasted a 38% increase in total spine numbers in the CA1. To determine if such increase in spines are functionally relevant, we collaborated with the laboratory of Dr. Xiangmin Xu. Using LSPS technology, we ultimately found that microglial elimination greatly increases excitatory neuronal connectivity, albeit in two month-old mice. In accordance with these findings, I also performed experiments to determine if microglial elimination, by way of increased synaptic connectivity, lowered the kainic acid-induced seizure threshold in adult mice, and found this hypothesis to be confirmed. My findings indicate that microglia mediate neuronal connectivity, as well as the functional outputs of such, in the adult brain. Excitingly, microglial manipulation allows for the opportunity to modify adult neural networks, and could be researched in the context of many neurodevelopmental critical periods and disorders.

Because long-term or even acute microglial elimination may not be clinically feasible, I also investigated the ability of microglial repopulation to rescue/reduce lesion-induced deficits. Adult mice were treated with PLX5622 for 14 days to deplete microglia, and then treatment was withdrawn for 21 days to stimulate repopulation of the microglial

compartment. Again, the neuronal lesion increased pro-inflammatory transcript levels, increased the number of $GFAP^+$ astrocytes, and induced deficits in elevated plus maze and Morris water maze. Strikingly, all of these effects were rescued or improved with microglial repopulation, with some benefits even exceeding those of microglial elimination. Moreover, the repopulating microglia appeared morphologically naïve in many regions of the brain, indicating at least a partial resetting of this cellular compartment. This study provides the first evidence that repopulating microglia have improved functionality in the context of a neurological insult. Our lab seeks to further characterize repopulated microglia, as well as to determine their therapeutic benefit in other models of aging and injury.

Beyond microglial dysfunction and senescence, I investigated other ways by which age-related changes contribute to neurodegeneration. Previous work I carried out revealed that the $CaV_{3.1}$ T-type calcium channel is downregulated with aging, both in mice and humans. Critically, pharmacological downregulation of this channel suppresses non-amyloidogenic processing, ultimately resulting in increased beta-amyloid levels, while genetic overexpression of $CaV_{3.1}$ increases non-amyloidogenic processing.

Together, my dissertation provides key insights as to how age- and insult-related changes contribute to the progression of dysfunction in the brain. My findings, coupled with the progression of the CSF1R inhibitors we employed to Phase 3 clinical trials, support the idea that microglia can be safely and effectively manipulated to improve functionality in individuals suffering from the ravages of aging, disease, or neurodevelopmental disorders.

REFERENCES

Abou-Khalil R, Yang F, Mortreux M, Lieu S, Yu YY, Wurmser M, Pereira C, Relaix F, Miclau T, Marcucio RS, Colnot C (2014) Delayed bone regeneration is linked to chronic inflammation in murine muscular dystrophy. Journal of bone and mineral research : the official journal of the American Society for Bone and Mineral Research 29:304-315.

Ajami B, Bennett JL, Krieger C, Tetzlaff W, Rossi FM (2007) Local self-renewal can sustain CNS microglia maintenance and function throughout adult life. Nature neuroscience 10:1538-1543.

Alliot F, Godin I, Pessac B (1999) Microglia derive from progenitors, originating from the yolk sac, and which proliferate in the brain. Brain research Developmental brain research 117:145-152.

Anderson MP, Mochizuki T, Xie J, Fischler W, Manger JP, Talley EM, Scammell TE, Tonegawa S (2005) Thalamic Cav3.1 T-type Ca2+ channel plays a crucial role in stabilizing sleep. Proceedings of the National Academy of Sciences of the United States of America 102:1743-1748.

Anekonda TS, Quinn JF, Harris C, Frahler K, Wadsworth TL, Woltjer RL (2011) L-type voltage-gated calcium channel blockade with isradipine as a therapeutic strategy for Alzheimer's disease. Neurobiol Dis 41:62-70.

Association As (2012) Alzheimer's disease facts and figures. Alzheimer's and Dementia: The Journal of the Alzheimer's Association 8:131-168.

Astori S, Wimmer RD, Prosser HM, Corti C, Corsi M, Liaudet N, Volterra A, Franken P, Adelman JP, Luthi A (2011) The Ca(V)3.3 calcium channel is the major sleep spindle pacemaker in thalamus. Proceedings of the National Academy of Sciences of the United States of America 108:13823-13828.

Baglietto-Vargas D, Medeiros R, Martinez-Coria H, LaFerla FM, Green KN (2013) Mifepristone alters amyloid precursor protein processing to preclude amyloid beta and also reduces tau pathology. Biol Psychiatry 74:357-366.

Baird DM, Rowson J, Wynford-Thomas D, Kipling D (2003) Extensive allelic variation and ultrashort telomeres in senescent human cells. Nature genetics 33:203-207.

Barger SW, Harmon AD (1997) Microglial activation by Alzheimer amyloid precursor protein and modulation by apolipoprotein E. Nature 388:878-881.

Beers DR, Henkel JS, Xiao Q, Zhao W, Wang J, Yen AA, Siklos L, McKercher SR, Appel SH (2006) Wild-type microglia extend survival in PU.1 knockout mice with familial amyotrophic lateral sclerosis. Proceedings of the National Academy of Sciences of the United States of America 103:16021-16026.

Berchtold NC, Cribbs DH, Coleman PD, Rogers J, Head E, Kim R, Beach T, Miller C, Troncoso J, Trojanowski JQ, Zielke HR, Cotman CW (2008) Gene expression changes in the course of normal brain aging are sexually dimorphic. Proceedings of the National Academy of Sciences of the United States of America 105:15605-15610.

Beschorner R, Nguyen TD, Gozalan F, Pedal I, Mattern R, Schluesener HJ, Meyermann R, Schwab JM (2002) CD14 expression by activated parenchymal microglia/macrophages and infiltrating monocytes following human traumatic brain injury. Acta neuropathologica 103:541-549.

Brodie MJ, Ben-Menachem E, Chouette I, Giorgi L (2012) Zonisamide: its pharmacology, efficacy and safety in clinical trials. Acta neurologica Scandinavica Supplementum:19-28.
Butovsky O, Siddiqui S, Gabriely G, Lanser AJ, Dake B, Murugaiyan G, Doykan CE, Wu PM, Gali RR, Iyer LK, Lawson R, Berry J, Krichevsky AM, Cudkowicz ME, Weiner HL (2012) Modulating inflammatory monocytes with a unique microRNA gene signature ameliorates murine ALS. The Journal of clinical investigation 122:3063-3087.
Calabrese B, Wilson MS, Halpain S (2006) Development and regulation of dendritic spine synapses. Physiology 21:38-47.
Castello NA, Nguyen MH, Tran JD, Cheng D, Green KN, LaFerla FM (2014) 7,8-Dihydroxyflavone, a small molecule TrkB agonist, improves spatial memory and increases thin spine density in a mouse model of Alzheimer disease-like neuronal loss. PloS one 9:e91453.
Charo IF, Myers SJ, Herman A, Franci C, Connolly AJ, Coughlin SR (1994) Molecular cloning and functional expression of two monocyte chemoattractant protein 1 receptors reveals alternative splicing of the carboxyl-terminal tails. Proceedings of the National Academy of Sciences of the United States of America 91:2752-2756.
Chitu V, Nacu V, Charles JF, Henne WM, McMahon HT, Nandi S, Ketchum H, Harris R, Nakamura MC, Stanley ER (2012) PSTPIP2 deficiency in mice causes osteopenia and increased differentiation of multipotent myeloid precursors into osteoclasts. Blood 120:3126-3135.
Chodobski A, Zink BJ, Szmydynger-Chodobska J (2011) Blood-brain barrier pathophysiology in traumatic brain injury. Translational stroke research 2:492-516.
Clarke WE, Berry M, Smith C, Kent A, Logan A (2001) Coordination of fibroblast growth factor receptor 1 (FGFR1) and fibroblast growth factor-2 (FGF-2) trafficking to nuclei of reactive astrocytes around cerebral lesions in adult rats. Molecular and cellular neurosciences 17:17-30.
Colton C, Wilcock DM (2010) Assessing activation states in microglia. CNS & neurological disorders drug targets 9:174-191.
Combrinck MI, Perry VH, Cunningham C (2002) Peripheral infection evokes exaggerated sickness behaviour in pre-clinical murine prion disease. Neuroscience 112:7-11.
Coniglio SJ, Eugenin E, Dobrenis K, Stanley ER, West BL, Symons MH, Segall JE (2012) Microglial stimulation of glioblastoma invasion involves epidermal growth factor receptor (EGFR) and colony stimulating factor 1 receptor (CSF-1R) signaling. Mol Med 18:519-527.
Corrigan JD, Selassie AW, Orman JA (2010) The epidemiology of traumatic brain injury. The Journal of head trauma rehabilitation 25:72-80.
Cribbs DH, Berchtold NC, Perreau V, Coleman PD, Rogers J, Tenner AJ, Cotman CW (2012) Extensive innate immune gene activation accompanies brain aging, increasing vulnerability to cognitive decline and neurodegeneration: a microarray study. Journal of neuroinflammation 9:179.

Cross DA, Alessi DR, Cohen P, Andjelkovich M, Hemmings BA (1995) Inhibition of glycogen synthase kinase-3 by insulin mediated by protein kinase B. Nature 378:785-789.
Cruz JC, Tseng HC, Goldman JA, Shih H, Tsai LH (2003) Aberrant Cdk5 activation by p25 triggers pathological events leading to neurodegeneration and neurofibrillary tangles. Neuron 40:471-483.
Dai XM, Ryan GR, Hapel AJ, Dominguez MG, Russell RG, Kapp S, Sylvestre V, Stanley ER (2002) Targeted disruption of the mouse colony-stimulating factor 1 receptor gene results in osteopetrosis, mononuclear phagocyte deficiency, increased primitive progenitor cell frequencies, and reproductive defects. Blood 99:111-120.
Damani MR, Zhao L, Fontainhas AM, Amaral J, Fariss RN, Wong WT (2011) Age-related alterations in the dynamic behavior of microglia. Aging cell 10:263-276.
de Groot CJ, Huppes W, Sminia T, Kraal G, Dijkstra CD (1992) Determination of the origin and nature of brain macrophages and microglial cells in mouse central nervous system, using non-radioactive in situ hybridization and immunoperoxidase techniques. Glia 6:301-309.
De I, Nikodemova M, Steffen MD, Sokn E, Maklakova VI, Watters JJ, Collier LS (2014) CSF1 overexpression has pleiotropic effects on microglia in vivo. Glia 62:1955-1967.
de Leon MJ, George AE, Stylopoulos LA, Smith G, Miller DC (1989) Early marker for Alzheimer's disease: the atrophic hippocampus. Lancet 2:672-673.
Demuro A, Smith M, Parker I (2011) Single-channel Ca(2+) imaging implicates Abeta1-42 amyloid pores in Alzheimer's disease pathology. The Journal of cell biology 195:515-524.
Derecki NC, Cronk JC, Lu Z, Xu E, Abbott SB, Guyenet PG, Kipnis J (2012) Wild-type microglia arrest pathology in a mouse model of Rett syndrome. Nature 484:105-109.
Dilioglou S, Cruse JM, Lewis RE (2003) Function of CD80 and CD86 on monocyte- and stem cell-derived dendritic cells. Experimental and molecular pathology 75:217-227.
Dogrul A, Gardell LR, Ossipov MH, Tulunay FC, Lai J, Porreca F (2003) Reversal of experimental neuropathic pain by T-type calcium channel blockers. Pain 105:159-168.
Elmore MR, Najafi AR, Koike MA, Dagher NN, Spangenberg EE, Rice RA, Kitazawa M, Matusow B, Nguyen H, West BL, Green KN (2014) Colony-stimulating factor 1 receptor signaling is necessary for microglia viability, unmasking a microglia progenitor cell in the adult brain. Neuron 82:380-397.
Elmore MRL, R.J.; West, B.L.; Green, K.N. (2015) Characterizing Newly Repopulated Microglia in the Adult Mouse: Impacts on Animal Behavior, Cell Morphology, and Neuroinflammation. PloS one.
Emerick MC, Stein R, Kunze R, McNulty MM, Regan MR, Hanck DA, Agnew WS (2006) Profiling the array of Ca(v)3.1 variants from the human T-type calcium channel gene CACNA1G: alternative structures, developmental expression, and biophysical variations. Proteins 64:320-342.

Erblich B, Zhu L, Etgen AM, Dobrenis K, Pollard JW (2011) Absence of colony stimulation factor-1 receptor results in loss of microglia, disrupted brain development and olfactory deficits. PloS one 6:e26317.
Etminan M, Gill S, Samii A (2003) Effect of non-steroidal anti-inflammatory drugs on risk of Alzheimer's disease: systematic review and meta-analysis of observational studies. Bmj 327:128.
Feng G, Mellor RH, Bernstein M, Keller-Peck C, Nguyen QT, Wallace M, Nerbonne JM, Lichtman JW, Sanes JR (2000) Imaging neuronal subsets in transgenic mice expressing multiple spectral variants of GFP. Neuron 28:41-51.
Fiala M, Liu QN, Sayre J, Pop V, Brahmandam V, Graves MC, Vinters HV (2002) Cyclooxygenase-2-positive macrophages infiltrate the Alzheimer's disease brain and damage the blood-brain barrier. European journal of clinical investigation 32:360-371.
Flanary BE, Streit WJ (2003) Telomeres shorten with age in rat cerebellum and cortex in vivo. Journal of anti-aging medicine 6:299-308.
Flanary BE, Sammons NW, Nguyen C, Walker D, Streit WJ (2007) Evidence that aging and amyloid promote microglial cell senescence. Rejuvenation research 10:61-74.
Floden AM, Combs CK (2011) Microglia demonstrate age-dependent interaction with amyloid-beta fibrils. Journal of Alzheimer's disease : JAD 25:279-293.
Garcia-Baquero R, Puerta P, Beltran M, Alvarez M, Sacristan R, Alvarez-Ossorio JL, Sanchez-Carbayo M (2013) Methylation of a Novel Panel of Tumor Suppressor Genes in Urine Moves Forward Non-Invasive Diagnosis and Prognosis in Bladder Cancer: A Two Center Prospective Study. The Journal of urology.
Giannakopoulos P, Herrmann FR, Bussiere T, Bouras C, Kovari E, Perl DP, Morrison JH, Gold G, Hof PR (2003) Tangle and neuron numbers, but not amyloid load, predict cognitive status in Alzheimer's disease. Neurology 60:1495-1500.
Ginhoux F, Merad M (2010) Ontogeny and homeostasis of Langerhans cells. Immunology and cell biology 88:387-392.
Go AS et al. (2014) Heart disease and stroke statistics--2014 update: a report from the American Heart Association. Circulation 129:e28-e292.
Godbout JP, Chen J, Abraham J, Richwine AF, Berg BM, Kelley KW, Johnson RW (2005) Exaggerated neuroinflammation and sickness behavior in aged mice following activation of the peripheral innate immune system. FASEB journal : official publication of the Federation of American Societies for Experimental Biology 19:1329-1331.
Green KN (2009) Calcium in the initiation, progression and as an effector of Alzheimer's disease pathology. J Cell Mol Med 13:2787-2799.
Green KN, Khashwji H, Estrada T, Laferla FM (2011) ST101 induces a novel 17 kDa APP cleavage that precludes Abeta generation in vivo. Annals of neurology 69:831-844.
Green KN, Demuro A, Akbari Y, Hitt BD, Smith IF, Parker I, LaFerla FM (2008) SERCA pump activity is physiologically regulated by presenilin and regulates amyloid beta production. The Journal of cell biology 181:1107-1116.
Guerreiro R et al. (2013) TREM2 variants in Alzheimer's disease. The New England journal of medicine 368:117-127.

Hains BC, Waxman SG (2006) Activated microglia contribute to the maintenance of chronic pain after spinal cord injury. The Journal of neuroscience : the official journal of the Society for Neuroscience 26:4308-4317.
Hamilton JA, Whitty G, Masendycz P, Wilson NJ, Jackson J, De Nardo D, Scholz GM (2008) The critical role of the colony-stimulating factor-1 receptor in the differentiation of myeloblastic leukemia cells. Molecular cancer research : MCR 6:458-467.
Hanisch UK (2013) Functional diversity of microglia - how heterogeneous are they to begin with? Frontiers in cellular neuroscience 7:65.
He Y, Rhodes SD, Chen S, Wu X, Yuan J, Yang X, Jiang L, Li X, Takahashi N, Xu M, Mohammad KS, Guise TA, Yang FC (2012) c-Fms signaling mediates neurofibromatosis Type-1 osteoclast gain-in-functions. PloS one 7:e46900.
Hefendehl JK, Neher JJ, Suhs RB, Kohsaka S, Skodras A, Jucker M (2014) Homeostatic and injury-induced microglia behavior in the aging brain. Aging cell 13:60-69.
Holmes C, Cunningham C, Zotova E, Woolford J, Dean C, Kerr S, Culliford D, Perry VH (2009) Systemic inflammation and disease progression in Alzheimer disease. Neurology 73:768-774.
Hsieh H, Boehm J, Sato C, Iwatsubo T, Tomita T, Sisodia S, Malinow R (2006) AMPAR removal underlies Abeta-induced synaptic depression and dendritic spine loss. Neuron 52:831-843.
Huang L, Keyser BM, Tagmose TM, Hansen JB, Taylor JT, Zhuang H, Zhang M, Ragsdale DS, Li M (2004) NNC 55-0396 [(1S,2S)-2-(2-(N-[(3-benzimidazol-2-yl)propyl]-N-methylamino)ethyl)-6-fluo ro-1,2,3,4-tetrahydro-1-isopropyl-2-naphtyl cyclopropanecarboxylate dihydrochloride]: a new selective inhibitor of T-type calcium channels. J Pharmacol Exp Ther 309:193-199.
Iftinca MC (2011) Neuronal T-type calcium channels: what's new? Iftinca: T-type channel regulation. J Med Life 4:126-138.
Ji K, Akgul G, Wollmuth LP, Tsirka SE (2013) Microglia actively regulate the number of functional synapses. PloS one 8:e56293.
Jonsson T et al. (2013) Variant of TREM2 associated with the risk of Alzheimer's disease. The New England journal of medicine 368:107-116.
Kierdorf K et al. (2013) Microglia emerge from erythromyeloid precursors via Pu.1- and Irf8-dependent pathways. Nature neuroscience 16:273-280.
Kirsten TB, Chaves-Kirsten GP, Chaible LM, Silva AC, Martins DO, Britto LR, Dagli ML, Torrao AS, Palermo-Neto J, Bernardi MM (2012) Hypoactivity of the central dopaminergic system and autistic-like behavior induced by a single early prenatal exposure to lipopolysaccharide. Journal of neuroscience research 90:1903-1912.
Kitamura T, Miyake T, Fujita S (1984) Genesis of resting microglia in the gray matter of mouse hippocampus. The Journal of comparative neurology 226:421-433.
Kitazawa M, Cheng D, Tsukamoto MR, Koike MA, Wes PD, Vasilevko V, Cribbs DH, LaFerla FM (2011) Blocking IL-1 signaling rescues cognition, attenuates tau pathology, and restores neuronal beta-catenin pathway function in an Alzheimer's disease model. Journal of immunology 187:6539-6549.

Kleinberger G et al. (2014) TREM2 mutations implicated in neurodegeneration impair cell surface transport and phagocytosis. Science translational medicine 6:243ra286.
Kleindienst A, Ross Bullock M (2006) A critical analysis of the role of the neurotrophic protein S100B in acute brain injury. Journal of neurotrauma 23:1185-1200.
Kleindienst A, McGinn MJ, Harvey HB, Colello RJ, Hamm RJ, Bullock MR (2005) Enhanced hippocampal neurogenesis by intraventricular S100B infusion is associated with improved cognitive recovery after traumatic brain injury. Journal of neurotrauma 22:645-655.
Kochi SK, Collier RJ (1993) DNA fragmentation and cytolysis in U937 cells treated with diphtheria toxin or other inhibitors of protein synthesis. Experimental cell research 208:296-302.
Kuhlman SJ, Olivas ND, Tring E, Ikrar T, Xu X, Trachtenberg JT (2013) A disinhibitory microcircuit initiates critical-period plasticity in the visual cortex. Nature 501:543-546.
Landfield PW, Pitler TA (1984) Prolonged Ca2+-dependent afterhyperpolarizations in hippocampal neurons of aged rats. Science 226:1089-1092.
Lee JW, Lee YK, Yuk DY, Choi DY, Ban SB, Oh KW, Hong JT (2008) Neuro-inflammation induced by lipopolysaccharide causes cognitive impairment through enhancement of beta-amyloid generation. Journal of neuroinflammation 5:37.
Lee P, Morley G, Huang Q, Fischer A, Seiler S, Horner JW, Factor S, Vaidya D, Jalife J, Fishman GI (1998) Conditional lineage ablation to model human diseases. Proceedings of the National Academy of Sciences of the United States of America 95:11371-11376.
Lin H, Lee E, Hestir K, Leo C, Huang M, Bosch E, Halenbeck R, Wu G, Zhou A, Behrens D, Hollenbaugh D, Linnemann T, Qin M, Wong J, Chu K, Doberstein SK, Williams LT (2008) Discovery of a cytokine and its receptor by functional screening of the extracellular proteome. Science 320:807-811.
Liu JS, Amaral TD, Brosnan CF, Lee SC (1998) IFNs are critical regulators of IL-1 receptor antagonist and IL-1 expression in human microglia. Journal of immunology 161:1989-1996.
Lopez JR, Lyckman A, Oddo S, Laferla FM, Querfurth HW, Shtifman A (2008) Increased intraneuronal resting [Ca2+] in adult Alzheimer's disease mice. Journal of neurochemistry 105:262-271.
Lopez-Arrieta JM, Birks J (2000) Nimodipine for primary degenerative, mixed and vascular dementia. Cochrane Database Syst Rev:CD000147.
Maezawa I, Jin LW (2010) Rett syndrome microglia damage dendrites and synapses by the elevated release of glutamate. The Journal of neuroscience : the official journal of the Society for Neuroscience 30:5346-5356.
Marcum ZA, Hanlon JT (2010) Recognizing the Risks of Chronic Nonsteroidal Anti-Inflammatory Drug Use in Older Adults. The annals of long-term care : the official journal of the American Medical Directors Association 18:24-27.
Marshak DR (1990) S100 beta as a neurotrophic factor. Progress in brain research 86:169-181.

Martini A, Battaini F, Govoni S, Volpe P (1994) Inositol 1,4,5-trisphosphate receptor and ryanodine receptor in the aging brain of Wistar rats. Neurobiology of aging 15:203-206.
Mayford M, Bach ME, Huang YY, Wang L, Hawkins RD, Kandel ER (1996) Control of memory formation through regulated expression of a CaMKII transgene. Science 274:1678-1683.
McKercher SR, Torbett BE, Anderson KL, Henkel GW, Vestal DJ, Baribault H, Klemsz M, Feeney AJ, Wu GE, Paige CJ, Maki RA (1996) Targeted disruption of the PU.1 gene results in multiple hematopoietic abnormalities. The EMBO journal 15:5647-5658.
Mildner A, Schmidt H, Nitsche M, Merkler D, Hanisch UK, Mack M, Heikenwalder M, Bruck W, Priller J, Prinz M (2007) Microglia in the adult brain arise from Ly-6ChiCCR2+ monocytes only under defined host conditions. Nature neuroscience 10:1544-1553.
Min KJ, Yang MS, Kim SU, Jou I, Joe EH (2006) Astrocytes induce hemeoxygenase-1 expression in microglia: a feasible mechanism for preventing excessive brain inflammation. The Journal of neuroscience : the official journal of the Society for Neuroscience 26:1880-1887.
Minagar A, Alexander JS (2003) Blood-brain barrier disruption in multiple sclerosis. Multiple sclerosis 9:540-549.
Mody M, Cao Y, Cui Z, Tay KY, Shyong A, Shimizu E, Pham K, Schultz P, Welsh D, Tsien JZ (2001) Genome-wide gene expression profiles of the developing mouse hippocampus. Proceedings of the National Academy of Sciences of the United States of America 98:8862-8867.
Mok S, Koya RC, Tsui C, Xu J, Robert L, Wu L, Graeber TG, West BL, Bollag G, Ribas A (2014) Inhibition of CSF-1 receptor improves the antitumor efficacy of adoptive cell transfer immunotherapy. Cancer research 74:153-161.
Morioka M, Kawano T, Yano S, Kai Y, Tsuiki H, Yoshinaga Y, Matsumoto J, Maeda T, Hamada J, Yamamoto H, Fukunaga K, Kuratsu J (2006) Hyperphosphorylation at serine 199/202 of tau factor in the gerbil hippocampus after transient forebrain ischemia. Biochemical and biophysical research communications 347:273-278.
Morrison RS, Wenzel HJ, Kinoshita Y, Robbins CA, Donehower LA, Schwartzkroin PA (1996) Loss of the p53 tumor suppressor gene protects neurons from kainate-induced cell death. The Journal of neuroscience : the official journal of the Society for Neuroscience 16:1337-1345.
Myczek K, Yeung ST, Castello N, Baglietto-Vargas D, LaFerla FM (2014) Hippocampal adaptive response following extensive neuronal loss in an inducible transgenic mouse model. PloS one 9:e106009.
Nagamoto-Combs K, McNeal DW, Morecraft RJ, Combs CK (2007) Prolonged microgliosis in the rhesus monkey central nervous system after traumatic brain injury. Journal of neurotrauma 24:1719-1742.
Nagarajan RP, Hogart AR, Gwye Y, Martin MR, LaSalle JM (2006) Reduced MeCP2 expression is frequent in autism frontal cortex and correlates with aberrant MECP2 promoter methylation. Epigenetics : official journal of the DNA Methylation Society 1:e1-11.

Neely KM, Green KN, LaFerla FM (2011) Presenilin is necessary for efficient proteolysis through the autophagy-lysosome system in a gamma-secretase-independent manner. J Neurosci 31:2781-2791.
Nimmerjahn A, Kirchhoff F, Helmchen F (2005) Resting microglial cells are highly dynamic surveillants of brain parenchyma in vivo. Science 308:1314-1318.
Olivas ND, Quintanar-Zilinskas V, Nenadic Z, Xu X (2012) Laminar circuit organization and response modulation in mouse visual cortex. Front Neural Circuits 6:70.
Orlowski D, Soltys Z, Janeczko K (2003) Morphological development of microglia in the postnatal rat brain. A quantitative study. International journal of developmental neuroscience : the official journal of the International Society for Developmental Neuroscience 21:445-450.
Oshima T, Ozono R, Yano Y, Higashi Y, Teragawa H, Miho N, Ishida T, Ishida M, Yoshizumi M, Kambe M (2005) Beneficial effect of T-type calcium channel blockers on endothelial function in patients with essential hypertension. Hypertension research : official journal of the Japanese Society of Hypertension 28:889-894.
Oules B, Del Prete D, Greco B, Zhang X, Lauritzen I, Sevalle J, Moreno S, Paterlini-Brechot P, Trebak M, Checler F, Benfenati F, Chami M (2012) Ryanodine receptor blockade reduces amyloid-beta load and memory impairments in Tg2576 mouse model of Alzheimer disease. The Journal of neuroscience : the official journal of the Society for Neuroscience 32:11820-11834.
Palop JJ, Jones B, Kekonius L, Chin J, Yu GQ, Raber J, Masliah E, Mucke L (2003) Neuronal depletion of calcium-dependent proteins in the dentate gyrus is tightly linked to Alzheimer's disease-related cognitive deficits. Proceedings of the National Academy of Sciences of the United States of America 100:9572-9577.
Pan XD, Zhu YG, Lin N, Zhang J, Ye QY, Huang HP, Chen XC (2011) Microglial phagocytosis induced by fibrillar beta-amyloid is attenuated by oligomeric beta-amyloid: implications for Alzheimer's disease. Molecular neurodegeneration 6:45.
Paolicelli RC, Bolasco G, Pagani F, Maggi L, Scianni M, Panzanelli P, Giustetto M, Ferreira TA, Guiducci E, Dumas L, Ragozzino D, Gross CT (2011) Synaptic pruning by microglia is necessary for normal brain development. Science 333:1456-1458.
Pardo-Manuel de Villena F, Heine-Suner D, Rodriguez de Cordoba S (1996) Ordering of the human regulator of complement activation gene cluster on 1q32 by two-colour FISH. Cytogenetics and cell genetics 72:339-341.
Parkhurst CN, Yang G, Ninan I, Savas JN, Yates JR, 3rd, Lafaille JJ, Hempstead BL, Littman DR, Gan WB (2013) Microglia promote learning-dependent synapse formation through brain-derived neurotrophic factor. Cell 155:1596-1609.
Patrick GN, Zhou P, Kwon YT, Howley PM, Tsai LH (1998) p35, the neuronal-specific activator of cyclin-dependent kinase 5 (Cdk5) is degraded by the ubiquitin-proteasome pathway. The Journal of biological chemistry 273:24057-24064.
Patrick GN, Zukerberg L, Nikolic M, de la Monte S, Dikkes P, Tsai LH (1999) Conversion of p35 to p25 deregulates Cdk5 activity and promotes neurodegeneration. Nature 402:615-622.
Penzes P, Cahill ME, Jones KA, VanLeeuwen JE, Woolfrey KM (2011) Dendritic spine pathology in neuropsychiatric disorders. Nature neuroscience 14:285-293.

Perez-Reyes E (2003) Molecular physiology of low-voltage-activated t-type calcium channels. Physiol Rev 83:117-161.
Perry VH, O'Connor V (2010) The role of microglia in synaptic stripping and synaptic degeneration: a revised perspective. ASN Neuro 2:e00047.
Pessac B, Godin I, Alliot F (2001) [Microglia: origin and development]. Bulletin de l'Academie nationale de medecine 185:337-346; discussion 346-337.
Peters A, Kaiserman-Abramof IR (1970) The small pyramidal neuron of the rat cerebral cortex. The perikaryon, dendrites and spines. Am J Anat 127:321-355.
Plane JM, Shen Y, Pleasure DE, Deng W (2010) Prospects for minocycline neuroprotection. Archives of neurology 67:1442-1448.
Prada CE, Jousma E, Rizvi TA, Wu J, Dunn RS, Mayes DA, Cancelas JA, Dombi E, Kim MO, West BL, Bollag G, Ratner N (2013) Neurofibroma-associated macrophages play roles in tumor growth and response to pharmacological inhibition. Acta neuropathologica 125:159-168.
Priller J, Flugel A, Wehner T, Boentert M, Haas CA, Prinz M, Fernandez-Klett F, Prass K, Bechmann I, de Boer BA, Frotscher M, Kreutzberg GW, Persons DA, Dirnagl U (2001) Targeting gene-modified hematopoietic cells to the central nervous system: use of green fluorescent protein uncovers microglial engraftment. Nature medicine 7:1356-1361.
Quesada A, Bui PH, Homanics GE, Hankinson O, Handforth A (2011) Comparison of mibefradil and derivative NNC 55-0396 effects on behavior, cytochrome P450 activity, and tremor in mouse models of essential tremor. European journal of pharmacology.
Rademakers R et al. (2012) Mutations in the colony stimulating factor 1 receptor (CSF1R) gene cause hereditary diffuse leukoencephalopathy with spheroids. Nature genetics 44:200-205.
Ramlackhansingh AF, Brooks DJ, Greenwood RJ, Bose SK, Turkheimer FE, Kinnunen KM, Gentleman S, Heckemann RA, Gunanayagam K, Gelosa G, Sharp DJ (2011) Inflammation after trauma: microglial activation and traumatic brain injury. Annals of neurology 70:374-383.
Renno T, Krakowski M, Piccirillo C, Lin JY, Owens T (1995) TNF-alpha expression by resident microglia and infiltrating leukocytes in the central nervous system of mice with experimental allergic encephalomyelitis. Regulation by Th1 cytokines. Journal of immunology 154:944-953.
Resende R, Ferreiro E, Pereira C, Resende de Oliveira C (2008) Neurotoxic effect of oligomeric and fibrillar species of amyloid-beta peptide 1-42: involvement of endoplasmic reticulum calcium release in oligomer-induced cell death. Neuroscience 155:725-737.
Riascos D, de Leon D, Baker-Nigh A, Nicholas A, Yukhananov R, Bu J, Wu CK, Geula C (2011) Age-related loss of calcium buffering and selective neuronal vulnerability in Alzheimer's disease. Acta neuropathologica 122:565-576.
Rim HK, Lee HW, Choi IS, Park JY, Choi HW, Choi JH, Cho YW, Lee JY, Lee KT (2012) T-type Ca2+ channel blocker, KYS05047 induces G1 phase cell cycle arrest by decreasing intracellular Ca2+ levels in human lung adenocarcinoma A549 cells. Bioorganic & medicinal chemistry letters 22:7123-7126.
Rio-Hortega P (1939) The Microglia. Lancet 233:1023-1026.

Roses AD (1996) Apolipoprotein E alleles as risk factors in Alzheimer's disease. Annual review of medicine 47:387-400.
Saijo K, Winner B, Carson CT, Collier JG, Boyer L, Rosenfeld MG, Gage FH, Glass CK (2009) A Nurr1/CoREST pathway in microglia and astrocytes protects dopaminergic neurons from inflammation-induced death. Cell 137:47-59.
Sandhir R, Onyszchuk G, Berman NE (2008) Exacerbated glial response in the aged mouse hippocampus following controlled cortical impact injury. Experimental neurology 213:372-380.
Sandmann S, Spormann J, Prenzel F, Shaw L, Unger T (2002) Calcium channel blockade limits transcriptional, translational and functional up-regulation of the cardiac calpain system after myocardial infarction. European journal of pharmacology 453:99-109.
Schafer DP, Lehrman EK, Kautzman AG, Koyama R, Mardinly AR, Yamasaki R, Ransohoff RM, Greenberg ME, Barres BA, Stevens B (2012) Microglia sculpt postnatal neural circuits in an activity and complement-dependent manner. Neuron 74:691-705.
Schilling M, Strecker JK, Schabitz WR, Ringelstein EB, Kiefer R (2009) Effects of monocyte chemoattractant protein 1 on blood-borne cell recruitment after transient focal cerebral ischemia in mice. Neuroscience 161:806-812.
Sequier JM, Hunziker W, Andressen C, Celio MR (1990) Calbindin D-28k Protein and mRNA Localization in the Rat Brain. The European journal of neuroscience 2:1118-1126.
Shi Y, Nenadic Z, Xu X (2010) Novel use of matched filtering for synaptic event detection and extraction. PLoS One 5:e15517.
Sierra A, Gottfried-Blackmore AC, McEwen BS, Bulloch K (2007) Microglia derived from aging mice exhibit an altered inflammatory profile. Glia 55:412-424.
Sierra A, Encinas JM, Deudero JJ, Chancey JH, Enikolopov G, Overstreet-Wadiche LS, Tsirka SE, Maletic-Savatic M (2010) Microglia shape adult hippocampal neurogenesis through apoptosis-coupled phagocytosis. Cell stem cell 7:483-495.
Splawski I, Yoo DS, Stotz SC, Cherry A, Clapham DE, Keating MT (2006) CACNA1H mutations in autism spectrum disorders. The Journal of biological chemistry 281:22085-22091.
Stevens B, Allen NJ, Vazquez LE, Howell GR, Christopherson KS, Nouri N, Micheva KD, Mehalow AK, Huberman AD, Stafford B, Sher A, Litke AM, Lambris JD, Smith SJ, John SW, Barres BA (2007) The classical complement cascade mediates CNS synapse elimination. Cell 131:1164-1178.
Stewart WF, Kawas C, Corrada M, Metter EJ (1997) Risk of Alzheimer's disease and duration of NSAID use. Neurology 48:626-632.
Streit WJ, Sammons NW, Kuhns AJ, Sparks DL (2004) Dystrophic microglia in the aging human brain. Glia 45:208-212.
Suzuki K, Sugihara G, Ouchi Y, Nakamura K, Futatsubashi M, Takebayashi K, Yoshihara Y, Omata K, Matsumoto K, Tsuchiya KJ, Iwata Y, Tsujii M, Sugiyama T, Mori N (2013) Microglial activation in young adults with autism spectrum disorder. JAMA Psychiatry 70:49-58.
Tang SC, Arumugam TV, Xu X, Cheng A, Mughal MR, Jo DG, Lathia JD, Siler DA, Chigurupati S, Ouyang X, Magnus T, Camandola S, Mattson MP (2007) Pivotal

role for neuronal Toll-like receptors in ischemic brain injury and functional deficits. Proceedings of the National Academy of Sciences of the United States of America 104:13798-13803.
Tetreault NA, Hakeem AY, Jiang S, Williams BA, Allman E, Wold BJ, Allman JM (2012) Microglia in the cerebral cortex in autism. Journal of autism and developmental disorders 42:2569-2584.
Thibault O, Landfield PW (1996) Increase in single L-type calcium channels in hippocampal neurons during aging. Science 272:1017-1020.
Tobinick EL, Gross H (2008) Rapid cognitive improvement in Alzheimer's disease following perispinal etanercept administration. Journal of neuroinflammation 5:2.
Toyota M, Ho C, Ohe-Toyota M, Baylin SB, Issa JP (1999) Inactivation of CACNA1G, a T-type calcium channel gene, by aberrant methylation of its 5' CpG island in human tumors. Cancer research 59:4535-4541.
Tremblay ME, Zettel ML, Ison JR, Allen PD, Majewska AK (2012) Effects of aging and sensory loss on glial cells in mouse visual and auditory cortices. Glia 60:541-558.
Trollor JN, Smith E, Agars E, Kuan SA, Baune BT, Campbell L, Samaras K, Crawford J, Lux O, Kochan NA, Brodaty H, Sachdev P (2012) The association between systemic inflammation and cognitive performance in the elderly: the Sydney Memory and Ageing Study. Age 34:1295-1308.
Valdearcos M, Robblee MM, Benjamin DI, Nomura DK, Xu AW, Koliwad SK (2014) Microglia dictate the impact of saturated fat consumption on hypothalamic inflammation and neuronal function. Cell reports 9:2124-2138.
Valero J, Mastrella G, Neiva I, Sanchez S, Malva JO (2014) Long-term effects of an acute and systemic administration of LPS on adult neurogenesis and spatial memory. Frontiers in neuroscience 8:83.
Veeranna, Kaji T, Boland B, Odrljin T, Mohan P, Basavarajappa BS, Peterhoff C, Cataldo A, Rudnicki A, Amin N, Li BS, Pant HC, Hungund BL, Arancio O, Nixon RA (2004) Calpain mediates calcium-induced activation of the erk1,2 MAPK pathway and cytoskeletal phosphorylation in neurons: relevance to Alzheimer's disease. The American journal of pathology 165:795-805.
Villeda SA et al. (2011) The ageing systemic milieu negatively regulates neurogenesis and cognitive function. Nature 477:90-94.
Wagner G, Icks A, Abholz HH, Schroder-Bernhardi D, Rathmann W, Kostev K (2012) Antihypertensive treatment and risk of dementia: a retrospective database study. International journal of clinical pharmacology and therapeutics 50:195-201.
Wake H, Moorhouse AJ, Jinno S, Kohsaka S, Nabekura J (2009) Resting microglia directly monitor the functional state of synapses in vivo and determine the fate of ischemic terminals. The Journal of neuroscience : the official journal of the Society for Neuroscience 29:3974-3980.
Wang Y, Szretter KJ, Vermi W, Gilfillan S, Rossini C, Cella M, Barrow AD, Diamond MS, Colonna M (2012) IL-34 is a tissue-restricted ligand of CSF1R required for the development of Langerhans cells and microglia. Nature immunology 13:753-760.
Wasserman JK, Yang H, Schlichter LC (2008) Glial responses, neuron death and lesion resolution after intracerebral hemorrhage in young vs. aged rats. The European journal of neuroscience 28:1316-1328.

West MJ, Coleman PD, Flood DG, Troncoso JC (1994) Differences in the pattern of hippocampal neuronal loss in normal ageing and Alzheimer's disease. Lancet 344:769-772.
Wiktor-Jedrzejczak W, Bartocci A, Ferrante AW, Jr., Ahmed-Ansari A, Sell KW, Pollard JW, Stanley ER (1990) Total absence of colony-stimulating factor 1 in the macrophage-deficient osteopetrotic (op/op) mouse. Proceedings of the National Academy of Sciences of the United States of America 87:4828-4832.
Xu X, Callaway EM (2009) Laminar specificity of functional input to distinct types of inhibitory cortical neurons. J Neurosci 29:70-85.
Xu X, Olivas ND, Levi R, Ikrar T, Nenadic Z (2010) High precision and fast functional mapping of cortical circuitry through a combination of voltage sensitive dye imaging and laser scanning photostimulation. J Neurophysiol 103:2301-2312.
Yamasaki TR, Blurton-Jones M, Morrissette DA, Kitazawa M, Oddo S, LaFerla FM (2007) Neural stem cells improve memory in an inducible mouse model of neuronal loss. The Journal of neuroscience : the official journal of the Society for Neuroscience 27:11925-11933.
Yang Y, Rosenberg GA (2011) Blood-brain barrier breakdown in acute and chronic cerebrovascular disease. Stroke; a journal of cerebral circulation 42:3323-3328.
Yirmiya R, Goshen I (2011) Immune modulation of learning, memory, neural plasticity and neurogenesis. Brain Behav Immun 25:181-213.
Zhan Y, Paolicelli RC, Sforazzini F, Weinhard L, Bolasco G, Pagani F, Vyssotski AL, Bifone A, Gozzi A, Ragozzino D, Gross CT (2014) Deficient neuron-microglia signaling results in impaired functional brain connectivity and social behavior. Nature neuroscience 17:400-406.
Zusso M, Methot L, Lo R, Greenhalgh AD, David S, Stifani S (2012) Regulation of postnatal forebrain amoeboid microglial cell proliferation and development by the transcription factor Runx1. The Journal of neuroscience : the official journal of the Society for Neuroscience 32:11285-11298.